UNIVERSITY OF CINCINNATI

Date: August 27, 2008

I, Kevin Parker,

hereby submit this work as part of the requirements for the degree of:

Doctor of Philosophy

in:

Chemistry

It is entitled:

Studies on Inclusion of a Thiol Flavor Constituent and Fatty Acids with beta-Cyclodextrin

This work and its defense approved by:

Chair: Dr. Apryll M. Stalcup

Dr. Patrick Limbach

Dr. James Mack

Studies on Inclusion of a Thiol Flavor Constituent and Fatty Acids with beta-Cyclodextrin

A dissertation submitted to the
Graduate School
of the University of Cincinnati

In partial fulfillment of the
requirements for the degree of

DOCTORATE OF PHILOSOPHY (Ph.D.)

In the Department of Chemistry
of the College of Arts and Sciences

August 2008

By

Kevin M. Parker

B.A., Chemistry
Hanover College, Hanover, IN, May 2003

Committee Chair: Dr. Apryll M. Stalcup

Studies on Inclusion of a Thiol Flavor Constituent and Fatty Acids with β-Cyclodextrin

Kevin M. Parker

ABSTRACT

The work presented in this dissertation aims to advance the application of using cyclodextrins to encapsulate flavoring compounds for enhanced retention and protection from environmental surroundings. Specifically, results of investigations are presented on the study of beta-cyclodextrin (β-CD) inclusion of 2-furfurylthiol (FFT) in the presence and absence of different fatty acids (FAs).

In Chapter 1, an overview is given on CD chemistry: its discovery, structural characteristics, inclusion complexation, and uses in industrial and chemical applications. The concept of ternary CD complexes is introduced, in which auxiliary compounds are used in conjunction with CD to achieve desirable traits not realized by simple binary inclusion complexes. The natural occurrence of some sulfur containing aroma and flavor compounds is discussed, specifically the importance of furanthiols in aroma and flavor chemistry. Chapter 1 concludes with an overview of the focused project of this dissertation, and its relation to past work in this field.

Chapter 2 describes studies on FFT complexation with β-CD in solution. Nuclear magnetic resonance (NMR) spectroscopy and its application to study CD inclusion complexes are detailed. Results of these experiments provide evidence for cavity

inclusion of FFT with β-CD, and a structure of the complex is proposed. A quantitative binding study is also discussed.

Chapter 3 details binding studies between FAs and β-CD, using capillary electrophoresis and isothermal titration calorimetry. Results obtained from these techniques can be used concurrently to quantitatively characterize these binary systems.

Chapter 4 carries the focus toward the study of solid encapsulation products of FFT with β-CD and β-CD/FAs in combination, with the goal of preparing a solid FFT formulation with ideal retention and environmental protection capabilities. Results are presented for FFT loading and retention in different solid materials that were prepared. The complexes prepared in the presence of ethanol exhibited the best FFT retention, and are further discussed.

Chapter 5 offers general conclusions. Additional experimental studies are suggested that could potentially help understand the properties of complexes that have been prepared, as well as opening the door for other possible ternary auxiliary compounds to potentially realize encapsulation characteristics not fulfilled by the β-CD/fatty acid combination.

Acknowledgements

Many people deserve thanks and appreciation for their support during my time in graduate school at the University of Cincinnati. I would first like to thank my advisor, Dr. Apryll Stalcup, for financial support, a place in her group, and for her role in the advancement of my knowledge in separations and analytical chemistry. More importantly, I sincerely thank her for many discussions regarding research advice, and also those focused on balancing a personal life with a professional career, encouragement of my abilities, and thoughtfulness into my life and development outside of chemistry. I will specifically miss your non-scientific analogies of chemistry theory that always seemed to not only clarify a difficult topic, but also make me laugh.

I would also like to acknowledge Dr. Pat Limbach and Dr. James Mack for serving on my Ph.D. committee. Particular appreciation is noted for their flexibility in scheduling and attending the many seminars I presented throughout my graduate studies, and for the tough questions that always tested my ability to think under pressure. Also, I would like to thank them for conversations had apart from chemistry.

Dr. Daisy-Malloy Hamburg, Dr. Douglas D. Richardson, and Dr. Kevin M. Kubachka merit special recognition for standing out from the rest of my peers I interacted with during my graduate studies. Many sincere thanks and appreciation for different perspectives they offered on class and examination materials and how to survive through the hard times that graduate school can present. Also, I especially enjoyed our study sessions that always seemed to turn into “let’s have just a couple of drinks.”

To the members of the Stalcup research group, thank you for making my experience in the lab an entertaining one. I have learned something from each and every single individual that has helped shape my personality and professionalism that I hope to carry away into my career.

Givaudan Flavors Corporation, specifically Dr. Alan Gabelman, deserves recognition for support of my project. Thank you for discussions on advancement of my academic career and the relationship between my research and your industry, and for the many on-site oral presentation opportunities throughout the past 3 years. I would also like to thank the Membrane Applied Science and Technology (MAST) Center at the University of Cincinnati, as funded by NSF, for financial support of this project.

I would like to extend my gratitude and appreciation for my family and friends for their support. Thank you for encouraging my endeavors and abilities, and for listening to my concerns even though you might not have understood what I was talking about.

Lastly, and most importantly, I would like to deeply thank my wife, Abbey, for her unconditional love and support. Thank you for encouraging me to go outside of my comfort zone, changing my mood when I thought I could not be optimistic, driving my self-esteem up by making me focus on my strengths instead of my weaknesses, and for just being by my side. Nothing makes me happier than the thought of continuing my journey through life with you, and I look forward to our adventures.

Studies on Inclusion of a Thiol Flavor Constituent and Fatty Acids with β-Cyclodextrin

Table of Contents

Chapter 1

Introduction

1.1 Cyclodextrins

1.1.1 Discovery

The first reference to the compounds later shown as cyclodextrins was made by Villiers in 1891 [1,2]. Villiers' studies on the enzymatic digestion of starch with *Bacillus amylobacter* isolated a crystalline substance he termed "cellulosine", owing to its similarity to cellulose with regard to its resistance to acid hydrolysis. At the beginning of the 20th century while studying studied heat resistant strains of bacteria, Schardinger noted that when digesting starch with his microorganisms, two different crystalline products were formed in small amounts that seemed to be identical to Villiers' "cellulosine" [1]. The isolated microbe was termed *Bacillus macerans* by Schardinger and the crystallized compounds "dextrins". Following Schardinger's work, Pringsheim is credited with discovering the complexing ability of dextrins with various organic molecules [1,3]. Later work revealed the structure of the Schardinger dextrins to be a series of cyclic oligosaccharides built up from individual glucose units via α-1-4-glycosidic linkages [1,2], and they were thusly named "cyclodextrins".

The cyclodextrin family is comprised of three major CDs, and several minor, less common ones. Cyclodextrin nomenclature reflects the number of glucose units in the cyclic oligomer, so that the three major forms of CDs are termed α-, β- and γ-CD, representing the

glucose hexamer, heptamer, and octamer, respectively. Higher homologues containing 9-12 glucose units were reported in the mid-20th century [4], and recent research has provided evidence for large-ring CDs containing as many as 35 residues present in the cyclic structure [5]**.** A 5-unit containing CD has also been synthesized and characterized [6]. By far, the parent cyclodextrins are the most characterized with respect to their physical and chemical properties.

1.1.2 Structural Characteristics

Schematic models of β-CD are shown in Figure 1.1. Several structural features of CDs result from the cyclic association of the glucose residues via their glycosidic linkages. The cylindrical structure of a CD molecule is commonly characterized as a truncated cone. One rim of the cone is lined by secondary hydroxyl groups, while the opposite rim is lined by primary hydroxyl groups. Free rotation of the latter reduces the effective diameter of cylinder at this rim, therefore leading to the truncated shape. The cavity of the cyclinder is lined by hydrogen atoms and glycosidic oxygen bridges. Computations of molecular hydrophilicity potential profiles reveal separate, distinct regions of CD hydrophobicity [2]. The internal cavity and the primary hydroxyl rim are hydrophobic, while the secondary hydroxyl rim is hydrophilic. Figure 1.2 shows a schematic representation of α-, β-and γ-CDs listed with their individual molecular dimensions.

The presence of hydroxyl groups on the native CDs confers their aqueous solubility. However, the creation of an internal hydrogen bond network is possible, formed through association between the secondary hydroxyl groups located on the C-2 and C-3 carbons of adjacent glucose residues. This secondary rim hydrogen bond belt is fully realized in β-CD,

Figure 1.1. Schematic models of β-CD.

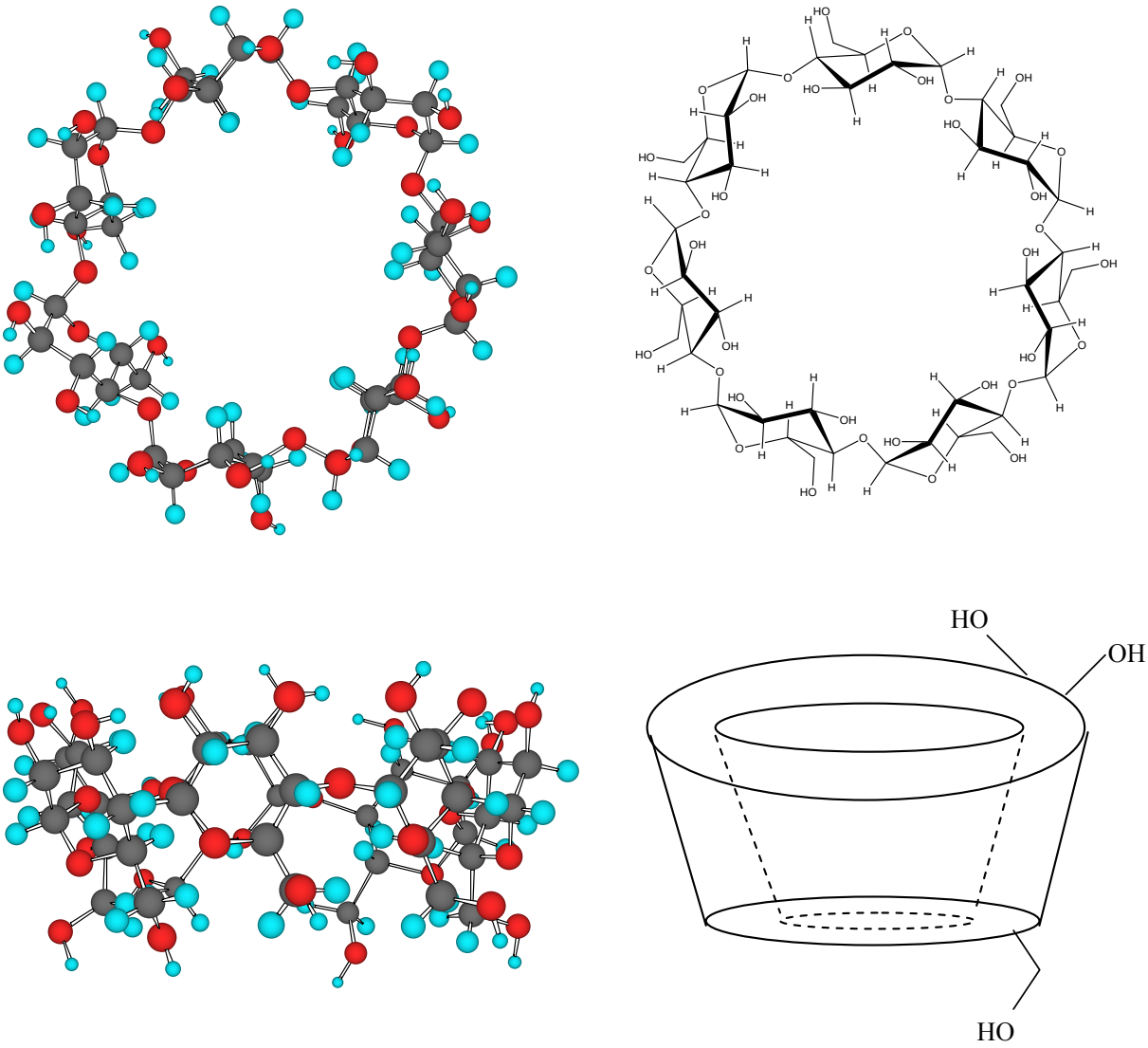

Figure 1.2. Schematic representation of the individual molecular dimension of α-, β-, and γ-CD.

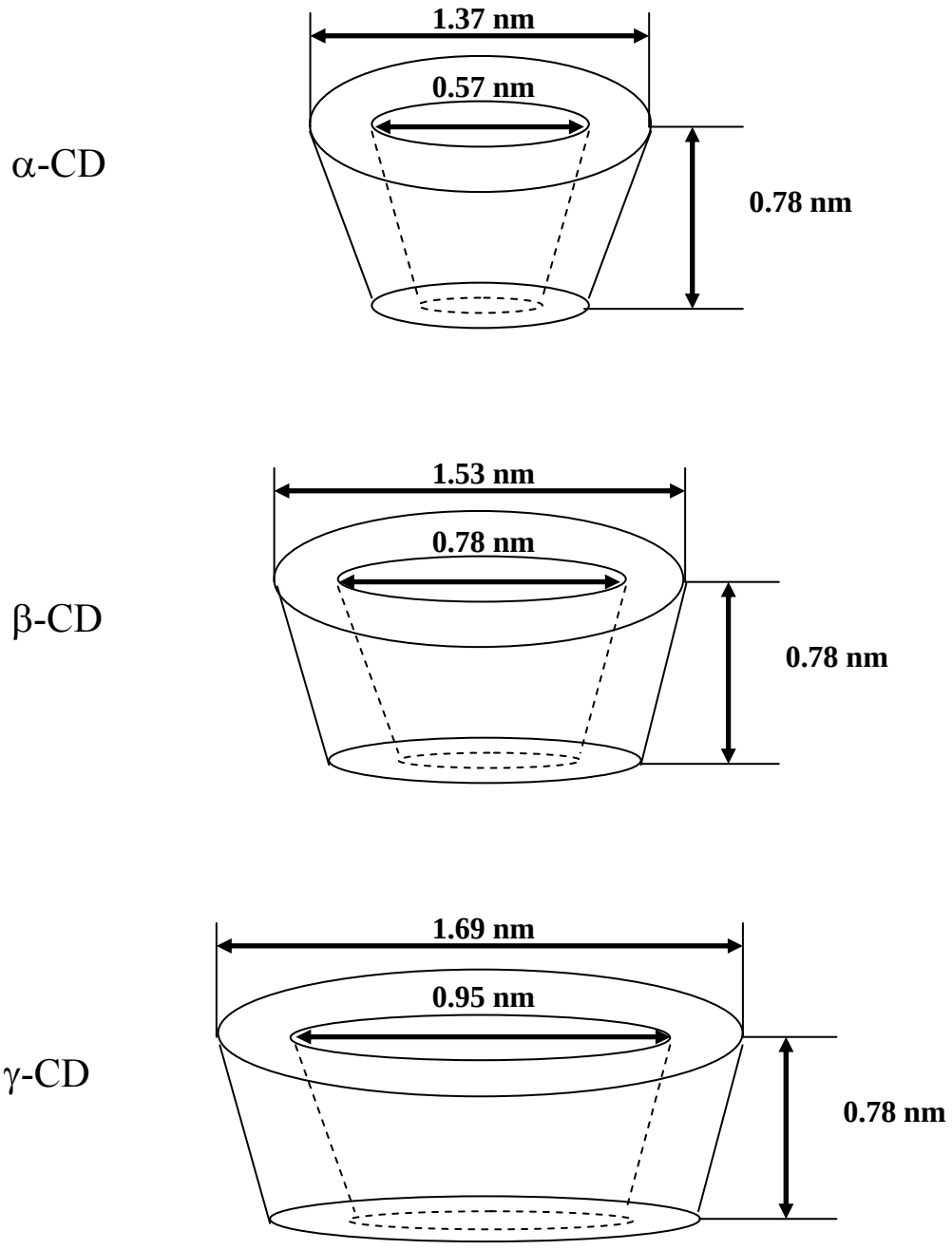

thereby leaving it the least water-soluble of the three native forms. Steric crowding of adjacent hydroxyl groups in α-CD distorts one glucose unit from a horizontal configuration, allowing only 4 of the 6 possible hydrogen bonds available to form according to this mechanism, and increasing its aqueous solubility compared to β-CD. The γ-CD has a non-coplanar, more flexible structure, and is therefore the most water soluble of the three major cyclodextrins [7].

1.1.3 Cyclodextrin Inclusion Complexes

1.1.3.1 Mechanism and Energetics of Inclusion

The inclusion of a guest in a CD cavity can be thought of essentially as an exchange of the included water molecules by a less polar guest species [1,2]. The "driving force" of this process is a combination of various effects dependent upon the guest and the CD. A major contributor to the inclusion mechanism is the substitution of energetically unfavorable polar-apolar interactions between the CD cavity and its included water molecules, and between water and an apolar guest compound, with favorable apolar-apolar interactions between the guest and cavity and polar-polar interactions between bulk water molecules and the released cavity-water molecules. Also contributing to the energetics of complex formation are: van der Waals interactions between the guest and host species; hydrogen bonding between some guests and host CDs; and, as seen in the case of α-CD, release of CD ring strain upon complexation. The latter contribution is not seen with β- or γ-CD because they are not strained in the "empty" state [1].

1.1.3.2 Factors Affecting Complexation

Geometric factors facilitate the formation of CD inclusion complexes in two ways: they are decisive on the types of guest molecules which can penetrate the CD cavity; and they determine the "tightness of fit" of the included guest and the CD cavity [1,2]. Therefore, one of the most influential factors on the ability of CDs to form inclusion complexes is geometric compatibility between the CD cavity and guest species. Consequently, the α-, β- and γ-CDs can fully include and form complexes with molecules of different size (Table 1.1) [1]. Complexation is possible with compounds significantly larger than the cavity dimensions of CDs, but in this case, only certain groups or side chains actually penetrate the host cavity.

The extent of complex formation also depends upon the polarity and ionization state of the guest molecule. Generally speaking, molecules can be complexed with CDs when they are less polar than water itself [1,2]. Highly hydrophilic, very water-soluble, highly hydrated species are not appropriate guest substances for any CDs regardless of their molecular dimensions. There is a positive correlation between complex stability and the hydrophobic character of the guest compound or certain parts of the guest compound. The addition of a methyl or ethyl group tends to improve the stability of the complex, whereas polar substituents commonly decrease the binding affinity [2]; for example, a systematic study on the complexation of cyclodextrins with various monosubstituted benzenes displays the dependence of the association equilibrium constant on substituent identity [8]. Furthermore, ionic species are commonly unfavored in complex formation [1,2,9]. However, this is not always true, as in some cases the ionized guest can form stronger inclusion complexes compared to their neutral counterparts [10]. The role of charge state therefore appears to be very guest/host pair-specific. And it should be noted that,

Table 1.1. Dependence of solute and CD cavity size on stability constants of inclusion complexes [9].

Guest	α-CD	β-CD	γ-CD
1,3-Butanediol	16 200	12 023	NR
4-Methoxycinnamic acid	10 300	658	NR
Adamantane carboxylic acid	130	330 000	24 000
Testosterone	5 058	7 450	16 500
Naphthalene	77	608	130
Anthracene	40	2 300	1 500
Phenanthrene	60	1 500	770

while charge and polarity are thought to play important roles in complex formation, these roles are considered less decisive than that of geometric fitting [2].

The complexation medium also plays a role in inclusion, because the presence of a third component can influence the inclusion equilibrium process in both directions [2]. Most complexation processes take place in aqueous solutions or at least in the presence of some water. However, some additives in the complexation media can facilitate or inhibit the inclusion process by influencing the hydrophobicity of the bulk water solvent [11,12,13,14,15], participating in competitive inclusion with the CD cavity [16,17], or through the formation of ternary complexes (Section 1.1.3.5).

Native CDs may be modified through functionalization of the primary and secondary hydroxyl groups. A variety of functionalized CDs have been prepared with either hydrophobic (e.g. methyl, propyl) or hydrophilic (sulfate, phosphate, quaternary amine) groups. The goal of such functionalization may be to: improve the solubility of the CD derivative and its inclusion complexes, alter fitting and association of specific guests to the CD cavity, or to form immobilized CD-containing structures for use in specific applications [18].

1.1.3.3 Methods of Studying Inclusion Complexes

Various techniques have been employed to study the effect of different structural and medium variables on complexation with CDs through the determination of binding constants (stability constants) and thermodynamic parameters responsible for the inclusion process, and also for the determination of molecular structure of inclusion complexes. Among the most common are spectroscopic (NMR, IR, UV-Vis), separations (CE, HPLC), calorimetric (ITC,

DSC), gravimetric (TGA) and mass spectrometric techniques. The use of these techniques to study CD inclusion complexes is detailed and reviewed in multiple literature sources [19,20,21,22,23,24,25]. The methods used in the research detailed in this dissertation (NMR, CE, ITC) are discussed in more detail in the subsequent chapters featuring experimental work.

1.1.3.4 Applications

One of the best realized industrial applications of CD inclusion complexes is in the pharmaceutical trade. The first patent on the use of CDs in drug formulations was issued in 1953 to Freudenberg and co-workers [1]. The possible advantageous effects of CDs with pharmaceuticals realized through this invention, and currently used today in drug formulations, include increased stability and decreased volatility of problematic ingredients, masked taste of necessary yet undesirable components, conversion of liquids and oils to easily handled and free-flowing powders, increased solubility, and increased bioavailability [1,2,26,30,27]. Table 1.2 lists examples of commercial pharmaceutical products available throughout the world whose formulation contains CDs to achieve at least one of these aforementioned advantages [28,29,30,31].

Use of CDs in the food industry offers many of the same advantages as those listed above for pharmaceutical applications [1,27,32,38]. One noticeable difference, compared to the pharmaceutical industry, is seen when considering CDs available for use. β-CD is the only CD, native or otherwise, currently recognized by the FDA as GRAS (Generally Regarded As Safe) for use in foods [33]. Other CDs (e.g. α- and γ-CD) have been the subject of investigations conducted by individual companies whose results indicate GRAS compatibility for certain

Table 1.2. CDs in commercial pharmaceutical products.

Cyclodextrin	Drug	Trade Name (Market)
α-CD	Alprostadil (PGE_1)	Prostavastin, Caverject, Edex, Rigidur, Prostandin500 (Europe, Japan, USA)
	Cefotiam hexetil HCl	Pansporin T (Japan)
	OP-1206	Opalmon (Japan)
β-CD	Benexate	Ulgut, Lonmiel (Japan)
	Cephalosporin (ME 1207)	Meiact (Japan, Europe)
	Cetirzine	Cetrizin (Europe)
	Chlordiazepoxide	Transilium (Argentina)
	Dexamethasone	Glymesason (Japan)
	Dextromethorphan	Rynathisol (Europe)
	Dinoprostone (PGE_2)	Prostarmon E (Japan)
	Diphynydramine HCl + chlortheophylline	Stada-Travel (Europe)
	Iodine	Mena-Gargle (Japan)
	Meloxicam	Mobitil (Egypt)
	Nicotine	Nicorette (Europe)
	Nimesulide	Nimedex, Mesulid (Europe)
	Nitroglycerin	Nitropen (Japan)
	Omeprazole	Omebeta (Europe)
	Tiaprofenic acid	Surgamyl (Europe)
	Piroxicam	Brexin, Cicladol, Flogene (Europe, Brazil)
2-Hydroxypropyl-β-CD	Cisapride	Propulsid (Europe)
	Hydrocortisone	Dexocort (Europe)
	Indomethacin	Indocid (Europe)
	Itraconazole	Sporanox (Europe, USA)
	Mitomycin	Mitozytrex, MitoExtra (USA)
Randomly methylated-β-CD	17β-Oestradiol	Aerodiol (Europe)
	Chloramphenicol	Clorocil (Europe)
Sulphobutylether β-CD	Aripiprazole	Abilify (USA)
	Maropitant	Cerenia (USA)
	Voriconazole	Vfend (Europe, USA)
	Ziprasidone mesylate	Geodon, Zeldox (Europe, USA)
2-Hydroxypropyl-γ-CD	Diclofenac sodium	Voltaren (Europe)
	Tc-99 Teoboroxime	Cardiotec (USA)

applications and at particular levels, but FDA affirmation has not followed [34,35]. Even with this limitation, various essential flavor mixtures and pure components have been successfully encapsulated by β-CD to form a stable encapsulated material [1,32,36,37,38], and several commercial products in use around the world utilize this technology in either final product form or in the manufacturing process (Table 1.3, [38]).

The utilization of CDs in a variety of separation techniques is a well known application of the inclusion complex forming ability. Indeed, the molecular discrimination and selectivity resulting from differences in stability constants between various guests and CDs represent the greatest advantage in utilizing CDs in different separation methods. Several extensive reviews detail CDs as chemically bonded or sorbed ligands to chromatographic stationary phases for GC and HPLC, as mobile phase additives in HPLC, and as buffer additives in different electrophoretic techniques [1,9,39,40,41,42,43,44,45,46,47]. One significant application of CDs in separations science focuses on chiral separations. While chromatographic, or electrophoretic, behavior of both enantiomers of a racemic mixture is modified upon complexation with CDs, the chiral environment imposed by CDs offers preferential binding of one enantiomer over the other. Through optimization of separation parameters, this binding discrimination is enough to result in enantioresolution.

The versatility of the CD inclusion complexation phenomenon has been exploited for use in various other chemical processes. These include areas such as reaction catalysis [1,48,49], agrochemical formulations [1,50], malodor entrapment [51], and soil cleanup [52,53,54].

Table 1.3. CDs in commercial food products.

Food Product Type	Trade Name (Market)
Low cholesterol cheese	Natual (France)
Flavored baking sugar	Cyroma-line (Hungary)
Low cholesterol butter	Balade (Belgium)
Low cholesterol eggs	Simply Eggs (USA)
Beer flavor standards	FlavorAktiv Standard Kit (Great Britain)
Chewing gum	Flavono (Japan)
Chocolate	Choco Bar (Japan)
Instant green tea	Poder Tea (Japan)
Dietary fiber drink	Gymet (Japan)
Instant tea drink	Stick Lemon (Japan)

1.1.3.5 Cyclodextrin Ternary Complexes

A complex is deemed "ternary" when two different guests, neither of them being water, are incorporated into the same CD cavity [1,2]. Evidence for the formation of multiple ternary complexes is presented throughout CD literature. Some of the earliest evidence on CD ternary complex formation revealed that organic solvents, such as diethyl ether and acetone, could be included in the CD cavity with other guests [55,56]. The effects of alcohols, both aliphatic and cyclic, on the binding properties of various aromatic guests, such as pyrene, with CDs are among the most studied. The role of alcohols in these complexes tend to increase the binding constant of the guest/CD complex, by either acting as a space regulator to fill the void in the CD cavity resulting from imperfect geometric matching between the principle guest and host [57,58,59,60], or to effectively lengthen the hydrophobic cavity of the host CD through H-bond formation with primary and secondary hydroxyl groups [61]. Different surfactants have also been shown to interact with these aforementioned guests by forming ternary complexes [62,63,64].

With such proof of the ternary complex formation concept mentioned above, applications of ternary CD complexes have been realized. In fact, the formation of ternary complexes is a strategy that has been used to achieve desirable traits not attained in more simple, binary systems. One specific application is in the field of room-temperature phosphorescence measurements, where ternary CD complexes can be used to decrease the phosphor's susceptibility to quenching by molecular oxygen, and to increase the rigidity of the included guest compound, both of which lead to better detection capabilities (i.e. lower detection limits, increased analytical sensitivity) [65,66,67,68]. Upon the formation of ternary complexes, degradation rates of certain guests have been slowed compared to the binary guest/CD complex

[69,70]. Solubility enhancement of guest/CD complexes has also been accomplished by incorporating a third component to form ternary complexes [71,72,73,74], thereby facilitating dissolution of the complex and release of the primary component into solution.

1.2 Sulfur-Containing Flavor and Aroma Constituents

1.2.1 Occurrence and Stability

The advancement of hyphenated gas chromatographic techniques, such as GC-MS and GC-Olfactometry, has expanded the flavor chemist's ability to identify compounds occurring, at times present only at trace levels, in natural materials [75]. Sulfur-containing flavor and aroma compounds are no exception, and the range of applicable characteristic flavors and aromas are dependent upon the actual sulfur functionality. Mercaptans (thiols), sulfides, thioesters, thiophenes, thiazoles, and dithiazines, lend their "notes" in various locations. For example, these compounds are present in sources such as garlic and onions, beef and pork, blackcurrant, coffee, and can possess the following flavor and/or aroma effects: roasted, burnt, green, fruity, tropical, vegetable-like, spicy, herbaceous, cheesy, and buillon-like (Figure 1.3 [75,76,77]).

While mercaptans are generally the most odorous of all aroma chemicals, they tend to be susceptible to oxidation resulting in a mixed product of various sulfides [77]. However, this tendency decreases in the order of primary > secondary > tertiary thiols. In fact, tertiary mercaptans like 4-methoxy-2-methyl-2-butanethiol can be resistant to oxidation upon storage for several years [77]. Monosulfides, while typically less odorous than mercaptans, have the advantage of greater chemical stability. They are not readily oxidized under conditions that

would force mercaptan oxidation. Di- and tri-sulfides, while similarly resistant to oxidation as monosulfides, possess weak S-S bonds that are susceptible to attack by nucleophiles**.** Rearrangement reactions give mixed products, dependent upon the aliphatic makeup present around the sulfide bond in the parent compound. Hydrolysis is the key "problem" reaction of S-alkyl thioesters with regard to their use in applications, while dithiazines display breakdown, but breakdown products were not identified [77].

Figure 1.3. Characteristic "notes" of some naturally occurring sulfur-containing compounds.

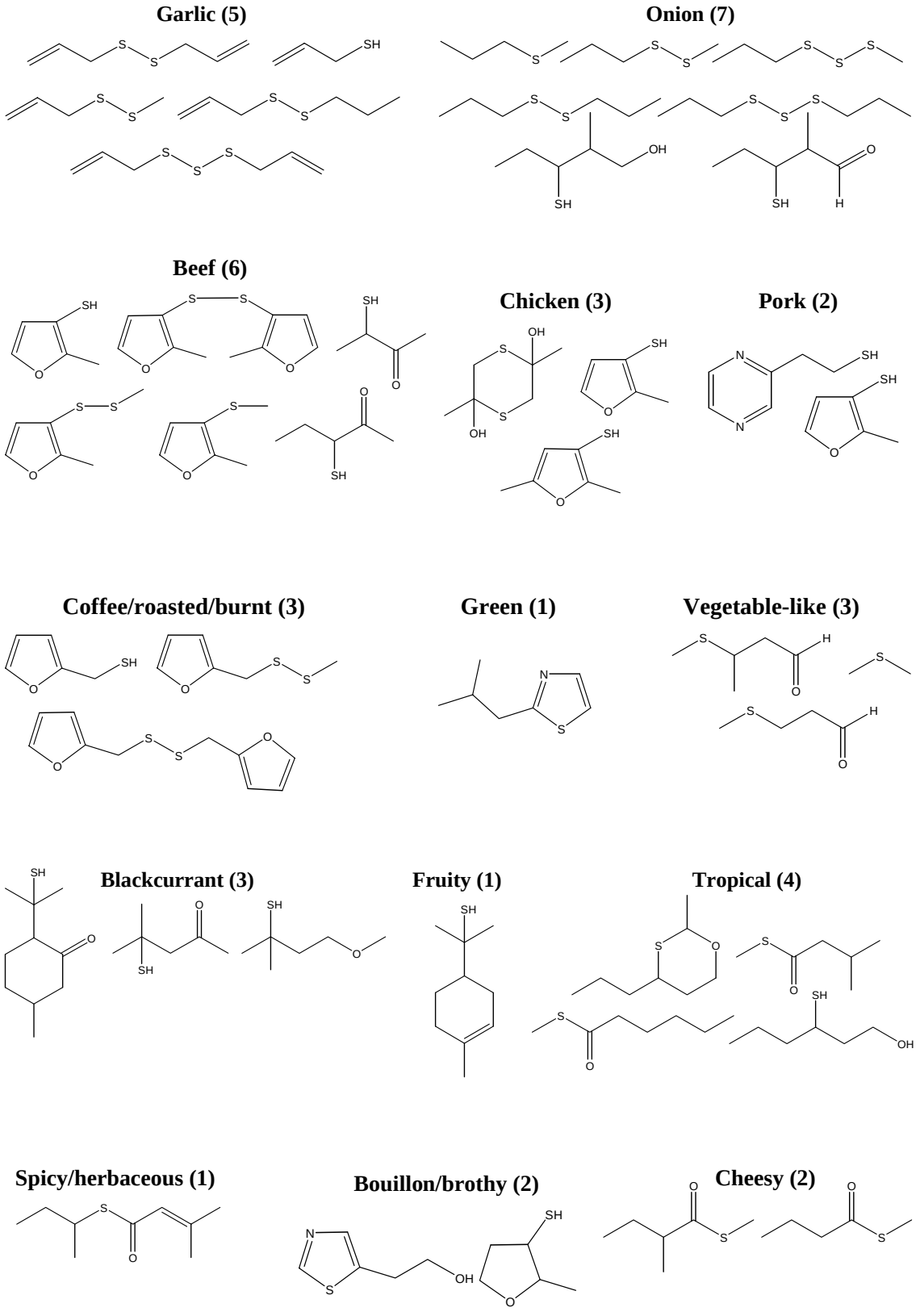

1.2.2 Furanthiols

Furanthiols possess the same attributes previously discussed for aliphatic mercaptans; they generally have the lowest odor thresholds and are subject to oxidation. However, their vulnerability to oxidation can be enhanced by the electron rich furan ring, when the thiol functionality is in conjugation with the π-electron network [77]. This effect is seen when comparing 2-furfurylthiol (FFT) and 2-methyl-3-furanthiol (MFT), where MFT is oxidized more readily because of the aforementioned conjugation effect [77,]. Furthermore, 2,5-dimethyl-3-furanthiol (DMFT) is oxidized even more readily than MFT, as the additional 5-methyl group adds electron density to the furan ring.

The significance in understanding the propensity of oxidation of furanthiols is revealed when considering that members of this family, such as FFT and MFT, are highly important constituents of familiar flavors and aromas [75,76,77]. While present in a variety of natural sources, FFT is the best-known contributor to the "burnt" or "roasted" scent of coffee, and has been determined to be the single most important aroma chemical in studies aimed at reconstituting this flavor. Meanwhile, MFT is naturally present in beef, pork, lamb and chicken. FFT is also present, at lower levels, in these same materials. With this being known, applications requiring "coffee" or "meat-like" flavoring and/or aroma would be well-suited to include these compounds. But, under oxidative conditions, slight differences between the desired and actual essence are possible because of decreased parent compound concentration and slight "off-notes" produced by the corresponding (mono-, di-, tri-) sulfide mixtures.

1.3 Specific Aims and Objectives

1.3.1 Selection of Model Flavor Component and Cyclodextrin

The work presented in this dissertation represents an investigation into the use of CDs as a potential encapsulation platform for a high-impact, character furanthiol. Specifically, 2-furfurylthiol (FFT) was chosen as the model odorant because of its high impact character and its susceptibility to loss through volatilization and oxidation. However, FFT is less prone to oxidation than other furanthiols, leading to greater ease in use as aqueous solutions [77,78,79]. β-CD was chosen to be the primary CD of the investigations because of the requirement that the encapsulation strategy must satisfy FDA approval; β-CD is the only CD, parent or functionalized, that is present on the FDA's GRAS (Generally Regarded As Safe) list for use in foods.

1.3.2 Past Studies on Cyclodextrin Encapulation of FFT

A literature survey reveals only two investigations into the encapsulating abilities of CDs for FFT. The first study was published in 1986 [80], where solid inclusion complexes of FFT with β-CD were prepared, and the retention and anti-oxidant capabilities of the solid complexes were characterized. Results indicated that FFT content in the prepared complex (6.8% w/w) was consistent during 3-week storage at 60^{o}C. Separate tests with storage in an oxygen environment at room temperature revealed much greater anti-oxidant properties of the β-CD/FFT complex, compared to an alternative formulation consisting of FFT simply adsorbed onto a lactose surface.

CD encapsulation of FFT was again reported in 2002 [81]. In this study, the effects of all three parent CDs (α-, β-, and γ-) on the retention of many labile flavor compounds during spray-drying was investigated. Initial retention from spray-drying an aqueous mixture displayed greatest FFT retention in the order of β- > γ- > α-CD, indicating that β-CD was best at preventing the thiol compound's loss during product formulation and drying. However, following a 4-week storage period at 20°C, α-CD was able to retain ~77% of FFT normalized for initial quantity determined immediately after spray-drying, while β- and γ-CD performed much worse with retentions of ~33% and 12%, respectively, under the same storage conditions.

Conflicting results from these past studies serve as motivation to further investigate the ability of β-CD to serve as an appropriate encapsulation platform for furanthiol compounds.

1.3.3 Extension into this Work

As mentioned in Section 1.1.3.2, CD inclusion complexation possesses a dependency on geometric fitting between a proposed guest and the CD cavity, where a better fit between the guest and cavity typically leads to increased complexation efficiency. With β-CD capable of fitting a molecule roughly the size of naphthalene within its hydrophobic cavity, FFT appears too small to form a well-fit inclusion complex.

It might be assumed that a "tighter fit" within the CD cavity would lead to greater realization of the benefits commonly achieved with CD encapsulation in flavoring and pharmaceutical applications (e.g. decreased volatility, protection from environmental hazards). Therefore, a ternary complex approach was theorized as a possible means of circumventing this mismatch in FFT/β-CD cavity size, where the co-inclusion of an auxiliary binding agent might

act a space regulator. In this role, by filling cavity void- space remaining after FFT inclusion, the ternary complex could possibly render the furanthiol less prone to loss through volatilization and oxidation.

The aims and objectives of the research described in this dissertation focus on understanding the capability of using β-cyclodextrin for encapsulating FM. In addition to studying the complexation of FM with β-CD as a simple binary mixture, fatty acids were selected as auxiliary agents for possible ternary complex formation. Included, as part of the research in this dissertation, is an investigation into the affinity of the fatty acids, separately, for β-CD.

1.4 References

[1] J. Szejtli, Cyclodextrin Technology. Kluwer Academic Publishers, Norwell, MA, 1988, and references herein.

[2] J. Szejtli, T. Osa, Comprehensive Supramolecular Chemistry, Vol 3, Cyclodextrins. Permagon, Oxford, 1996, and references herein.

[3] H. Pringsheim, Chemistry of the Saccharides. McGraw-Hill, New York, NY, 1932, p. 281.

[4] D. French, A.O. Pulley, J.A. Effenberger, M.A. Rougvie, M. Abdullah, Arch. Biochem. Biophys. 111 (1965) 153.

[5] H. Ueda, T. Endo, in H. Dodziuk (Editor), Cyclodextrins and Their Complexes. Wiley-VCH, Weinheim, Germany, 2006, p. 370.

[6] T. Nakagawa, K. Ueno, M. Kashiwa, J. Watanabe, Tetrahedron Lett. 35 (1994) 1921.

[7] J. Szejtli, Chem. Rev. 98 (1998) 1743.

[8] Q.X. Guo, S.H. Luo, Y.C. Liu, J. Inclusion Phenom. Mol. Recognit. Chem. 30 (1998) 173.

[9] E. Schneiderman, A.M. Stalcup, J. Chromatogr., B. 745 (2000) 83.

[10] R. Bergeron, R. Rowan, Bioorg. Chem. 5 (1976) 425.

[11] L.A. Godinez, S. Patel, C.M. Criss, A.E. Kaifer, J. Phys. Chem. 99 (1995) 17449.

[12] X. Shen, M. Belletete, G. Durocher, Langmuir 13 (1997) 5830.

[13] G. Castronuovo, V. Elia, M. Niccoli, F. Velleca, J. Inclusion Phenom. Macrocyclic Chem. 44 (2002) 229.

[14] B.W. Muller, E. Albers, J. Pharm. Sci. 80 (1991) 599.

[15] E. Junquera, E. Aicart, J. Phys. Chem. B 101 (1997) 7163.

[16] C.H. Evans, M. Partyka, J.V. Stam, J. Inclusion Phenom. Macrocyclic Chem. 38 (2000) 381.

[17] T. Furuta, H. Yoshii, A. Miyamoto, A. Yasunishi, H. Hirano, Supramol. Chem. 1 (1993) 321.

[18] J. Szejtli, Pure Appl. Chem. 76 (2004) 1825.

[19] Y. Inoue, Annu. Rep. NMR Spectrosc. 27 (2003) 59.

[20] H. Dodziuk, Cyclodextrins and Their Complexes. Wiley-VCH, Weinheim, Germany, 2006.

[21] L. Zhou, R. Thompson, R.A. Reamer, C. Miller, C. Welch, D.K. Ellison, J.M. Wyvratt, J. Chromatogr. A 987 (2003) 409.

[22] M.M. Meier, M.T.B. Luiz, B. Szpoganicz, V. Soldi, Thermochim. Acta 375 (2001) 153.

[23] Y. Dotsika, Y.L. Loukas, J. Am. Soc. Mass Spectrom. 14 (2003) 1123.

[24] S.R. Gratz, A.M. Stalcup. Anal. Chem. 70 (1998) 5166.

[25] K.L. Larsen, W. Zimmermann, J. Chromatogr. A 836 (1999) 3.

[26] K. Uekama, F. Hirayama, H. Arima, in H. Dodziuk (Editor), Cyclodextrins and Their Complexes. Wiley-VCH, Weinheim, Germany, 2006, p. 381.

[27] J.S. Pagington, Chem. Br., 23 (1987) 455.

[28] T. Loftsson, D. Duchene, Int. J. Pharm. 329 (2007) 1.

[29] M.E. Brewster, T. Loftsson, Adv. Drug Delivery Rev. 59 (2007) 645.

[30] M.E. Davis, M.E. Brewster, Nat. Rev. Drug Discovery 3 (2004) 1023.

[31] F. Giordano, C. Novak, J.R. Moyano, Thermochim. Acta 380 (2001) 123.

[32] J. Szejtli, L. Szente, E. Banky-Elod, Acta Chimica Academiae Scientiarum Hungaricae, 101 (1979) 27.

[33] http://www.cfsan.fda.gov/~dms/eafus.html

[34] http://www.cfsan.fda.gov/~rdb/opa-g155.html

[35] http://www.cfsan.fda.gov/~rdb/opa-g046.html

[36] H. Hashimoto, in H. Dodziuk (Editor), Cyclodextrins and Their Complexes. Wiley-VCH, Weinheim, Germany, 2006, p. 452.

[37] G.A. Reineccius, S.J. Risch, Perfumer & Flavorist 11 (1986) 1.

[38] L. Szente, J. Szejtli, Trends Food Sci. Technol. 15 (2004) 137.

[39] E. Smolkova-Keulemansova, J. Chromatogr. 251 (1982) 17.

[40] T. Cserhati, E. Forgacs, Cyclodextrins in Chromatography. The Royal Society of Chemistry, Cambridge, UK, 2003.

[41] H. Issaq, J. Liq. Chromatogr. 11 (1988) 2131.

[42] C. Mitchell, D. Armstrong, Chiral Separations; Methods and Protocols 243 (2004) 61.

[43] H. Aboul-Enein, I. Ali, Chiral Separations by Liquid Chromatography and Related Technologies. Marcell Dekker, New York, NY, 2003.

[44] B. Chankvetadze, in H. Dodziuk (Editor), Cyclodextrins and Their Complexes. Wiley-VCH, Weinheim, Germany, 2006, p. 119.

[45] S. Fanali, F. Kilar, J. Capillary Electrophor. 1 (1994) 72.

[46] E. Diacu, L. Mutihac, A. Barbu, Rev. Roum. Chim. 50 (2005) 165.

[47] C.E. Evans, A.M. Stalcup, Chirality 15 (2003) 709.

[48] M. Komiyama, E. Monflier, in H. Dodziuk (Editor), Cyclodextrins and Thier Complexes. Wiley-VCH, Weinheim, Germany, 2006, p. 93.

[49] L. Barr, P.G. Dumanski, C.J. Easton, J.B. Harper, K. Lee, S.F. Lincoln, A.G. Meyer, J.S. Simpson, J. Inclusion Phenom. Macrocyclic Chem. 50 (2004) 19.

[50] E. Morillo, in H. Dodziuk (Editor), Cyclodextrins and Their Complexes. Wiley-VCH, Weinheim, Germany, 2006, p. 459.

[51] T. Trinh, J.P. Cappel, P.A. Geis, M.L. McCarty, D Pilosof, S.S. Zwerdling, H.B. Tordil, U.S. Patent No. 5593670 (1997).

[52] X. Wang, M.L. Brusseau, Environ. Sci. Technol. 29 (1995) 2632.

[53] M.E. Lindsey, G. Xu, J. Lu, M.A. Tarr, Sci. Total Environ. 307 (2003) 215.

[54] G. Yardin, S. Chiron, Chemosphere 62 (2006) 1395.

[55] K. Takeo, T. Kuge, Agric. Biol. Chem. 36 (1972) 2615.

[56] J. Szetjli, Z. Budai, Acta Chim. Acad. Sci. Hung., 94 (1977) 383.

[57] A. Nakajima, Bull. Chem. Soc. Jpn. 57 (1984) 1143.

[58] S. Hamai, T. Ikeda, A. Nakamura, H. Ikeda, A. Ueno, F. Toda, J. Am. Chem. Soc. 114 (1992) 6012.

[59] J. Zung, A. Munoz de la Pena, T.T. Ndou, I.M. Warner, J. Phys. Chem. 94 (1991) 6701.

[60] A. Munoz de la Pena, T.T. Ndou, J.B. Zung, K.L. Greene, D.H. Live, I.M. Warner, J. Am. Chem. Soc. 113 (1991) 1572.

[61] G. Patonay, K. Fowler, A. Shapira, G. Nelson, I.M. Warner, J. Inclusion Phenom. 5 (1987) 717.

[62] H.E. Edwards, J.K. Thomas, Carbohydr. Res.65 (1978) 173.

[63] E.A. Cummings, T.T. Ndou, V.K. Smith, I.M. Warner, Appl. Spectrosc. 47 (1993) 2129.

[64] S. Hashimoto, J.K. Thomas, J. Am. Chem. Soc. 107 (1985) 4655.

[65] H.R. Zhang, S.Y. Guo, L. Li, M.Y. Cai, Anal. Chim. Acta 463 (2002) 135.

[66] V.B. Nazarov, V.G. Avakyan, E.I. Bagrii, T.G. Vershinnikova, M.V. Alfimov, Russ. Chem. Bull. International Edition 54 (2005) 2752.

[67] B. Tang, X. Wang, G. Wang, Y. Wang, Z. Chen, Analyst (Cambridge, U.K.) 130 (2005) 1038.

[68] J.J. Wu, Y. Wang, J.B. Chao, L.N. Wang, W.J. Jin, J. Phys. Chem. B 108 (2004) 8915.

[69] M. Valero, C. Carrillo, J. Photochem. Photobiol., B 74 (2004) 151.

[70] C. Garnero, M. Longhi, J. Pharm. Biomed. Anal. 45 (2007) 536.

[71] P. Mura, M.T. Faucci, A. Manderioli, G. Bramanti, J. Inclusion Phenom. Macrocyclic Chem. 39 (2001) 131.

[72] M. M. Al Omari, M.B. Zughul, J.E.D. Davies, A.A. Badwan, J. Inclusion Phenom. Macrocyclic Chem. 54 (2006) 159.

[73] M.D. Veiga, F. Ahsan, Eur. J. Pharm. Sci. 9 (2000) 291.

[74] P. Mura, G.P. Bettinetti, M. Cirri, F. Maestrelli, M. Sorrenti, L. Catenacci, Eur. J. Pharm. Biopharm. 59 (2005) 99.

[75] D. Rowe, Perfumer & Flavorist 25 (2000) 1.

[76] D. Rowe, Perfumer & Flavorist 27 (2002) 24.

[77] D. Rowe, K. Auty, S. Jameson, P. Setchell, G. Carter-Jones, Perfumer & Flavorist 29 (2004) 2.

[78] T. Hofmann, P. Schieberle, W. Grosch, J. Agric. Food Chem. 44 (1996) 251.

[79] I. Blank, E.C. Pascual, S. Devaud, L.B. Fay, R.H. Stadler, C. Yeretzian, B.A. Goodman, J. Agric. Food Chem. 50 (2002) 2356.

[80] L. Szente, J. Szejtli, J. Food Sci. 51 (1986) 1024.

[81] T.A. Reineccius, G.A. Reineccius, T.L. Peppard, J. Food Sci. 67 (2002) 3271.

Chapter 2

Investigating 2-Furfurylthiol Binding with β-Cyclodextrin Using NMR Spectroscopy

2.1 Introduction

This chapter details solution state equilibria studies undertaken to quantify the strength of binding between 2-furfurylthiol (FFT) and β-cyclodextrin (β-CD). The encapsulation of FFT by β-CD has been studied previously in the solid state [1,2], but no work exists for studying this system in solution. While these previous studies assume FFT insertion into the β-CD cavity as the interaction responsible for complexation, this work aims to provide evidence for the cavity inclusion of FFT and give information on the structural orientation of the formed complex in solution. Information gleaned through these studies can offer quantitative information on the strength of binding between FFT and β-CD, and could be useful later when the complex formation is studied in the preparation of solid complexes (Chapter 4).

Several comprehensive reviews have been published on the use of nuclear magnetic resonance (NMR) spectroscopy in studying cyclodextrin inclusion [3,4,5]. Similar to other instrumental techniques used in the study of complexation equilibria, NMR can estimate a binding constant quantitatively through the use of well established mathematical treatments of the experimental data [5,6]; this will be discussed in Section 2.2. Furthermore, structural elucidation is an advantage of using NMR to study complex formation, where both 1-D and 2-D

NMR can offer information on the structural orientation of the interacting guest and host in the formed inclusion complex.

2.2 NMR Theory

2.2.1 Basic Principles

In NMR spectroscopy, the application of an external magnetic field to a sample containing spin-active nuclei results in non-identical energy states for the magnetic spin quantum numbers of opposite signs [5,7]. That is to say, the magnetic spin quantum number +1/2 and -1/2 are present at different energy levels, a phenomenon that is not observed in the absence of said applied field. A collection of identical, non-interacting nuclei absorbs electromagnetic radiation at an appropriate frequency applied perpendicular to the external magnetic field, resulting in transitioning of the atomic nuclei between the different spin energy levels; this represents the observable signal output of NMR spectroscopy. The utility of NMR spectroscopy for analytical purposes arises from the fact that chemically different types of a given nucleus (i.e. all ^{1}H nuclei in a sample) are subject to differing degrees of electron shielding. This phenomenon results from the circulation of electrons about a nucleus, and the extent of electron shielding varies the energy gap between nuclei energy states under the application of an external magnetic field. The variation in band gap results in the chemically different nuclei requiring varying frequencies of precession between the different spin energy states (Equation 2.1) [5].

$$\nu = \frac{\gamma B_o(1-\sigma)}{2\pi} \qquad (2.1)$$

In the previous equation, B_o, γ, ν, and σ represent the applied magnetic field strength, nuclei magnetogyric ratio constant, nuclei resonance frequency, and the shielding constant for a specific nucleus, respectively.

An NMR spectrum displays signal intensities for each chemically different nucleus of the sample at their respective chemical shifts, a parameter used to normalize NMR data. The relationship between chemical shift, δ, and absorption frequency, is defined by Equation 2.2 [7],

$$\delta = \frac{(\nu_s - \nu_r)}{\nu_r} * 10^6 = (\sigma_r - \sigma_s) * 10^6 \qquad (2.2)$$

where ν_s and σ_s, and ν_r and σ_r, represent the resonance frequency and shielding constant for the sample nucleus and a reference nucleus, respectively. As a function of the above equation, δ, is reported in units of parts per million (ppm).

2.2.2 Study of CD Inclusion Complexes

2.2.2.1 Structural Elucidation

Figure 2.1 displays the schematic structure and proton assignments of β-CD and FFT molecules. In the field of cyclodextrin complexation chemistry, the inclusion interaction is commonly probed by monitoring the chemical shifts of the CD-H3 and CD-H5 protons because of their respective orientations toward the interior of the CD cavity [8,9]. Upon inclusion of an aromatic guest compound into the cavity, these protons typically experience an upfield change in

their chemical shifts; this is because of an increase in electron shielding provided by the aromatic ring current of the guest molecule [10]. Chemical shifts for other CD protons located on the exterior surface of the CD molecule, CD-H1, CD-H2 and CD-H4, remain relatively unperturbed compared to the probed protons [8], thereby providing more evidence that the complexation truly is an inclusion phenomenon.

The 2-D NOESY (Nuclear Overhauser Effect correlation SpectrscopY) and its related ROESY (Rotating frame nuclear Overhauser Effect correlation SpectrscopY) NMR techniques are commonly used when studying CD inclusion complexes [11,12,13,14] because of their ability to showcase dipolar cross-relaxation between spins in a close spatial proximity such [15]. The application of this phenomenon to CD inclusion complex chemistry can yield information to be used for structural elucidation of the inclusion complex, highlighting structural orientation of the guest molecule within the cavity [3].

Figure 2.1. Structural schematic and proton assignments of a) β-CD and b) FFT.

a)

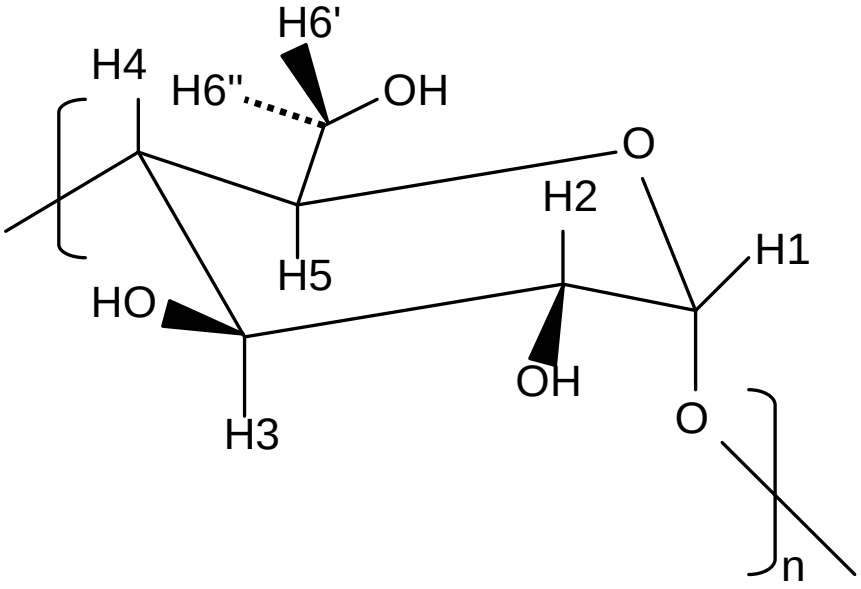

b)

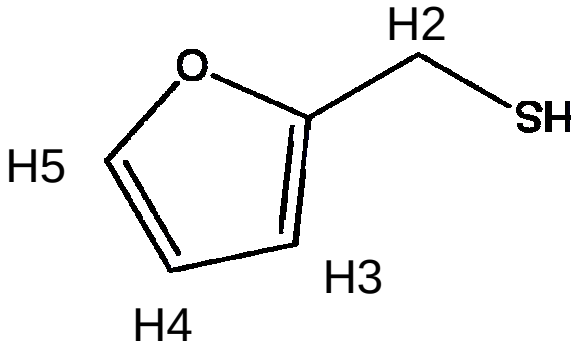

2.2.2.2 Quantitative Estimation of Binding Constants

As discussed in Section 2.2.1, the resonance frequency of a specific nucleus is dependent upon its chemical environment; complex formation can be probed based on this principle if the differences in absorption frequencies are sufficient [16]. Complexation dynamics affect the observable NMR spectrum in terms of exchange rate between the free versus complexed states. Binding systems undergoing slow exchange, meaning the nucleus in the free and complexed states will precess many times at their respective resonancy frequencies, ν_f and ν_c, before exchanging states, result in separate signals observed in the NMR spectrum with areas respective of the molar fractions of the free and bound species. Decreasing the complexed and free states' occupational lifetimes leads to the observation of a single signal, present as the weighted average between the two absorption frequencies. This averaging of absorption frequencies, and henceforth observable chemical shifts, typically occurs when lifetimes of the free and complexed states are 10^{-3} seconds or shorter [5,17], and can be described by Equation (2.3) [16]:

$$\delta_{obs} = \chi_f \delta_f + \chi_c \delta_c \tag{2.3}$$

In the above equation, δ_{obs} is the observed chemical shift of a nucleus in the presence of a binding partner, and δ_f and δ_c are the chemical shifts of the same nucleus in the fully free and complexed states, respectively, each weighted by its fractional occupancy (χ).

By using mass balance equations and the equilibrium expression for a 1:1 association, and by referencing all chemical shifts back to that of the free species, Equation (2.4) can be derived.

$$\delta_{obs} - \delta_f = \frac{(\delta_C - \delta_f) K_{1:1}[L]}{1 + K_{1:1}[L]} \tag{2.4}$$

The binding constant, *K*, and the theoretical value for the chemical shift of the nucleus in the fully complexed state, $\Delta\delta_C$, (as $\delta_C - \delta_f$) can be calculated through nonlinear regression analysis. The experimental dataset consists of observed changes in the analyte's proton chemical shift, $\Delta\delta_{obs}$ (as $\delta_{obs} - \delta_f$), at several different ligand concentrations *[L]* added to the analyte solution. The use of Equation (2.4) requires that the free ligand concentration at equilibrium, *[L]*, can be assumed equal to total ligand concentration added to analyte solution. Typically, this requirement is met if the minimum ligand concentration utilized is at least ten times the analyte concentration.

If, however, this assumption cannot be made because of experimental design, a different derivation of Equation (2.3) must be used [18]. Strict mass balance is followed to arrive at an expression for the concentration of the complex (A-L) formed dependent upon concentrations of the analyte (A_o) and ligand (L_o) species and their respective ratio ($R=L_o/A_o$) (Equation 2.5).

$$[\text{A-L}] = A_o \left[\left(1 + R + \frac{1}{KA_o} \right) - \sqrt{\left(1 + R + \frac{1}{KA_o} \right)^2 - 4R} \right] \tag{2.5}$$

Substitution of Equation (2.5) into Equation (2.3) yields a new binding isotherm equation (Equation 2.6),

$$\Delta\delta_{obs} = \frac{\Delta\delta_C}{2}\left[\left(1 + R + \frac{1}{KA_o}\right) - \sqrt{\left(1 + R + \frac{1}{KA_o}\right)^2 - 4R}\right] \quad (2.6)$$

and by using a constant analyte concentration, A_o, nonlinear regression can be applied to determine a value for K and $\Delta\delta_C$ for a series of $\Delta\delta_{obs}$ exhibited at various R values of the samples analyzed by NMR.

2.3 Experimental

β-cyclodextrin was purchased from Fluka (Buchs, Switzerland), while 2-furfurylthiol was purchased from Sigma-Aldrich (St. Louis, MO, USA). Deuterium oxide (D_2O) was purchased from Cambridge Isotope Laboratories, Inc. (Andover, MA, USA). Stock solutions of β-CD and FFT were prepared in D_2O, and working solutions analyzed by NMR were prepared by mixing appropriate volumes of the stock solutions to give desired concentrations. Preliminary studies were done with 1.0 x 10^{-3} M solutions of FFT and β-CD. For the first set of titration experiments, β-CD working concentration was held constant at 2.0 x 10^{-4} M, while FFT varied from 0-8.6 x 10^{-3} M. In a second set of titration experiments, FFT concentration was held constant at 9.4 x 10^{-4} M, and β-CD varied from 0-1.0 x 10^{-2} M. One dimensional ^{1}H-NMR spectra were recorded on a Bruker Avance 400 MHz spectrometer at 25^{o}C, and the HDO signal was used as an internal chemical shift reference . Nonlinear regression analysis of the titration experimental datasets to calculate binding constants was performed using Origin 7.0 (OriginLab Corp., Northampton, MA, USA).

Two dimensional ^{1}H-NMR experiments (NOESY and ROESY) were conducted on a Bruker DMX 500 MHz spectrometer. The sample solution consisted of 1mM each FFT and β-CD in D_2O.

2.4 Results and Discussion

2.4.1 Inclusion Complex Structural Elucidation

Figure 2.2 displays NMR spectra and signal assignments for 1mM FFT and 1mM β-CD, separately and in an equimolar mixture. Because only slight chemical shift variations were observed between the free and equimolar mixtures, NMR titrations were conducted to collect chemical shift data over a larger range of FFT:β-CD molar ratios.

Figure 2.2. ^{1}H NMR spectra of 1mM a) β-CD, b) FFT, and c) 1:1 mixture, in D_2O. Peak notations are defined in Figure 2.1.

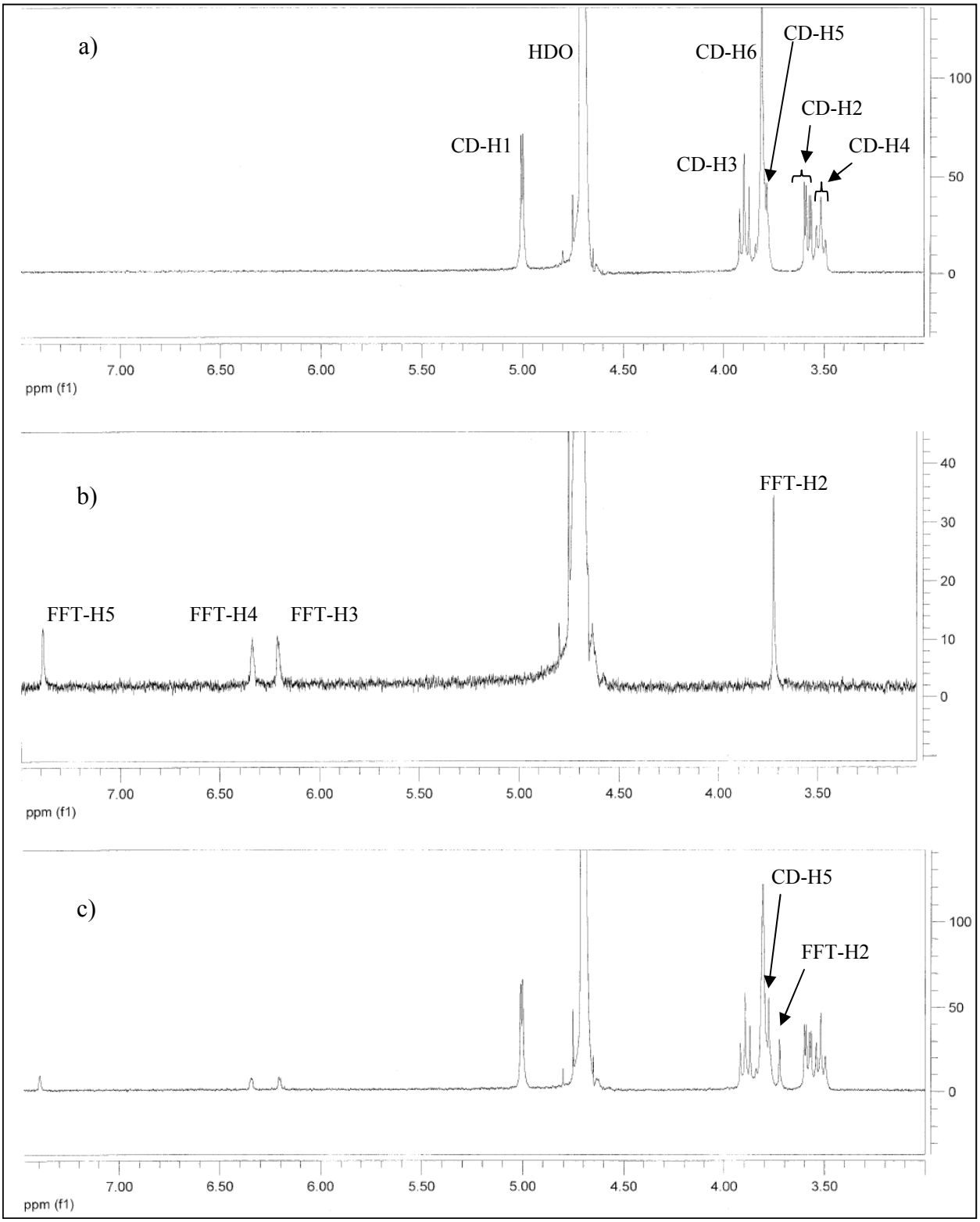

2.4.1.1 β-CD Titration with FFT

Table 2.1 lists the observed changes in chemical shifts, $\Delta\delta_{obs}$ for the β-CD protons for a variety of binary solutions containing different FFT concentrations. The cavity protons, CD-H3 and CD-H5, show chemical shift deviation in the upfield direction upon addition of FFT. This is consistent with previous works presented in the literature for the inclusion of aromatic guest compounds within the CD cavity [4,8,9]. As stated earlier, electron shielding of the cavity protons results from the ring current of the aromatic moiety in the presence of the external magnetic field [10]. While the magnitudes of the cavity proton chemical shift are not as great as those for other aromatic guest/CD systems [8,9,19], it cannot be denied that the relative shifts in this study do show the cavity protons are more affected by FFT addition than the others. Furthermore, the ΔδCD-H5 is likely underestimated because observation at the higher FFT concentrations is compromised because of overlap with the methylene protons of the guest. Additionally, the CD-H6 protons displayed a similar upfield change in their chemical shift, similar in magnitude to the CD-H3 protons.

Comparison of the induced chemical shifts of the CD protons can been used to define guest compound orientation within the cavity [4]. In this manner, the respective CD-H3 and CD-H5 shifts can be qualitatively interpreted in terms of the spatial relationship between these protons and the guest's aromatic moiety. Furthermore, it has been suggested that the ratio of the ΔδH5/ΔδH3 values has been used as a measure of the depth of guest penetration into the cavity [10]; this characterization inherently places the penetration point of reference from the wider, secondary hydroxyl rim of the cavity. Induced chemical shift of the CD-H6 protons is often drawn upon to conclude insertion of the guest species from the narrower primary hydroxyl rim of

CD [20]. Inferring the arrangement of the FFT/β-CD inclusion complex in this titration experiment using this reasoning alone is not possible. While the most significant induced chemical shifts are observed with CD-H5, thereby leading to the conclusion that the aromatic ring of FFT must occupy cavity space nearer the primary hydroxyl rim, any further supposition on exact inclusion orientation is ambiguous because of similar induced shifts for CD-H3 and CD-H6.

Table 2.1. Induced chemical shift changes of the β-CD protons at various FFT concentrations, referenced back to the chemical shift of β-CD alone in solution. Experimental conditions described in text. A negative value indicates an upfield change in the NMR spectrum.

FFT_o, M	ΔδH1, ppm	ΔδH2, ppm	**ΔδH3, ppm**	ΔδH4, ppm	**ΔδH5, ppm**	**ΔδH6, ppm**
0	0	0	**0**	0	**0**	**0**
1.91×10^{-3}	-0.003	0.001	**-0.009**	0.00	**-0.024**	**-0.011**
3.81×10^{-3}	-0.007	-0.002	**-0.017**	-0.003	**-0.036***	**-0.017**
5.24×10^{-3}	-0.009	-0.003	**-0.020**	-0.004	**-0.029***	**-0.019**
7.15×10^{-3}	-0.008	-0.001	**-0.022**	-0.001	**-0.038***	**-0.020**
8.58×10^{-3}	-0.010	-0.003	**-0.026**	-0.003	**-***	**-0.020**

2.4.1.2 FFT Titration with β-CD

In addition to monitoring the β-CD protons, guest molecule proton chemical shifts can be observed to further support inclusion and offer insight on structural orientation of the guest with respect to the host cavity [19]. Table 2.2 displays the calculated observed changes in chemical shifts for the FFT protons for a series of binary solutions of constant FFT concentration titrated with increasing concentrations of β-CD. Two of the three FFT aromatic protons (FFT-H4 and FFT-H5) experience a downfield shift in their observed signal upon the addition of β-CD. This is consistent with trends observed for other aromatic guest species included by cyclodextrins [19,20,21,22]; a hydrophobic medium effect has been offered for this induced downfield shift [23]. These results further validate the assumption that the observed chemical shifts of the CD cavity protons discussed in Section 2.4.1.1 are due to aromatic ring inclusion in the CD cavity.

Observed chemical shift variations for the FFT protons can possibly help reduce the structural ambiguity offered by CD titration results. In combination with the results discussed for the CD protons, the FFT-H4 and H-5 protons should be located nearer to CD-H5 in the cavity upon inclusion complexation. By defining this as our point of reference, situation of the aromatic ring with the $–CH_2$-SH substituent toward the secondary hydroxyl (wider) rim would place FFT-H3 still in the cavity, near CD-H3, and would presumably induce a downfield shift in its resonance as well. The upfield induced shift for FFT-H3 (Table 2.2) does not support this presumption, and FFT orientation in the cavity in this manner is not indicated. Going back to our point of reference where FFT-H4/H5 are situated near CD-H5, the possibility of $–CH_2$-SH orientation toward the primary hydroxyl rim would place FFT-H3 near the primary hydroxyl (narrower) cavity opening. This would effectively place it in a chemical environment different

than that experienced by the other aromatic protons, thus likely resulting in differences in field shift directions for the FFT protons. This inclusion orientation is given further support by the evidence that the observed induced shifts of CD-H6 in the upfield (electron shielded) direction in CD titration experiments.

Table 2.2. Induced chemical shift changes of the FFT protons at various β-CD/FFT concentration ratios, referenced back to the chemical shift of FFT alone in solution. Experimental conditions described in text. A positive value indicates a downfield change in the NMR spectrum.

CD_o/FFT_o	ΔδH2, ppm	ΔδH3, ppm	ΔδH4, ppm	ΔδH5, ppm
0	0	0	0	0
1.26	0.005	-0.001	0.010	0.012
2.08	0.005	-0.003	0.010	0.015
5.25	0.009	-0.0075	0.022	0.032
8.06	0.006	-0.0165	0.024	0.036
10.5	0.010	-0.016	0.031	0.045

2.4.1.3 2-D NMR Results

Preliminary 2-D NMR experiments were performed for possible confirmation of the proposed structure of the inclusion complex offered in the previous sections. Figure 2.3 diplays the NOESY and ROESY spectra for a solution containing 1mM each of FFT and β-CD. The observed cross-peaks are the same in both spectra, and represent spatial proximity of CD-H1 with CD-H2, CD-H4, and the CD-H5/H6 group. No correlation signals were observed between FFT and CD protons.

The lack of FFT/β-CD cross peaks in the 2-D spectra could be a manifestation of a poor geometrical fitting between the guest and host cavity (See Chapter 1 Section 1.2.3.2 and Table 1.1). Under the assumption of a poor guest/host size match, the resulting inclusion complex would likely be weakly bound in solution. Based upon the theory discussed in Section 2.2.2.1 for a quantitative model of NMR binding, both FFT and β-CD would likely remain in their respective uncomplexed forms, thereby limiting the $\Delta\delta$ value that would be observed. It is therefore assumed that the tendency of FFT and β-CD to remain uncomplexed because of weak binding is the reason behind the relatively small induced chemical shift values. This could also lead to the lack of guest/cavity correlation peaks in the 2-D spectra, especially considering that a 1:1 (FFT:β-CD) molar ratio was used for the 2-D experiments; as noted in Tables 2.1 and 2.2 relatively large $\Delta\delta$ values are not observable without using one binding partner in much greater excess than the other.

Figure 2.3. a) NOESY and b) ROESY spectra acquired for a 1 mM solution each of FFT and β-CD in D_20. Peaks labeled according to Figure 2.1. --- indicates cross-peak identification.

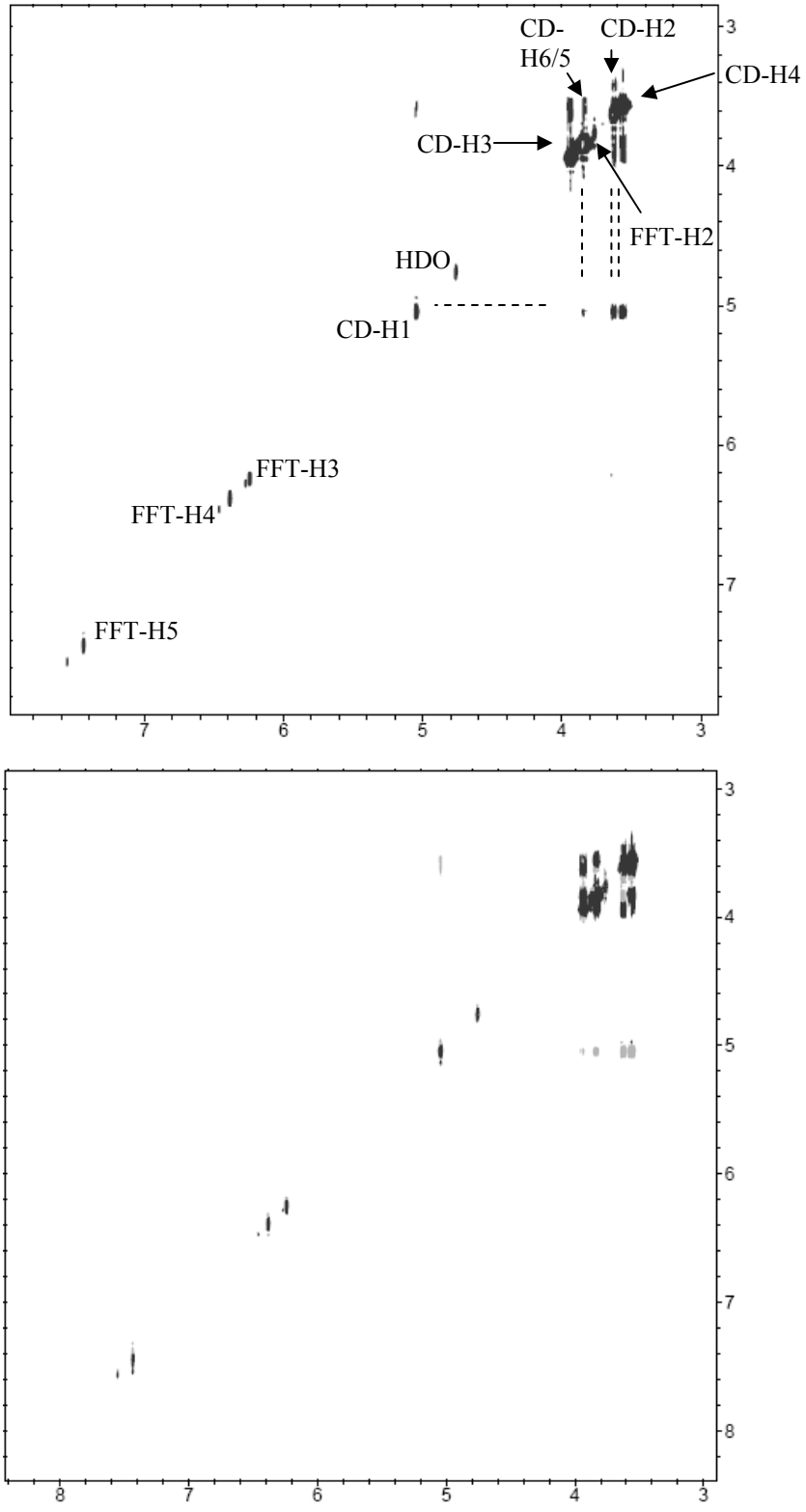

2.4.2 Calculating a Binding Constant for FFT/β-CD Inclusion

A binding constant for the association of FFT with β-CD can be estimated by using the chemical shift variation data presented in Tables 2.1 and 2.2 in conjunction with Equations (2.4) and (2.6). Determination of a binding constant related to the β-CD cavity inclusion of FFT requires the use of signal variations that are suggestive of complex formation. The assigned protons for this study that meet this requirement are CD-H3, CD-H5, FFT-H4 and FFT-H5, based upon past reports in the literature describing the induced chemical shift trends for other aromatic/CD inclusion complexes [4,8,9,19,20,21,22].

Equation (2.4) can be used for the experiments with constant β-CD concentration and increasing FFT concentrations in binary mixtures. However, because of interference between the CD-H5 and FFT-H2 signals at the higher FFT concentrations used, interpretation of the chemical shift for CD-H5 could not be done unambiguously. Therefore, only observed chemical shift data of the CD-H3 proton can be used. Figure 2.4 displays this experimental dataset in conjunction with the best-fit line of nonlinear regression. For experiments with solutions containing constant FFT concentration and varying β-CD concentrations, Equation (2.6) is used to calculate the binding parameters. Figures 2.5 and 2.6 display the FFT experimental dataset along with the best-fit line of nonlinear regression. The calculated results of the regressions are displayed in Table 2.3.

Figure 2.4. ■ Experimental binding isotherm generated from data of Table 2.1. --- Best fit curve of nonlinear regression analysis according to Equation (2.4).

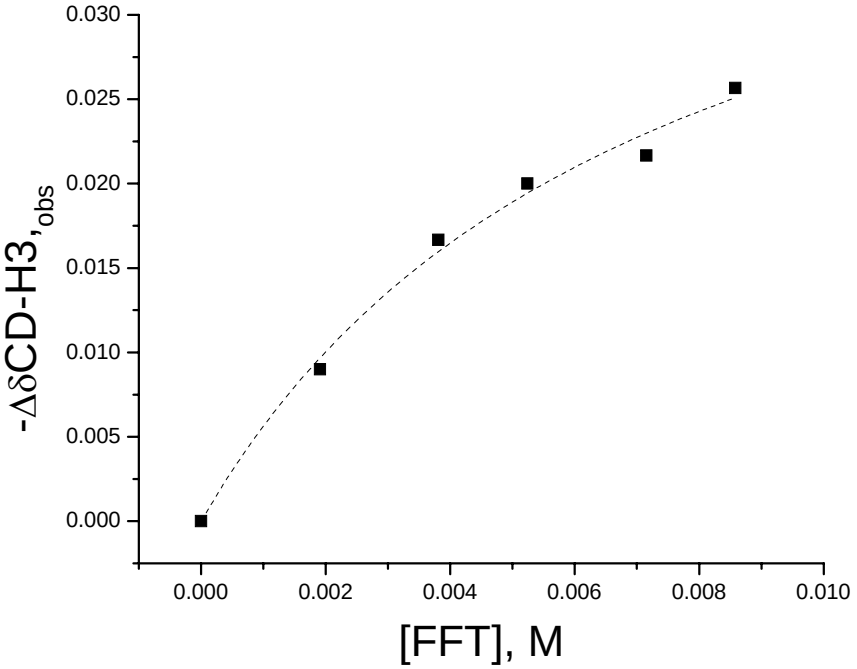

Figure 2.5. ■ Experimental binding isotherm generated from data of Table 2.2. --- Best fit curve of nonlinear regression analysis according to Equation (2.6).

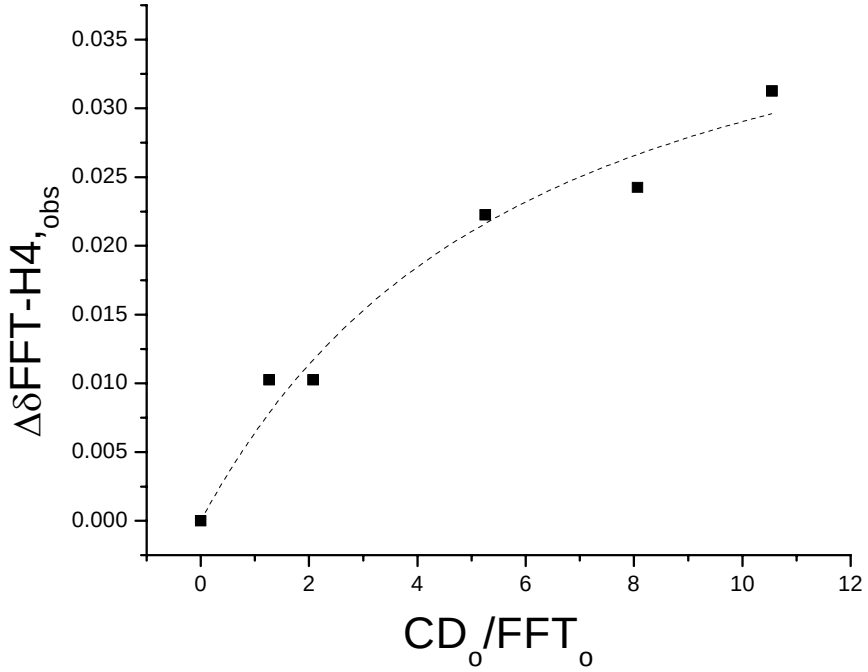

Figure 2.6. ■ Experimental binding isotherm generated from data of Table 2.2 --- Best fit curve of nonlinear regression analysis according to Equation (2.6).

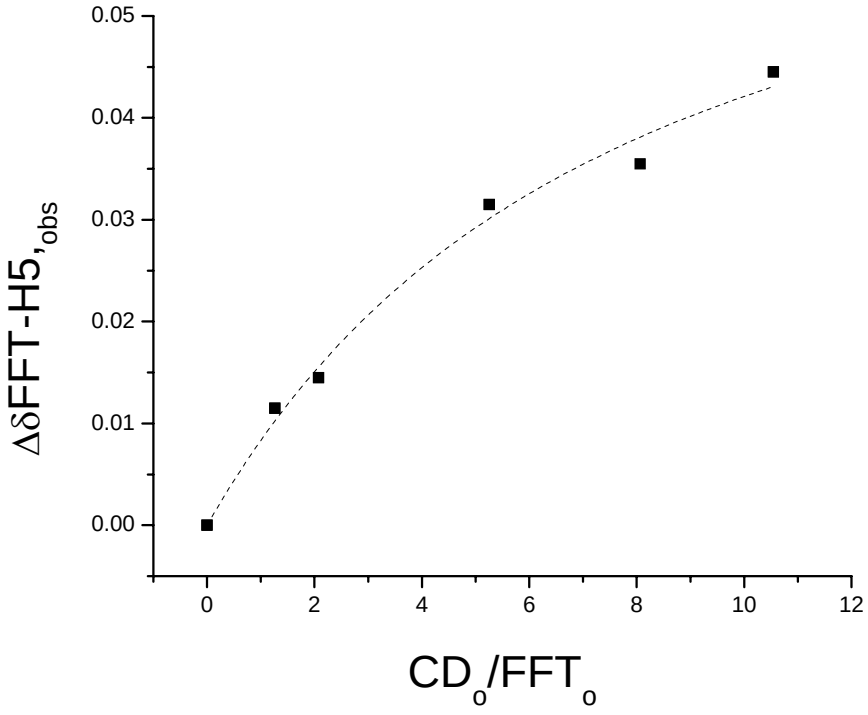

Table 2.3. Calculated binding constants (and standard error) from nonlinear regression analysis of chemical shift data for selected protons.

Proton	**K (± standard error)**	**$\Delta\delta_c$**	**R^2**
CD-H3	140. (32.9)	0.0461 (0.00593)	0.992
FFT-H4	204 (86.1)	0.0451 (0.00819)	0.975
FFT-H5	155 (43.9)	0.0727 (0.00997)	0.991

The calculated binding constants presented in Table 2.3 are consistent taking into regard the standard error of the estimate, independent of the proton dataset used (100-200 M^{-1}). This could be used to further validate the proposed inclusion complex structure (Section 2.4.1.1 and 2.4.1.2) that assumes these portions of the guest/host molecules are indeed those that are involved in complex formation, regardless of the lacking evidence in 2-D spectra. To test this premise, a binding constant was calculated for FFT-H3 induced chemical shifts listed in Table 2.2; the calculated binding constant in this case (1.48 ± 13.9 M^{-1}; isotherm not shown) is much different than those presented in Table 2.3, suggesting its non-involvement in cavity inclusion and adding further evidence to the proposed inclusion complex orientation of Section 2.4.1.2.

2.5 Summary

NMR titration experiments have aided in gathering evidence for the interaction between FFT and β-CD to be that of inclusion complex formation. This is the first reported work of studying this system in solution, and provides supporting evidence that CDs may be a useful technology for the encapsulation of FFT. This work also adds credence to previous investigations of the FFT/β-CD interaction in the solid state, where FFT cavity inclusion was assumed [1,2].

On the basis of complementary information obtained in 1-D titrations, the proposed inclusion complex structure is based upon the aromatic moiety of FFT within the β-CD cavity near the primary (narrow) cavity opening. With this as the frame of reference, NMR titration data obtained for FFT suggest the thiol functionality to orient toward the primary opening.

Estimation of a binding constant using induced chemical shift data for the protons associated with the involved moieties of inclusion also supports this proposed structure.

The preliminary 2-D results perhaps do not indicate guest/host inclusion because of the relatively weak binding between FFT and β-CD. Conversations with Dr. Pearl Tsang at the University of Cincinnati, with whom this preliminary work was performed, revealed the prospect of varying experimental conditions to hopefully improve the possibility of observing the guest/host interaction. These include decreased temperature to slow the kinetics of inclusion, thus increasing the likelihood observing a signal due to the spatial proximity of the guest/host compounds, or the use of more complicated 2-D NMR pulse sequences to study the interaction.

2.6 References

[1] L. Szente, J. Szejtli, J. Food Sci. 51 (1986) 1024.

[2] T.A. Reineccius, G.A. Reineccius, T.L. Peppard, J. Food Sci. 67 (2002) 3271.

[3] H-J Schneider, F. Hacket, V. Rüdiger, Chem. Rev. 98 (1998) 1755.

[4] Y. Inoue, in G.A. Webb (Editor), Annu. Rep. NMR Spectrosc. 27 (2003) 59.

[5] A. Ejchart, W. Kozminski, in H. Dodziuk (Editor), Cyclodextrins and Their Complexes. Wiley, Weinheim, Germany, 2006, p. 231.

[6] L. Fielding, Tetrahedron 56 (2000) 6151.

[7] D.A. Skoog, F.J. Holler, T.A. Nieman (Editors), Principles of Instrumental Analysis, 5th ed. Harcourt Brace & Company, Philadelphia, PA, 1998.

[8] P.V. Demarco, A.L. Thakkar, Chem. Commun. (1970) 2.

[9] A.L. Thakkar, P.V. Demarco, J. Pharm. Sci. 60 (1971) 652.

[10] M.V. Rekharsky, R.N. Goldberg, F.P. Schwarz, Y.B. Tewari, P.D. Ross, Y. Yamashoji, Y. Inoue, J. Am. Chem. Soc. 117 (1995) 8830.

[11] A. Guerrero-MaRtinez, G. Gonzalez-Gaitano, E.M Murciano, G. Tardajos, J. Inclusion Phenom. Macrocyclic Chem. 57 (2007) 251.

[12] T. Carofiglio, R. Fornasier, L. Jicsinszky, G. Saielli, U. Tonellato, R. Vetta, Eur. J. Org. Chem. (2002) 1191.

[13] S.M. Ali, S.K. Upadhyay, Magn. Reson. Chem. 46 (2008) 676.

[14] S. Sagiraju, B.S. Jursic, Carbohydr. Res. 343 (2008) 1180.

[15] D. Neuhaus, M.P. Williams, The Nuclear Overhauser Effect in Structural and Conformational Analysis, 2nd Ed. Wiley-VCH, New York, NY, 2000.

[16] K.A. Connors, Binding Constants: The Measurement of Molecular Complex Stability. Wiley-Interscience, New York, NY, 1987, p. 189.

[17] J. Sandstrom, Dynamic NMR Spectroscopy, Academic Press, London, 1982.

[18] K. Hirose, J. Inclusion Phenom. Macrocyclic Chem. 39 (2001) 193.

[19] H. Choi, A.M. Knevel, C. Chang, Pharm. Res. 9 (1992) 690.

[20] L.M.A. Pinto, L.F. Fraceto, M.H.A. Santana, T.A. Pertinhez, S.O. Junior, E. de Paula, J. Pharm. Biomed. Anal. 39 (2005) 956.

[21] H. Jiang, H. Sun, S. Zhang, R. Hua, Y. Xu, S. Jin, H. Gong, L. Li, J. Inclusion Phenom. Macrocyclic Chem. 58 (2007) 133.

[22] S.M. Ali, S.K. Upadhyay, A. Maheshwari, J. Inclusion Phenom. Macrocyclic Chem. 59 (2007) 351.

[23] M.E. Amato, K.B.Lipkowitz, G.M.Lombardo, G.C.Pappalardo, Magn. Reson. Chem. 36 (1998) 693.

Chapter 3

Affinity Capillary Electrophoresis and Isothermal Titration Calorimetry for the Determination of Fatty Acid Binding with β-Cyclodextrin

3.1 Introduction

For the purposes of this work outlined in the Chapter 1, relating the strength and stoichiometry of binding of β-cyclodextrin (β-CD) with fatty acid (FA) as a function of chain length and double bond presence might provide useful information when the ternary complex approach (2-furfurylthiol/FA/β-CD) is investigated. A survey of the literature reveals a wide variety of analytical techniques have been used to characterize the interactions between different fatty acids and CDs. These include: gravimetric [1,2], UV-Vis and NMR spectroscopic [3,4,5,6,7], conductimetric [8], volumetric [9,10] and calorimetric [2,11] studies. Commonly, the inclusion complexes are defined by binding stoichiometry and binding constants (K), with each technique adopting similar binding equations that generally differ only because of differences in the physical property measured during the course of the experiment. While the binding constant determined by each method is usually consistent, a discrepancy is apparent in the stoichiometry of these systems. Some reports provide data assuming a 1:1 binding stoichiometry [3,5,6,7,8,10], but in some studies [4,9,10] values are given for the step-wise association of multiple β-CD molecules onto a given fatty acid molecule, while still others [1,2,8,12] infer the onset of higher stoichiometry with increasing number of carbons (N_C) in the alkyl chain of the acid without providing binding constant values. Table 3.1 lists a range of

values calculated for the binding constant, assuming differing stoichiometries of interaction, sampled from References [3,4,5,6,7,8,9,10].

The goal of this experimental work was to investigate the capability of capillary electrophoresis (CE) and isothermal titration calorimetry (ITC) for studying several fatty acid/β-CD complexes. There are multiple reports in the literature on different guest/CD binding systems as studied by CE [13,14,15,16,17]. The advantages of using CE to study such interactions include requiring small amounts of sample, generally short analysis times and the wide range of binding pairs and experimental approaches that can be utilized [18,19].

Several guest/CD interactions have been characterized using ITC [11,20,21], including some with ITC in conjunction with CE [22,23,24]. One of the most important features of ITC lies in its ability to simultaneously determine binding stoichiometry, binding constant and reaction enthalpy. Indeed, ITC is the only technique that can establish all of these binding parameters from a single experiment. Other advantages include the measurement of a heat signal, a nearly universal property of binding reactions, and favorable signal-to-noise ratio that is necessary when using very dilute solutions of strongly interacting systems with large binding constants [25].

To the best of our knowledge, this work represents the first report of a CE investigation of binding between fatty acids and CDs to determine binding stoichiometry and binding constant. Further, it should be noted that while ITC has been used to study shorter chain fatty acids with CDs [11], this is the first ITC report of complexes formed between longer chain fatty acids and β-CD. As will be shown, CE and ITC provide consistent and complementary information on these interacting systems.

Table 3.1. Sample of binding constants (K) reported in literature [3-10] for differing stoichiometries of interaction (n) between some fatty acids and β-CD.

Fatty Acid	**Overall n (FA:β-CD)**	$K_{1:1}$	$K_{1:2}$
Octanoate	1:1	$(4.6\text{-}6.6) \times 10^2$	-
	1:2	5.7×10^2	27
Decanoate	1:1	$(0.7\text{-}5.1) \times 10^3$	-
	1:2	$(4.1\text{-}4.8) \times 10^3$	55-81
Dodecanoate	1:1	$(0.2\text{-}2.8) \times 10^4$	-
	1:2	2.8×10^4	2.5×10^2

3.2 Theory

3.2.1 Capillary Electrophoresis

Analyte mobility under the influence of an electric field, μ_{ep}, is described by the following fundamental equation of CE,

$$\mu_{ep} = \frac{l * L}{V} * \left(\frac{1}{t} - \frac{1}{t_{eof}} \right) \tag{3.1}$$

where l is the capillary length in centimeters from injection inlet to detection window, L is the capillary total length, V is applied voltages in volts, t is the migration time in seconds of the analyte of interest and t_{eof} is the migration time corresponding to an electroosmotic flow marker. Affinity capillary electrophoresis (ACE), one of the CE methods to determine binding constants, involves monitoring the change in mobility an analyte experiences with the addition of a binding ligand to the CE run buffer [18,26]. Calculation of a binding constant based upon this experimental observation is described through the following set of Equations (3.2-3.7) [13,15,16,17,18,19,26,27,28,29,30,31,32,33].

For a 1:1 binding system in the presence of a binding ligand in the BGE, an analyte's mobility is defined by the Equation (3.2):

$$\mu_{ep}^{L} = \chi_f * \mu_{ep,f} + \chi_c * \mu_{ep,c} \tag{3.2}$$

where μ_{ep}^{L} represents the observed analyte mobility in the presence of ligand in the BGE, $\mu_{ep,f}$ and $\mu_{ep,c}$ the mobilities of the free and fully complexed analyte, respectively, and χ_f and χ_c the mole fractions of the analyte in these forms. Further increase in the concentration of a binding ligand in the BGE results in further deviation of μ_{ep}^{L} from $\mu_{ep,f}$ (Figure 3.1).

The presence of a binding ligand in the BGE can impart changes in analyte mobility independent of the binding interaction; the most common of these arises from variable solution viscosities, η, dependent on the concentration of binding ligand in BGE [13,15,17,18,33]. A viscosity correction factor, ν, can be calculated for each BGE composition by injecting an analyte onto the capillary and monitoring the time required to push the analyte plug past the detection window using a constant pressure. The correction factor, ν, is directly related to the measured time required for a given ligand concentration in the BGE, t, relative to the measured time required for zero ligand concentration in the BGE, t^o, as defined by Equation (3.3):

$$\nu = \left(\frac{\eta}{\eta^o} \right) = \left(\frac{t}{t^o} \right) \tag{3.3}$$

The product of ν and μ_{ep}^{L} at each BGE composition replaces the y-term of Equation 3.2 to give a viscosity-corrected value for the observed electrophoretic mobility at a given ligand concentration.

Figure 3.1. Electropherograms of 2-octenoic acid (50 μM) with different concentrations of β-CD in the BGE: (a) 0 mM, (b) 1.0 mM and (c) 2.0 mM. Experimental conditions described in text.

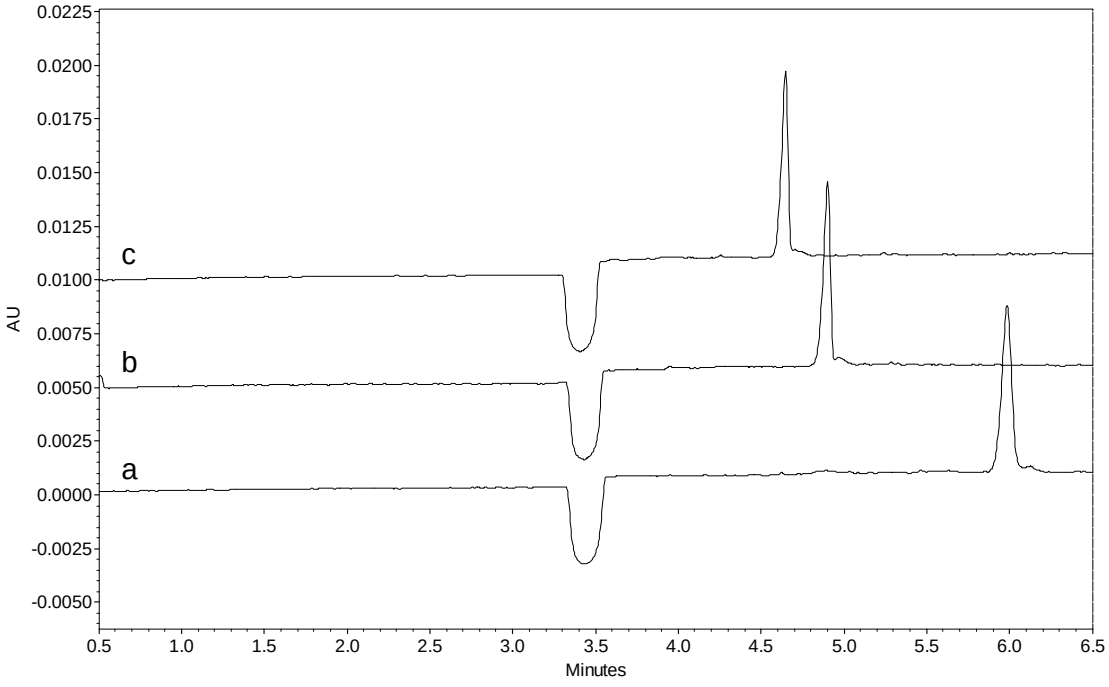

Through the use of the 1:1 equilibrium expression and mass balance equations, and by referencing all mobilities back to that of the free analyte, $\mu_{ep,f}$, Equation (3.2) can be rewritten as Equation 3.4.

$$\nu\mu_{ep}^{L} - \mu_{ep,f} = \frac{(\mu_{ep,FA\text{-}CD} - \mu_{ep,f})K_{1:1}[L]}{1 + K_{1:1}[L]} \tag{3.4}$$

A binding constant, *K*, and the mobility of the fully bound complex, $\mu_{ep,FA\text{-}CD}$, can be estimated using a constant sample concentration while varying the concentration of binding ligand in the BGE, *[L]*, and fitting the data to Equation (3.4) using nonlinear regression analysis.

Three different linear transformations of Equation (3.4) are commonly reported to calculate the binding parameters. These are often termed the Double reciprocal (3.5), Y-reciprocal (3.6) and X-reciprocal (3.7) equations, and are shown below.

$$\frac{1}{(\nu\mu_{ep}^{L} - \mu_{ep,f})} = \frac{1}{(\mu_{ep,FA\text{-}CD})K_{1:1}[L]} + \frac{1}{(\mu_{ep,FA\text{-}CD} - \mu_{ep,f})} \tag{3.5}$$

$$\frac{[L]}{(\nu\mu_{ep}^{L} - \mu_{ep,f})} = \frac{1}{(\mu_{ep,FA\text{-}CD} - \mu_{ep,f})}[L] + \frac{1}{(\mu_{ep,FA\text{-}CD} - \mu_{ep,f})K_{1:1}} \tag{3.6}$$

$$\frac{(\nu\mu_{ep}^{L} - \mu_{ep,f})}{[L]} = -K_{1:1}(\nu\mu_{ep}^{L} - \mu_{ep,f}) + K_{1:1}(\mu_{ep,FA\text{-}CD} - \mu_{ep,f}) \tag{3.7}$$

While both nonlinear and linear regression have been used to calculate the binding parameters, nonlinear regression is noted to be better because the experimental error associated with the parameters is distorted upon transformation into the linear forms [18,31]. However, as will be explained later, the use of the linear transformation equations (3.5) and (3.7) to display data has some unique advantages over the nonlinear form of the binding equation.

3.2.2 Isothermal Titration Calorimetry

The use of ITC to study binding systems relies upon the change in heat experienced during stepwise injections of one of the binding constituents (Ligand) into the other (Macromolecule). This heat change is related to the molar ratio of the binding partners (L/M); thereby, the resulting isotherm can then be used to determine binding stoichiometry, binding constant and reaction enthalpy. The following set of equations show how these binding parameters are calculated [25]. For brevity, only the expressions for 1:1 binding will be shown, with β-CD defined as the ligand and fatty acid as macromolecule.

Equation (3.8) can be derived through mass balance and stability constant equations. It relates the binding constant, initial and equilibrium concentrations of β-cyclodextrin (c_{CD} and *[CD]*, respectively) and of fatty acid (c_{FA} and *[FA]*) and of the complex (*[FA-CD]*).

$$[\text{FA-CD}]^2 + [\text{FA-CD}] * \left(-c_{\text{CD}} - c_{\text{FA}} - \frac{1}{\text{K}} \right) + c_{\text{CD}} c_{\text{FA}} = 0 \qquad (3.8)$$

Upon addition of β-CD to the fatty acid solution, the change in *[FA-CD]* can be expressed in terms of the heat change, *dQ*:

$$dQ = d[\text{FA-CD}] * \Delta H * V_o \tag{3.9}$$

in which ΔH is the reaction enthalpy and V_0 is the initial cell volume. Substitution of (3.8) into (3.9) yields Equation (3.10):

$$\frac{1}{V_0} * \frac{dQ}{dc_{CD}} = \Delta H * \left(\frac{1}{2} + \frac{1 - \frac{1+r}{2} - \frac{c_{CD}}{2c_{FA}}}{\sqrt{\frac{c_{CD}^{\,2}}{c_{FA}^{\,2}} - 2 * \frac{c_{CD}}{c_{FA}} * (1-r) + (1+r)^2}} \right) \tag{3.10}$$

where

$$r = \frac{1}{Kc_{FA}} \tag{3.11}$$

An iterative nonlinear least squares regression analysis is used to fit experimental data to Equation (3.10), resulting in calculated values of K and ΔH. Similar models may be derived for different binding modes and stoichiometries.

3.3 Experimental

3.3.1 Materials

Sodium octanoate ($C_8O_2^-Na^+$), sodium dodecanoate ($C_{12}O_2^-Na^+$), and β-cyclodextrin (β-CD) were obtained from Fluka (Buchs, Switzerland). Sodium decanoate ($C_{10}O_2^-Na^+$), 2-octenoic acid ($C_6{=}C_2O_2^-H^+$), and monobasic sodium phosphate monohydrate were purchased from Sigma (St. Louis, MO, USA). The 9-decenoic acid ($C{=}C_9O_2^-H^+$) was purchased from Oakwood Products (West Columbia, SC, USA). Dibasic sodium phosphate and sodium hydroxide were acquired from Fisher Scientific (Fair Lawn, NJ, USA). All reagents were used without further purification.

3.3.2 Instrumentation and Methods

3.3.2.1 Capillary Electrophoresis

All CE experiments were performed using a Beckman P/ACE MDQ automated capillary electrophoresis system (Beckman Coulter, Inc., Fullerton, CA, USA) equipped with a UV detector and interfaced to a personal computer. Fused-silica capillary (75-μm i.d., 40.2 cm total length, 30.0 cm injection inlet to detection window) was purchased from Polymicro Technologies (Phoenix, AZ, USA).

The electrophoresis background electrolyte (BGE) consisted of a 25 mM phosphate buffer, pH 7, containing different concentrations of β-CD (0-12.0 mM). These BGE solutions

were degassed and filtered through a 0.2-μm filter (Nalge Nunc International Corp., Rochester, NY, USA) before use. Stock solutions (1.0 mM) of the fatty acids were prepared by dissolving an appropriate amount in 2.5 mM phosphate buffer. Working samples of these fatty acids were then prepared by dilution of the stock by 2.5 mM phosphate buffer to a final concentration of 50 μM. Prior to use, the capillary was rinsed with 0.1N NaOH in a 50% methanol/water solution at 40 psi for three minutes, followed by distilled, deionized water at 40 psi for three minutes, and finally phosphate buffer at 40 psi for five minutes. The capillary was then allowed to equilibrate overnight. Between injections, the same rinsing procedure was used, with the exception that the β-CD/phosphate BGE was the final rinse. Fatty acid samples were injected hydrodynamically at 0.5 psi for five seconds. Electrophoresis was performed under normal polarity with an applied voltage of 10 kV, and direct UV detection of the fatty acids was achieved at 200 nm. All experiments were performed in triplicate at 25^{o}C. Viscosity correction factor measurements were conducted by injecting 2-octenoic acid onto the capillary at each BGE composition and monitoring the time required to push the sample plug past the detection window using a constant pressure of 5 psi.

Nonlinear regression analysis of the datasets was performed using Origin 7.0 (OriginLab Corp., Northampton, MA, USA) with user-defined fitting functions. Linear transformations of the binding isotherms were constructed using Microsoft Excel.

3.3.2.2 Isothermal Titration Calorimetry

ITC experiments were conducted using a MicroCal Omega ITC microcalorimeter following standard instrumental procedure [34] (MicroCal, Northampton, MA, USA). All

titrations were performed with a 250-μL injection syringe and a stir rate of 400-500 rpm. Experiments were performed at 25°C ± 1°C, with each titration consisting of 16-29 steps, 10-30 μL each, at 240-300 second intervals. A 25 mM phosphate buffer, pH 7, was used to prepare the β-CD (~12.0 mM) and fatty acid (~1.0 mM) solutions used for calorimetric experiments. Each binding system was studied in duplicate.

Analogous to the changes in solution viscosity in ACE leading to inaccurate estimation of binding parameters, trials involving β-CD injections into buffer and buffer injections in FA were performed to account for potential heats of dilution, which can contribute to instrumental response apart from the binding interaction. These trials did not produce measurable heat signals.

Stoichiometries, binding constants and reaction enthalpies were determined by nonlinear regression analysis of the binding isotherms using built-in binding models within MicroCal Origin 2.9 software package (MicroCal, Northampton, MA, USA).

3.4 Results and Discussion

The results obtained for this study are separated in the following sections according to the two different methods utilized, ACE and ITC. With each method, steps taken to construct accurate binding isotherms are first discussed, followed by the presentation of the calculated binding data. Finally, a comparison of the results obtained with ACE and ITC is offered to determine a binding stoichiometry, and trends in the calculated binding constants are discussed.

3.4.1 Affinity Capillary Electrophoresis

3.4.1.1 Constructing the binding isotherm

Prior to the use of Equation (3.4) to determine binding constants by ACE, constraints on the β-CD additive concentrations used to collect electrophoretic mobility data of the fatty acids must be recognized. The criteria for selecting the range of additive concentrations used to investigate binding between the selected fatty acids and β-CD is based upon the following three considerations:

- **Higher order interactions**
- **[β-CD]>>[FA] encountered in capillary**
- **Error minimization**

Strategies adopted from the literature were used to assess the adequacy of the initially employed β-CD concentration range (0-12 mM) in fulfilling these three conditions.

Consideration 1: Higher order interactions. Investigating the possibility of higher stoichiometric interactions using ACE requires a wide additive range in the BGE, as interactions which might not contribute to the mobility shift at low additive concentrations could play a significant role at the higher concentrations [17]. Bowser and Chen were the first to show that the linear transformations of ACE data (e.g. X-reciprocal) could be used to investigate interacting, higher order binding. To examine the presence of 1:2 (FA:CD) along with 1:1 interactions in this study, the β-CD concentration range was extended to near its solubility limit (~1.9% w/w in H_20) , and the data was plotted according to the X-reciprocal equation. Curvature at the higher additive concentrations (toward the minimum of the y-axis) is indicative of higher

order binding. The X-reciprocal plots can be seen in Figure 3.2**;** the plots for $C_8O_2^-$, $C_6{=}C_2O_2^-$, $C_{10}O_2^-$ and $C{=}C_9O_2^-$ display continued linearity at the highest CD concentrations, thus supporting 1:1 binding, and Equation (3.4) can be used to estimate the binding parameters.

The $C_{12}O_2^-$ X-reciprocal plot is shown again in Figure 3.3 for closer inspection of data transformation. The slight curvature seen in the plot for $C_{12}O_2^-$ near the y-axis minimum could be indicative of higher order binding taking place (1:1 plus 1:2; FA:CD). If higher order binding in the $C_{12}O_2^-$/β-CD system is occurring, then another expression is needed for interacting 1:2 (analyte:ligand) binding, which can be derived based on the following reaction equation:

$$\mathrm{FA} + 2\mathrm{CD} \xleftrightarrow{K_{1:1}} \mathrm{FA\text{-}CD} + \mathrm{CD} \xleftrightarrow{K_{1:2}} \mathrm{FA\text{-}CD_2} \tag{3.12}$$

Mobility data obtained at different β-CD concentrations in the background electrolyte can be fit to Equation 3.13 using nonlinear regression [17]:

$$(\nu\mu_{ep}{}^{L} - \mu_{ep,f}) = \frac{(\mu_{ep,FA\text{-}CD} - \mu_{ep,f})K_{1:1}[CD] + (\mu_{ep,FA\text{-}CD2} - \mu_{ep,f})K_{1:1}K_{1:2}[CD]^2}{1 + K_{1:1}[CD] + K_{1:1}K_{1:2}[CD]^2} \tag{3.13}$$

with the new parameters, $\mu_{ep,FA\text{-}CD2}$ and $K_{1:2}$, representing the mobility of the 1:2 ($FA:CD_2$) complex and the association constant of this complex, respectively.

Figure 3.2. X-reciprocal plots to investigate higher order binding.

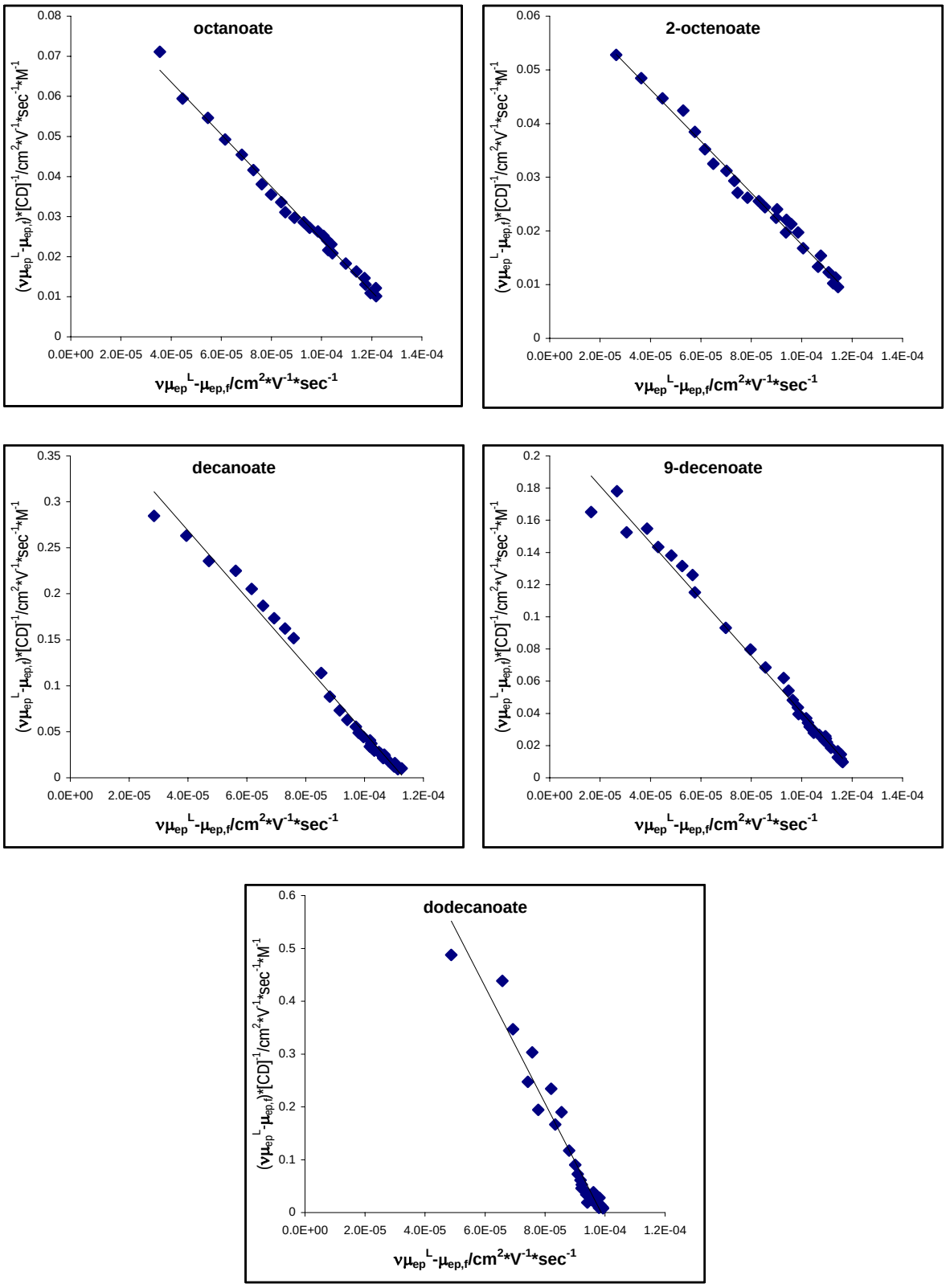

Figure 3.3. Redisplayed X-reciprocal plot for $C_{12}O_2$-/β-CD binding.

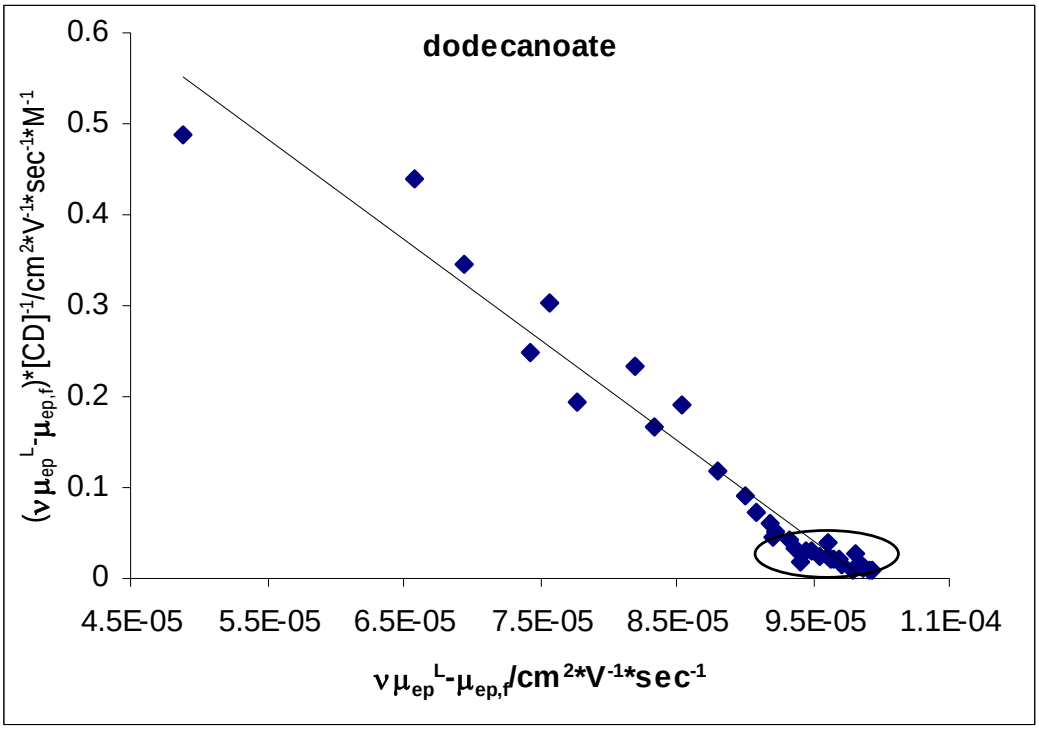

Consideration 2: [β-CD]>>[FA] encountered in capillary. The amount of injected analyte (fatty acid) must be small compared to β-CD encountered in the capillary [13,14,27,32,35]. In Equation (3.4), the term *[L]* represents the free β-CD concentration present in the background electrolyte after binding equilibrium is established. To simplify the equilibrium expression, this term is approximated by the total β-CD concentration that is added to the background electrolyte before the experiment is performed. This substitution is justified if the concentration of β-CD used is greater than the concentration of injected FA and/or if the binding is not particularly strong. This concentration requirement must also be met to avoid saturation of β-CD present in the BGE that can occur if the analyte concentration is too high or if the system under study experiences tight binding.

This issue of sample overloading is most critical at the lowest additive concentrations; at greater concentrations, sufficient additive is present in the background electrolyte to shift the analyte mobility to the correct value. In the presence of β-CD saturation due to sample overloading, the plots of the linear transformations show deviations in linearity at the lowest β-CD concentrations employed in the BGE [27]. Figure 3.4 displays the double-reciprocal plot, and the X-reciprocal plots are shown a second time in Figure 3.5 respectively, for the five fatty acid analytes of this study. Positive deviations in linearity on the y-axis at the x-axis maxima (low β-CD concentrations) of the double-reciprocal plots, coupled with negative deviations in linearity on the y-axis at the x-axis minima (low β-CD concentrations) of the X-reciprocal plots, indicate concentrations of β-CD at which sample overloading is present. These points are seen for $C_{10}O_2^-$, $C{=}C_9O_2^-$ and $C_{12}O_2^-$ corresponding to a β-CD concentration of 0.10 mM. These points are noted in their respective plots and the corresponding data points of the nonlinear binding isotherms are removed before calculation of the binding parameters. Elimination of

these points from the transformation plots, with subsequent linear regression, revealed that two more points in the $C_{10}O_2^-$ plots were characteristic of sample overloading at 0.15 mM and 0.20 mM β-CD in the BGE. However, sample overloading was not apparent at the same concentrations of β-CD in the BGE for $C_{12}O_2^-$, despite its greater binding. Hence, data collected at 0.15 mM and 0.20 mM β-CD were not eliminated from the datasets as it was unclear if sample overloading was occurring.

Figure 3.4. Double reciprocal plots used to investigate sample overloading (ligand saturation) present at lower β-CD concentrations employed in the BGE. Circled points are excluded from the dataset before binding parameters are calculated.

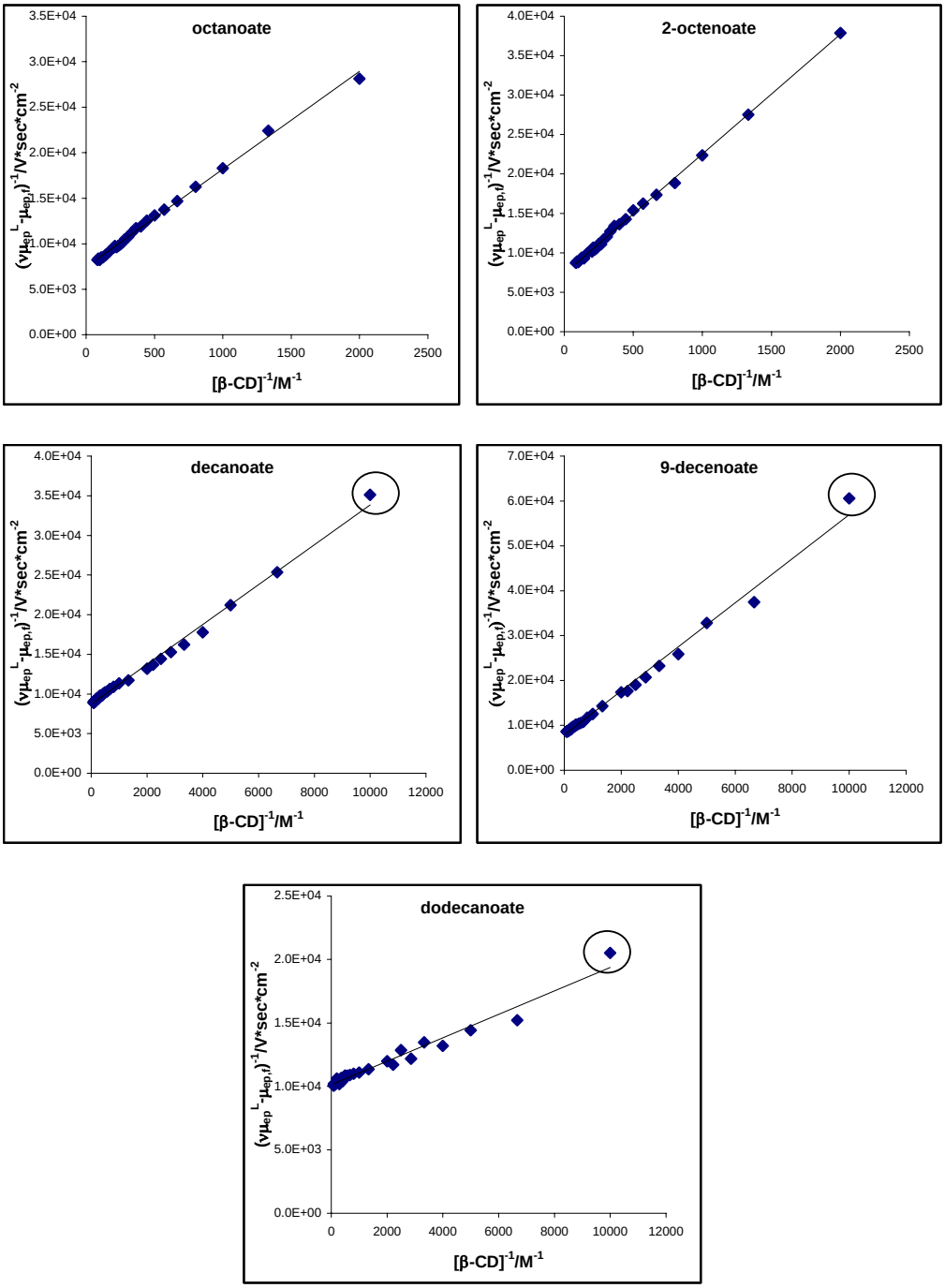

Figure 3.5. X-reciprocal plots used to investigate sample overloading (ligand saturation) at the lower β-CD concentrations employed in the BGE. Circled points are excluded from the dataset before binding parameters are calculated.

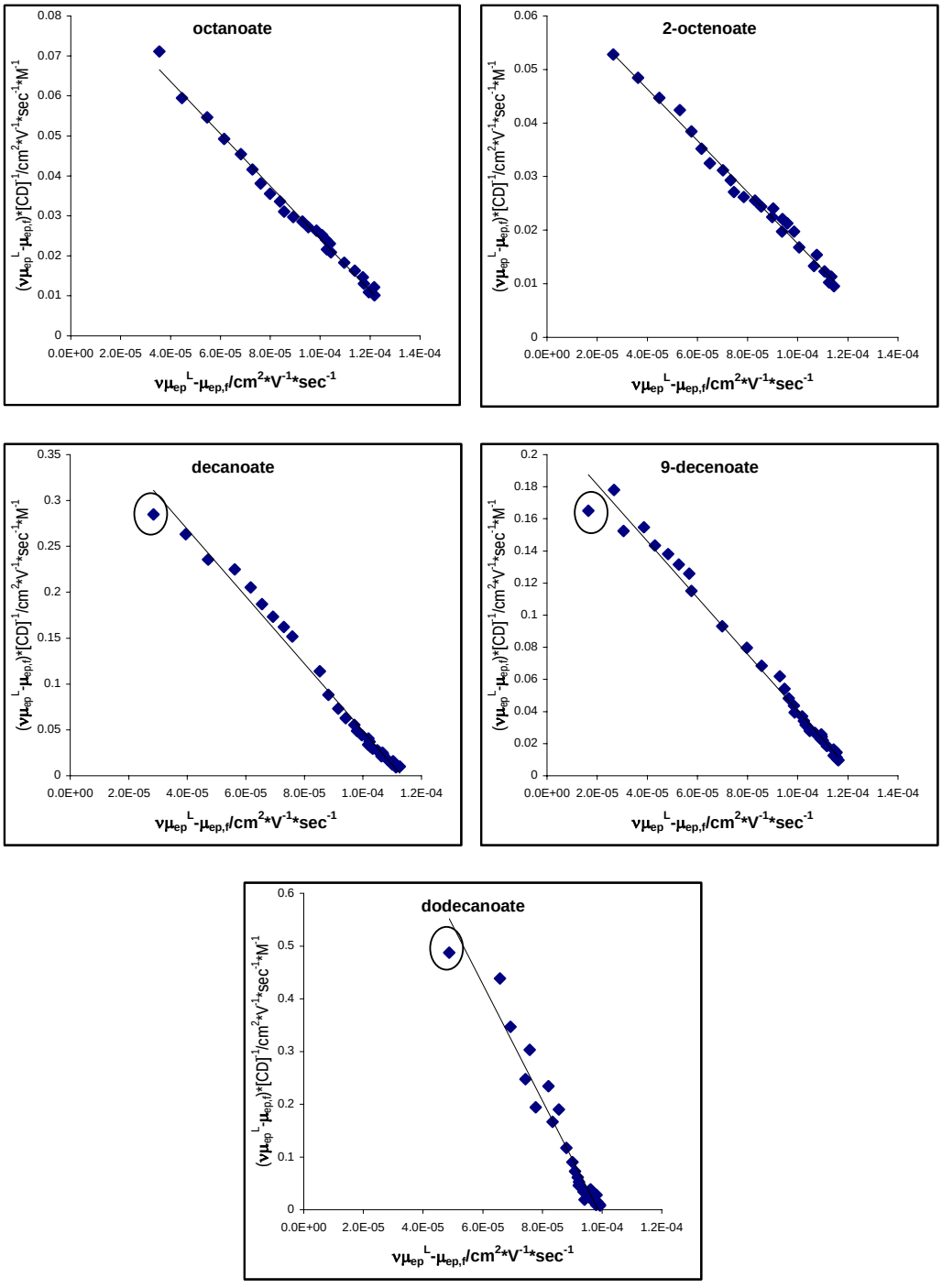

Consideration 3: Error minimization. The error associated with estimated binding constants and complex mobilities from ACE data is dependent upon the additive concentrations and the respective fatty acid mobility shifts used for calculation by the nonlinear fitting procedure. Sources have cited that error is minimized when the fraction of analyte in the complexed form lies in the range of 0.2-0.8 [13,17,31]. Therefore, while fatty acid mobility data was collected from 0-12.0 mM β-CD in the BGE, it is not advisable to use this entire dataset to calculate the binding parameters.

Each fatty acid requires a different β-CD concentration range in the BGE to minimize error, as the fatty acid/β-CD binding affinities will inherently determine what CD concentrations result in each fatty acid being complexed at the correct fraction. The opposite of the slopes in the X-reciprocal plots (Equation (3.7)) were used to approximate the binding constant of each fatty acid/CD pair. These approximated binding constants, K_{app}, are listed in Table 3.2, and the β-CD concentration ranges satisfying the desirable fatty acid complexed fraction range (0.2-0.8) at each K_{app} are shown as well. It should be noted that the β-CD concentration that is calculated to comply with this range is based upon the FA/CD systems interacting with a 1:1 stoichiometry.

Table 3.2. Concentration range of β-CD in the BGE satisfying the fraction of analyte in the bound form to be 0.2-0.8 for ACE experiments (assumes 1:1 stoichiometry).

Fatty Acid	**K_{app}**	**[β-CD] range, mM**
octanoate	650	0.4-6.2
2-octenoate	480	0.5-8.3
decanoate	3600	0.07-1.1
9-decenoate	1700	0.1-2.4
dodecanoate	11000	0.02-0.36

After removal of the mobility data points that were collected outside the requirements of **Considerations 2** and **3,** the remaining dataset was used to construct the binding isotherms for each of the fatty acid/β-CD pairs. These isotherms are displayed in Figure 3.6. In addition, because higher order stoichiometry was suspected as a possibility with the $C_{12}O_2^-$/β-CD system, a second isotherm was constructed for this system using the mobility data points collected throughout the entire β-CD concentration range employed in the BGE, thereby fulfilling **Consideration 1**, but ignoring **Consideration 3**.

Figure 3.6 Corrected binding isotherms with β-CD range satisfying Consideration 2 and Consideration 3. *$C_{12}O_2^-$ full isotherm shown because higher order binding was suspected (Consideration 1).

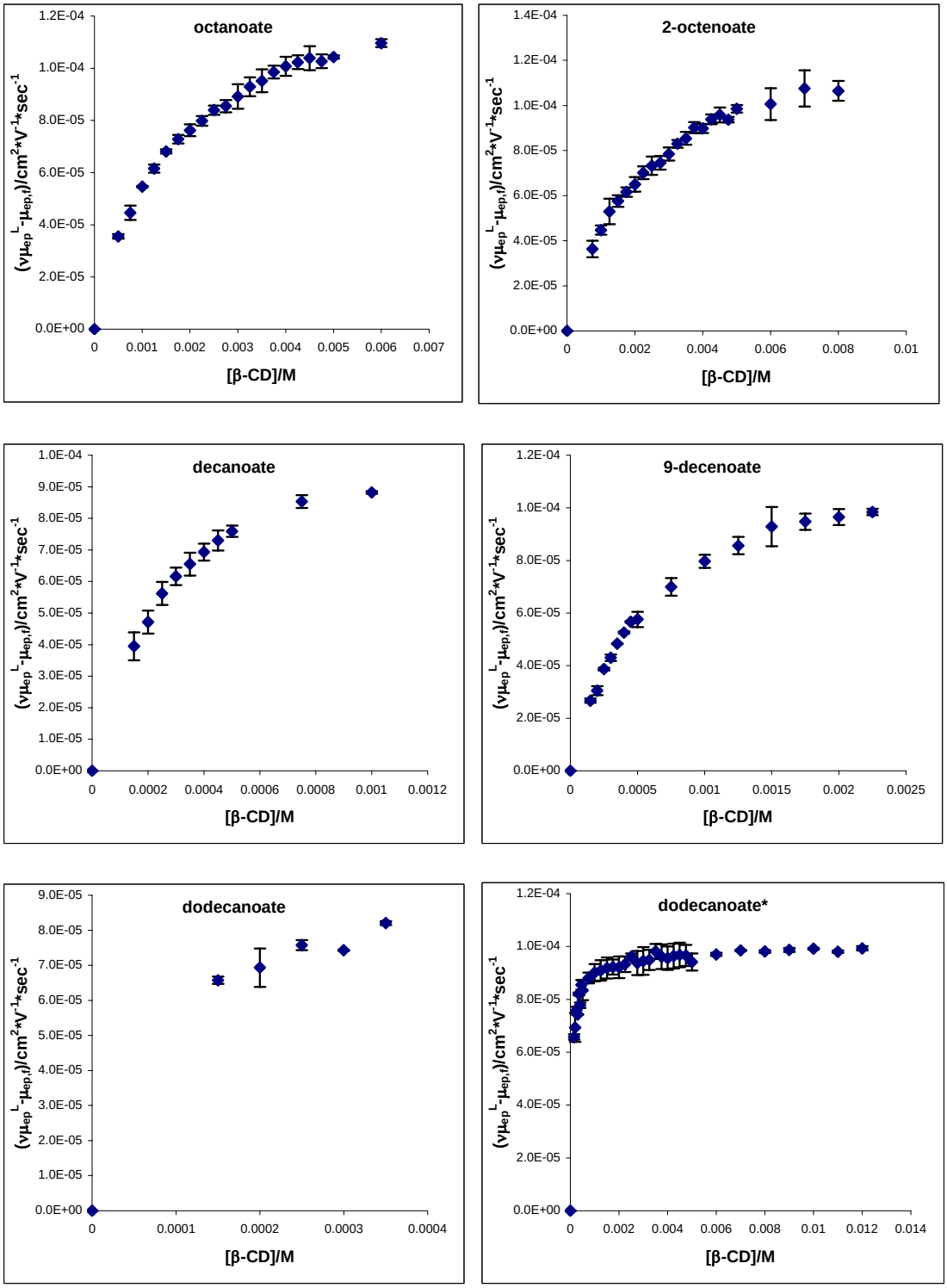

3.4.1.2 Calculating the binding parameters

Based on the 1:1 stoichiometry assumed from the linearity of the transformed data seen in Figure 3.2, the nonlinear isotherms were used to calculate the parameters for 1:1 binding by regression analysis according to Equation (3.4). Because higher order stoichiometry was suspected with the $C_{12}O_2^-$/β-CD system, $\Delta\mu_{ep}$ data collected over the entire β-CD range was used to also determine the binding parameters according to Equation (3.13). The results are shown in Table 3.3. General observation of the estimated binding constants for the 1:1 interactions reveals an order of magnitude increase with the addition of two methylene groups within the alkyl chain, while unsaturation in the chain contributes to a slightly lower binding constant. For $C_{12}O_2^-$, the 1:2 interacting binding model (Equation (3.13)) yields a 1:1 binding constant comparable to that determined by Equation (3.4), while also returning a 1:2 association constant two orders of magnitude lower than that for the first. This finding is consistent with other reports studying the same system by different methods (see Table 3.1).

Table 3.3. Binding constants (and standard errors) determined by ACE. Values represent those of the best fit curve to the average Δμep for three trials determined at each β-CD concentration in the BGE. "1:1" describes Equation (3.4) and "1:1 plus 1:2" describes Equation (3.13).

Fatty Acid	**Model**	$\mathbf{K_{1:1}}$	$\mathbf{K_{1:2}}$	$\mathbf{R^2}$
octanoate	1:1	6.4 (±0.2) $x10^2$	-	0.998
2-octenoate	1:1	4.7 (±0.2) $x10^2$	-	0.996
decanoate	1:1	3.7 (±0.2) $x10^3$	-	0.997
9-decenoate	1:1	1.8 (±0.05) $x10^3$	-	0.999
dodecanoate	1:1	1.4 (±0.4) $x10^4$	-	0.996
	1:1 plus 1:2	1.4 (±0.2) $x10^4$	1.3 (±2.4) $x10^2$	0.994

3.4.2 Isothermal Titration Calorimetry

3.4.2.1 Constructing the binding isotherm

Similar to the requirements discussed earlier regarding the construction of binding isotherms with ACE data, ITC possesses restrictions in selection of concentrations to employ. These restrictions are based upon the following considerations:

- **[Titrant] > [binding partner]**
- **[FA] < critical micelle concentration**
- **[Binding partner] selection**

Consideration 1 and **Consideration 2: [Titrant] > [binding partner]** and **[FA] < critical micelle concentration**. The first condition is required by standard ITC operation, as the titrant solution is added at very small volumes (i.e. ~250 μL total) into ~1.4 mL solution containing its binding partner, and the final molar ratio of titrant/partner typically exists as 1.5-2.0. The second condition accounts for additional phenomena apart from the binding interaction (e.g. micellization) that can produce heat signals that distort the ITC data. In this study, it was necessary to remain below the critical micelle concentration of the fatty acids (e.g. ~30 mM for $C_{12}O_2^-$) [8], eliminating the possibility of heats of micellization/demicellization. These two conditions, in conjunction with each other, limit the choice of titrant to β-CD. As a note, the approximate [β-CD] chosen to use was 12.0 mM, near its maximum aqueous solubility.

Consideration 3: [Binding partner] selection. With β-CD chosen as the titrant, the fatty acid concentration ([FA]) loaded into the ITC cell must be selected. In ITC theory, the shape of the binding isotherm is dependent upon the initial [FA] loaded into the cell, as well as its binding constant with titrant. It is clear that a higher [FA] would be advisable, as this would produce a more defined isotherm from which it is easier to find the best fit binding parameters, and would be concentrated enough to produce a minimum heat signal when titrated with β-CD [25]. However, this [FA] must also be dilute enough so that complete discharge of the titrant into the cell solution extends to a high enough molar ratio to construct as complete of a binding isotherm as possible. The latter is even more important in this study, where the stoichiometry of the systems is somewhat elusive. To comply with both requirements, a [FA] was chosen to be approximately 1.0 mM.

Isotherms resulting from the titration of four of the five fatty acids with β-CD are displayed in Figure 3.7. The $C_8O_2^-$/β-CD system did not produce a heat signal large enough to be studied by ITC, regardless of the experimental conditions.

Figure 3.7.Example ITC binding isotherms of the fatty acid/β-CD pairs.

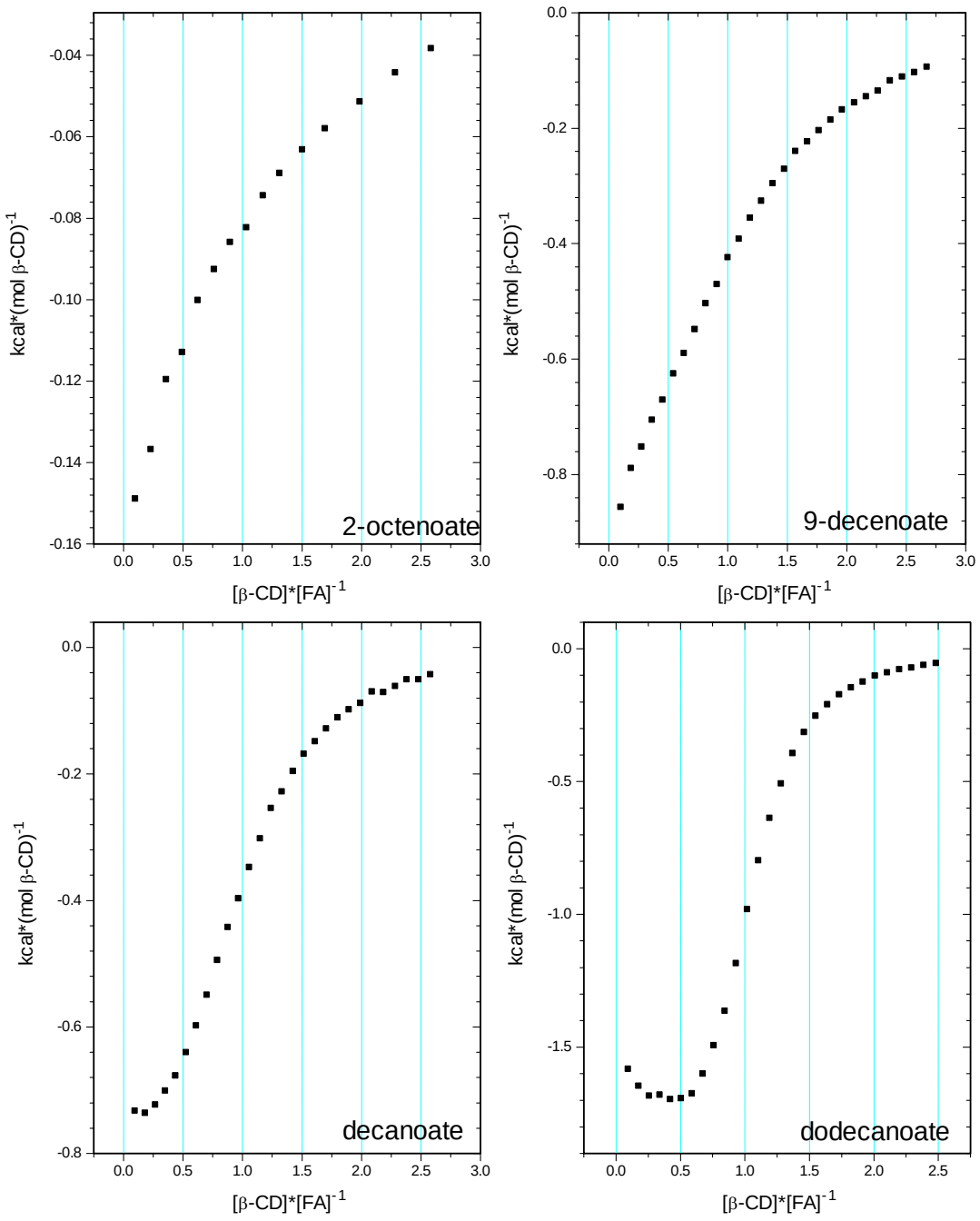

3.4.2.2 Calculating the binding parameters

Two models describing differing stoichiometries of binding were used to determine the best fit values of the parameters by nonlinear regression. The first model utilized for ITC data analysis is herein termed the **"one set of sites" (single site)** model (i.e. Equation (3.10)), and is used to determine the binding parameters if the stoichiometry of interaction is known to be either 1:1, or in the case of higher order stoichiometry, all binding sites possess the same K and ΔH [36]. For example, if a 1:2 (FA:CD) interaction is present, and the FA binds both CDs with the same K and ΔH, then fitting the data with the "one set of sites" model should indicate the higher stoichiometry.

The second binding model, herein termed the **"interacting sites"** model, is used to define the binding parameters K and ΔH for a system in which multiple ligands bind to a macromolecule in an interacting manner (i.e. reaction Equation (3.12)). As noted in the *Introduction*, many literature sources cite higher order binding between β-CD and the fatty acids chosen in this work at 1:2 (FA:CD); in this work the "interacting sites" model was used to fit the data according to a 1:2 interacting binding process. The fit parameters obtained through nonlinear regression analysis of ITC data according to the two different models are shown in Table 3.4; the values represent the weighted averages of the mean and standard error of the binding parameters determined for two trials per fatty acid/β-CD pair [37].

Table 3.4. Parameters (and standard errors) calculated from ITC generated binding isotherms. "Single" denotes one set of sites model; "Interacting" describes a model based on general reaction Equation (3.12). *n fixed at 1 because model would not converge otherwise.

Fatty Acid	Model	n (CD:FA)	$K_{1:1}$ ave	$K_{1:2}$ ave	ΔH_1 ave (cal*mol^{-1})	ΔH_2 ave (cal*mol^{-1})	X^2
2-octenoate	Single	1*	6.7 (±0.4) x10^2	-	-3.7 (±0.1) x10^2	-	13
	Interacting	2	2.6 (±0.2) x10^2	5.0 (±0.3) x10^3	-4.0 (±0.1) x10^2	2.5 (±0.2) x10^2	7.6
decanoate	Single	1.03 (±0.01)	6.6 (±0.2) x10^3	-	-8.8 (±0.1) x10^2	-	56
	Interacting	2	5.5 (±0.2) x10^3	8.0 (±0.2) x10^2	-8.3 (±0.04) x10^2	-1.4 (±0.1) x10^2	45
9-decenoate	Single	1.05 (±0.01)	2.2 (±0.05) x10^3	-	-1.3 (±0.02) x10^3	-	39
	Interacting	2	1.9 (±0.03) x10^3	1.3 (±0.03) x10^3	-1.1 (±0.01) x10^3	-94 (±11)	40
dodecanoate	Single	1.10 (±0.01)	2.6 (±0.2) x10^4	-	-1.8 (±0.02) x10^3	-	2800
	Interacting	2	1.1 (±0.1) x10^5	7.0 (±0.7) x10^3	-1.7 (±0.01) x10^3	-3.2 (±0.3) x10^2	1900

The 1:1 binding constants estimated using the "one set of sites" model show the same trend as seen with those calculated using ACE; strength of binding increases with increasing alkyl chain length and decreases with the presence of a double bond in the chain. In the case of the "interacting sites" model, this trend is seen in the $K_{1:1}$ constants, but is not apparent in the $K_{1:2}$ values. This latter trend is not consistent with results found by studying similar systems using different methods (Table 3.1). For the saturated acids, the $K_{1:2}$ values are less than the $K_{1:1}$ values. This trend is consistent to that seen for the $C_{12}O_2$-/β-CD system studied by ACE, and also with trends seen in other fatty acid/β-CD pairs using different methods (Table 3.1).

3.4.3 Comparison of ACE and ITC Results

3.4.3.1 Stoichiometry of binding

This section of the discussion focuses on how information from ACE and ITC can be used together to elucidate binding stoichiometry. The stoichiometry for the fatty acids $C_8O_2^-$, $C_6{=}C_2O_2^-$, $C_{10}O_2^-$ and $C{=}C_9O_2^-$ are discussed first. Then, the steps taken in concluding the stoichiometry for the $C_{12}O_2^-$/β-CD system are discussed.

As stated in the section covering the ACE results, the linear transformations of the data for the fatty acids (except $C_{12}O_2^-$) clearly suggest a 1:1 interaction with β-CD. It should be noted, however, that the transformation plots may also be linear in the case of multiple ligand (CD) molecules binding to the fatty acid in a non-interacting manner (e.g. with the same affinity) [38,39]. Hence, ACE cannot distinguish which stoichiometry best defines the dataset if non-interacting binding is occurring. However, ITC can distinguish an equal affinity, multi-ligand

binding phenomenon from a single ligand/guest interaction. Use of the "one set of sites" model would calculate $n \approx 2$, and furthermore, the middle of the steepest part of the titration curve would align at a molar ratio of ~2 along the X-axis of the binding isotherm [36]. Because this is clearly not the case in this work, as exhibited by Table 3.4 and Figure 3.7, the linearity present in the transformation plots of the ACE data for all fatty acids, except $C_{12}O_2^-$, must be 1:1, and this stoichiometry of interaction was chosen as the one that best describes these fatty acid/β-CD systems.

In the case of $C_{12}O_2^-$, the ACE linear transformations show the possibility of an interacting binding process occurring. Comparison of the binding constants calculated from the ACE data derived from both the 1:1 (Equation (3.4)) and 1:1 plus 1:2 (Equation (3.13)) binding models reveals that both models yield results that make physical sense (Table 3.3), regardless of the error associated with $K_{1:2}$ being greater than the calculated parameter itself. If 1:2 binding is occurring, this high error can most likely be attributed to the non-fulfillment of **ACE Consideration 3**, as the fraction of the analyte complexed as $FA:CD_2$ is 0.01-0.61 throughout the β-CD concentration range used to study the $C_{12}O_2^-$/CD system, thereby not minimizing the error associated with the calculation of $K_{1:2}$. Previously published results of ACE derived binding constants for systems known to bind in the 1:2 interacting manner also revealed standard errors greater than the parameters themselves when **ACE Consideration 3** could not be satisfied [17]. Therefore, the high error associated with $K_{1:2}$ should not be used as a factor in determining which model best describes the $C_{12}O_2^-$/β-CD interaction.

Selection of a model for $C_{12}O_2^-$/β-CD binding based upon the goodness of fit is also not clear. More complex models (i.e. 1:1 plus 1:2) commonly fit data better as more parameters are present [40], but in the case of the ACE calculated binding constants, the fit provided by the

simpler model (1:1) is better than that of the complex model. On the other hand, the X^2 values from fitting the ITC data to the two models reveal a better fit when the more complex model (interacting sites) is used.

Further comparison of the ACE derived binding constants to those calculated using ITC can lead to the conclusion of stoichiometry for $C_{12}O_2^-$/β-CD binding. Examination of the calculated binding parameters reveals that the ITC "interacting sites" model's first association constant, $K_{1:1}$, appears to be too large, especially when compared to the parameter calculated using the ACE model describing the same binding event. Indeed, the difference in this case appears as almost a full order of magnitude, much greater than the differences seen for other binding models and other fatty acids investigated. In fact, this result is also much greater than any binding constant reported in the literature for $C_{12}O_2^-$/β-CD binding (Table 3.1). These comparisons seem to suggest that the 1:2 stoichiometric ITC model may calculate values that are unreliable or possess little scientific meaning; but, under the conditions of these experiments, the definitive stoichiometry of the $C_{12}O_2^-$/β-CD interaction cannot be concluded but more consistent cross-technique values are obtained using the 1:1 model.

3.4.3.2 Magnitude of the binding constant

Comparison of Table 3.3 and Table 3.4 reveals differences in the values of the binding constant calculated, dependent upon the instrumental method used. Which one provides more accurate results may be a question of the steps taken to assure that the measurable term (i.e. $\Delta\mu$ or q) is dependent upon the binding phenomenon alone. In the ACE portion of the study, careful consideration was given to sample overloading (ligand saturation) that would lead to a

negative error in estimating the binding constant. Work was also done to eliminate points from the dataset that lie outside the suggested complexed analyte range before nonlinear regression analysis was performed. In the ITC work, experiments were conducted to account for heat affects arising from FA and CD dilution; as noted earlier, no measurable heat was detected in these experiments. In another study investigating the use of CE and ITC to study the binding between alkyloxyethylene surfactants and cyclodextrins [24], the binding constants estimated by ITC were consistently greater than those determined by CE, which is the same trend seen in this work. Regardless of the differences in calculated binding constants between ACE and ITC, both reveal the same trends associated with FA/β-CD binding strength dependent upon chain length and the presence of a site of unsaturation.

3.4.3.3 Trends in the calculated binding constants

Alkyl chain length and unsaturation both affect the binding strength between the fatty acids and β-CD. These trends, apparent in both methods utilized (Table 3.3 and Table 3.4), are consistent with previous studies investigating the same systems (Table 3.1), as well as other studies on shorter chain fatty acids with cyclodextrins [11].

One of the advantages of ITC over CE is the direct estimation of binding enthalpy, ΔH, which in conjunction with the estimated binding constant, allows the calculation of the free energy and entropy of binding (ΔG and ΔS, respectively). Examination of these thermodynamic parameters displayed in Table 3.4 aids in the explanation of the dependence of binding constant on the structural features of the fatty acids. As the stoichiometry was concluded to be 1:1, all thermodynamic data is that calculated using the ITC "one set of sites" model.

Table 3.4. Calculated thermodynamic parameters for the fatty acid/β-CD systems studied by ITC.

Fatty Acid	$K_{1:1}$	ΔG (kJ*mol^{-1})	ΔH (kJ*mol^{-1})	ΔS (J*mol^{-1}*K^{-1})
2-octenoate	6.7×10^{2}	-1.6×10^{1}	-1.6	49
decanoate	6.6×10^{3}	-2.2×10^{1}	-3.7	61
9-decenoate	2.2×10^{3}	-1.9×10^{1}	-5.4	46
dodecanoate	2.6×10^{4}	-2.5×10^{1}	-7.5	59

For the saturated acids, as the number of methylene groups in the chain increases, so does the magnitude of the binding constant, and consequently the apparent free energy (ΔG) becomes more favorable; this trend is also present for the unsaturated acids. Inspection of the other thermodynamic parameters reveals that this trend is an enthalpy-driven event, as the entropy is relatively independent of the chain length (e.g. 6.1 $x10^{-2}$ for $C_{10}O_2^-$ vs. 5.9 $x10^{-2}$ for $C_{12}O_2^-$). This is consistent with numerous other reports studying similar interacting systems [7,11], and the further decrease in ΔH as the chain lengthens is attributed to an increase in the number of interactions and a decrease in the molecular distance between the guest and host. Another contributing factor to the negative ΔH is the release of water molecules from the β-CD cavity upon the inclusion of a guest compound [22].

For a given chain length, the presence of a double bond in the chain decreases the binding of the fatty acid with β-CD. Closer examination of the thermodynamic results for the decanoate/9-decenoate pair reveals trends that are similar to other studies on similar systems [11]. Regardless of the more negative ΔH value as the chain is unsaturated, the magnitudes of ΔG and consequently K become less favorable; this trend contradicts that observed for increasing alkyl chain length mentioned previously. This binding affinity decrease must then be an entropic effect. While the entropy contribution to binding is positive for all of the acids, because of the favorable environment introduced by the nonpolar cyclodextrin cavity and the dehydration of the guest compound [7,11], the entropy is less positive for the unsaturated acid; this is likely related to the greater loss of freedom of motion the unsaturated acid experiences compared to the saturated acid as they are bound within CD [11]. It is this entropy difference that is responsible for the decreased binding for an unsaturated acid with β-CD.

3.5 Summary

Under the conditions of our experiments, it was concluded that these fatty acids interact with β-CD with a 1:1 association, a topic that, as mentioned in the introduction, is a point of inconsistency in the literature, and was one motivation behind this study. This conclusion was bolstered by the fact that two instrumental techniques, each relying upon different physical properties of the host/guest system, provided complementary information that led to the conclusion of this binding stoichiometry. Also, the calculated binding constants of the two methods were the same order of magnitude, and the cross-method comparison is consistent with previous work done in our lab comparing CE and ITC for binding studies of other systems. The work presented here demonstrates the utility of using ACE and ITC to study the binding between fatty acids and β-CD, systems that have been widely studied by a variety of other techniques. Similar binding affinities and trends in the binding constant are consistent with those determined by these other techniques. The thermodynamic parameters and their dependence on the structural features of the fatty acids are also consistent with other methods determining thermodynamic values.

3.6 References

[1] H. Schlenk, D.M. Sand, J. Am. Chem. Soc. 83 (1961) 2312.

[2] M.M. Meier, M.T. Bordignon-Luiz, B. Szpoganics, V. Soldi, Thermochim. Acta 375 (2001) 153.

[3] L.D. Wilson, S.R. Siddall, R.E. Verrall, Can. J. Chem. 75 (1997) 927.

[4] S.G. Skoulika, C.A. Georgiou, M.G. Polissiou, J. Inclusion Phenom. Macrocyclic Chem. 34 (1999) 85.

[5] M.M. Meier, M.T. Bordignon-Luiz, P.J. Farmer, B. Szpoganicz, J. Inclusion Phenom. Macrocyclic Chem. 40 (2001) 291.

[6] S. Lima, B.J. Goodfellow, J.J.C. Teixeira-Dias, J. Phys. Chem. A 108 (2004) 10044.

[7] G. Gonzalez-Gaitano, G. Tardajos, J. Chem. Educ. 81 (2004) 270.

[8] R. Palepu, J.E. Richardson, V. Reinsborough, Langmuir 5 (1989) 218.

[9] G. Gonzalez-Gaitano, T. Sanz-Garcia, G. Tardajos, Langmuir 15 (1999) 7963.

[10] L.D. Wilson, R.E. Verrall, J. Phys. Chem. B 101 (1997) 9270.

[11] M.V. Rekharsky, M.P. Mayhew, R.N. Goldberg, P.D. Ross, Y. Yamashoji, Y. Inoue, J. Phys. Chem. B 101 (1997) 87.

[12] L. Szente, J. Szejtli, J. Szeman, L. Kato, J. Inclusion Phenom. Macrocyclic Chem. 6 (1993) 339.

[13] C. Karakasyan, M. Taverna, M. Millot, J. Chromatogr. A 1032 (2004) 159.

[14] B. Steinbock, P.P. Vichaikul, O. Steinbock, J. Chromatogr A 943 (2002) 139.

[15] S.R. Gratz, A.M. Stalcup, Anal. Chem. 70 (1998) 5166.

[16] M. Cirri, F. Maestrelli, S. Orlandini, S. Furlanetto, S. Pinzauti, P. Mura, J. Pharm. Biomed. Anal. 37 (2005) 995.

[17] M.T. Bowser, D.D.Y. Chen, Anal. Chem. 70 (1998) 3261.

[18] H.H. Ruttinger, in R.H.H. Neubert, H.H. Ruttinger (Editors), Affinity Capillary Electrophoresis in Pharmaceutics and Biopharmaceutics. Marcel Dekker, New York, NY, 2003.

[19] K.L. Rundlett, D.W. Armstrong, Electrophoresis 22 (2001) 1419.

[20] M.V. Rekharsky, R.N. Goldberg, F.P. Schwarz, Y.B. Tewari, P.D. Ross, Y. Yamashoji, Y. Inoue, J. Am. Chem. Soc. 117 (1995) 8830.

[21] Y. Liu, Y.W. Yang, E.C. Yang, X.D. Guan, J. Org. Chem. 69 (2004) 6590.

[22] E. Schneiderman, A.M. Stalcup, J. Inclusion Phenom. Macrocyclic Chem. 43 (2002) 37.

[23] A.R. Stettler, P. Krattiger, H. Wennemers, M.A. Schwarz, Electrophoresis 28 (2007) 1832.

[24] E. Schneiderman, B. Perly, E. Brooks, A.M. Stalcup, J. Inclusion Phenom. Macrocyclic Chem. 43 (2002) 43.

[25] T. Wiseman, S. Williston, J.F. Brandts, L. Lin, Anal. Biochem. 179 (1989) 131.

[26] F. Robey, in J.P. Landers (Editor), Handbook of Capillary Electrophoresis. CRC Press, Boca Raton, FL, 1997, p. 591.

[27] F. Lynen, F. Borremans, P. Sandra, Electrophoresis 22 (2001) 1974.

[28] W. Wei, Z.J. Zhang, H.X. Ju, Chromatographia 59 (2004) 513.

[29] R. Kuhn, R. Frei, M. Christen, Anal. Biochem. 218 (1994) 131.

[30] F.A. Gomez, L.Z. Avila, Y. Chu, G.M. Whitesides, Anal. Chem. 66 (1994) 1785.

[31] M.T. Bowser, D.D.Y. Chen, J. Phys. Chem. A 102 (1998) 8063.

[32] K.L. Rundlett, D.W. Armstrong, J. Chromatogr. A 721 (1996) 173.

[33] Y. Tanaka, S. Terabe, J. Chromatogr. B. 768 (2002) 81.

[34] Operators Manual for OMEGA-Isothermal Titration Calorimeter. MicroCal Inc., Northampton, MA, 1993.

[35] S. Bose, J. Yang, D.S. Hage, J. Chromatogr. B 697 (1997) 77.

[36] ITC Data Analysis in Origin, Tutorial Guide. MicroCal Inc., Northampton, MA, 1993.

[37] F. Rossini, in F. Rossini (Editor), Experimental Thermochemistry. Interscience, New York, NY, 1956, p. 297.

[38] C. Galbusera, D.D.Y. Chen, Curr. Opin. Biotechnol. 14 (2003) 126.

[39] C. Galbusera, M. Thachuk, E.D. Lorenzi, D.D.Y. Chen, Anal. Chem. 74 (2002) 1903.

[40] H. Motulsky, Fitting Models to Biological Data Using Linear and Nonlinear Regression : A Practical Guide to Curve Fitting. Oxford University Press, New York, NY, 2004.

Chapter 4

Preparation and Properties of Solid State β-Cyclodextrin Inclusion Complexes of 2-Furfurylthiol

4.1 Introduction

This chapter details an experimental investigation into the complex properties between 2-furfurylthiol (FFT) and β-cyclodextrin (β-CD) in the solid state, when prepared in the absence and presence of the proposed fatty acid (FA) co-inclusion binding agents. This work is a key requirement in identifying the capability of the β-CD binary and ternary encapsulation platform for future use in an industrial application. Furthermore, this work aims to offer complementary information to the existing contradictory reports in the literature on the FFT/CD solid complex [1,2].

The preparation of solid inclusion complexes to assess the utility of the CD encapsulation strategy has been reported for a variety of different guest compounds. Typically, the characteristics achieved by encapsulating guest are the same as those discussed in Chapter 1; they include: decreased volatility, isolation from environmental hazards, increased water solubility, and conversion to an easily handled powder form [3,4]. Complexation is most commonly achieved in solution, but can performed using dry techniques; the most common of these involve cogrinding or mechanochemical activation [5]. The dry techniques offer the advantage of eliminating the extra effort involved in eliminating excess water from the prepared complex. When prepared in solution, the final product must be isolated and dried through one of

many techniques, many times in combination. These isolation strategies include spray- or freeze-drying, centrifugation, drying with heat, or drying with desiccant. These techniques are used in both the academic and industrial settings, for initial complexation investigations and in for use in large-batch applications. For this work, complexation was achieved in solution, to mirror past work done for the FFT/β-CD system. Specifically, a co-precipitation approach was used as it is noted to be the most convenient and suitable for initial laboratory evaluation [6].

Analytical characterization of solid complexes can be accomplished through the use of different techniques, such as nuclear magnetic resonance spectroscopy, differential scanning calorimetry, thermogravimetric analysis, and powder X-ray diffraction [7,8,9,10]; quantification of a loaded guest compound is usually accomplished by chromatographic techniques, with gas chromatography often chosen for flavors and aromas because of the volatile nature of many of the guest species investigated [4,11,12,13]. Communication with an Industrial Sponsor of this work illuminated problems with using GC for this work, as was evidenced by their unsuccessful efforts to fully extract FFT from the β-CD complex in their previous studies [14]. To circumvent this issue, a capillary electrophoresis (CE) method with UV detection for quantification was proposed in which direct dissolution of the FFT/CD complex in an aqueous solution with subsequent electrophoresis in a highly basic buffer allows for deprotonation of the thiol functionality, thereby increasing solubility and allowing separation from neutral sulfide oxidation by-products [15].

4.2 Materials and Methods

4.2.1 Reagents

All reagents were the same as described in Chapters 2 and 3, with the addition of 2-nonenoic acid purchased from MP Biomedicals Inc. (Solon, OH, USA). The CE background electrolyte (BGE) was prepared by dissolving an appropriate amount of tribasic sodium phosphate in distilled deionized water to give a 10 mM solution, and the pH was adjusted with a concentrated sodium hydroxide solution to pH 12. The BGE was passed through a 0.2 μM filter (Nalge Nunc International Corp, Rochester, NY, USA) before use.

4.2.2 Preparation of Solid Complexes

Several solid inclusion complexes were prepared consistent with a procedure described by Szente and Szejtli [1,4]. Briefly, 1.0-g of β-CD hydrate was dissolved in 10-mL of one of the following solutions, further referred to herein as **Medium I-Medium IV**:

I. Unbuffered distilled deionized water

II. 100 mM phosphate buffer, pH 7.0

III. 100 mM phosphate buffer, pH 2.5

IV. Aqueous solution of ethanol (2:1, H_20:EtOH)

The β-CD solution was heated to ~55^{o}C in a water bath with vigorous stirring. To this solution, 1-mL of a 2-furfurylthiol stock solution (1% v/v in: **I.** H_2O; **II.** phosphate buffer pH 7.0; **III**. phosphate buffer pH 2.5; **IV**. EtOH) was added dropwise. The FFT/β-CD mixture was continually stirred and allowed to cool to room temperature for 4.5 hours, after which the precipitated mixture was refrigerated at ~4^{o}C for 16 hours. The solid was isolated by centrifugation at 1550 rpm for 20 minutes, transferred to a watchglass, and dried over phosphorous pentoxide for an additional 24 hours.

To test the effect of fatty acid presence on the encapsulating ability of β-CD for FFT, the following were added separately to **Media I-IV**., thereby creating a number of **Treatments**:

Sodium octanoate	$C_8O_2^-Na^+$
Sodium decanoate	$C_{10}O_2^-Na^+$
Sodium dodecanoate	$C_{12}O_2^-Na^+$
2-octenoic acid	$C_6{=}C_2O_2^-H^+$
2-nonenoic acid	$C_7{=}C_2O_2^-H^+$
9-decenoic acid	$C{=}C_9O_2^-H^+$

The above notations will be used throughout the remaining work for consistency purposes only. The pKa values for these acids are ~4.8, and their anionic and neutral ionization states in Medium II (pH 7.0; anionic) and Medium III (pH 2.5; neutral) are understood. The number of solid complexes of each Medium/Treatment combination (M/T) for this study is presented in Table 4.1. In general, more complexes were prepared with the saturated FA treatments because

of the relative abundance of literature* studying their interactions with CDs compared to the unsaturated acids, whose use in these studies is offered as a preliminary investigation into the question of alkyl chain unsaturation alteration of the FA treatment effect on FFT/β-CD complexation. Also, more complexes of the "No Fatty Acid" treatment for **Media I** and **IV** were prepared; reasoning for this was based on preparing a complex of this type as a 'check' of the preparation protocol when preparing complexes across different M/T combinations.

* See Chapter 3, Section 3.1 for references

Table 4.1. Number of complexes prepared for each Medium/Treatment combination.

	FATTY ACID TREATMENT						
MEDIUM	*No Fatty Acid*	$C_8O_2^-Na^+$	$C_{10}O_2^-Na^+$	$C_{12}O_2^-Na^+$	$C_6{=}C_2O_2^-H^+$	$C_7{=}C_2O_2^-H^+$	$C{=}C_9O_2^-H^+$
I.	4	2	2	2	1	1	1
II.	2	2	2	2	2	2	2
III.	2	2	2	2	2	2	2
IV.	5	1	1	1	0	0	0

4.2.3 Determination of β-CD Complexation Efficacy

The performance of the β-CD encapsulation platform was evaluated by quantifying the amount of FFT in the prepared solids immediately after preparation, and again in 7-day intervals, throughout the course of 4-week storage. The solids were contained in clear glass vials left open to the ambient atmosphere, and were stored on the shelf at room temperature. A quantification sample consisted of a weighed portion of the solid complex diluted with 1mM phosphate solution (1/10 ionic strength of CE BGE) to give a final concentration of ~0.5-1.0 mg/mL. The sample solution was sonicated for approximately 3 minutes, and subsequently analyzed according to the CE method described below. Determination of FFT in the solid material (mg FFT/g complex) was calculated according to the quantified FFT concentration in solution, and by accounting for the sample portion mass initially weighed and the volume of sample solution prepared. FFT content was determined in this manner for 3 separate portions of each solid complex prepared.

4.2.4 Instrumentation

4.2.4.1 Capillary Electrophoresis

Conditioning of the fused-silica capillary (60 cm total length) was completed by consecutive flushing with 0.1 M NaOH, distilled deionized water, and the phosphate BGE, each at 40 psi for 5 minutes. The capillary was then allowed to equilibrate in the BGE overnight. Between runs, the capillary was flushed with phosphate BGE at 40 psi for 2 minutes. Sample

injection, 0.5 psi for 5 sec, was performed at the capillary outlet (e.g. detector end), and electrophoresis was performed under reversed polarity with an applied potential between 15-18 kV; this effectively shortened the length of capillary from injection site to detection window to 10 cm. Direct UV detection was accomplished at 214 nm.

FFT calibration standards were prepared in range of 25-800 μM in 1 mM phosphate prepared by dilution of the BGE. Corrected peak areas (area/migration time) were used for instrument calibration. New calibration standards were prepared, and curves constructed, for analyses performed on different days throughout the course of these studies.

4.2.4.2 Inductively Coupled Plasma-Mass Spectrometry (ICP-MS)

An Agilent 7500CE ICP-MS was used for sulfur quantification of some FFT/β-CD complexes prepared as part of this study. Calibration and sample solutions were prepared from the CE calibration and sample solutions by 50x dilution with the 1mM phosphate solution. Continuous flow injection at 0.4 mL/min was used for sample introduction. The system was flushed with 1mM phosphate between sample injections to reduce sample carryover. Quantification of sulfur (^{32}S m/z) was completed by averaging 5 replicate signal acquisitions for each sample.

4.2.4.3 Nuclear Magnetic Resonance (NMR) Spectroscopy

A Bruker Avance 400-MHz NMR spectrometer was used for identification of components of some of the prepared solid complexes. Portions of the solids were dissolved in DMSO-d_6, and ^{1}H-NMR spectra were acquired.

4.3 Results and Discussion

4.3.1 Evaluating the CE Method

The biggest concern with using the CE method described above is oxidation of FFT in the sample solution. While previous studies have shown FFT to be relatively stable in aqueous solutions compared to other furanthiols [15,16], the oxidation of mercaptans is enhanced in the deprotonated form [17]. Therefore, a simple test was conducted by evaluating a series of 6 FFT calibration standards immediately, and at 2 hours, after preparation. Analysis of the two calibration curves (Figure 4.1) revealed no meaningful statistical difference in the calculated regression parameters ($P_{slope} = 0.67$; $P_{intercept} = 1.00$) [18].

A secondary test was conducted by quantifying FFT by the CE method described above, followed by sulfur quantification in the same samples using ICP-MS. Three portions each from two different solid samples were taken and analyzed by CE and ICP-MS. Under the assumptions that FFT in the solid complex accounts for nearly all of the sulfur content, and that FFT oxidation is negligible in the time between CE sample prep and analysis, then CE quantification of FFT and ICP-MS quantification of sulfur should equate to the same value of FFT originally

present in the solid samples. Results indicated no statistical difference in the FFT value determined by CE versus ICP-MS (Table 4.2).

Figure 4.1. Comparison of instrument calibration curves to test for FFT stability in CE sample solution matrix.

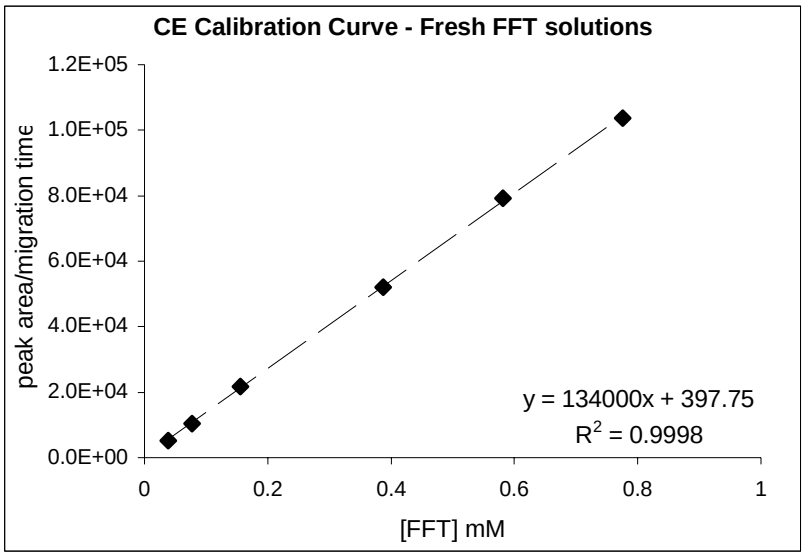

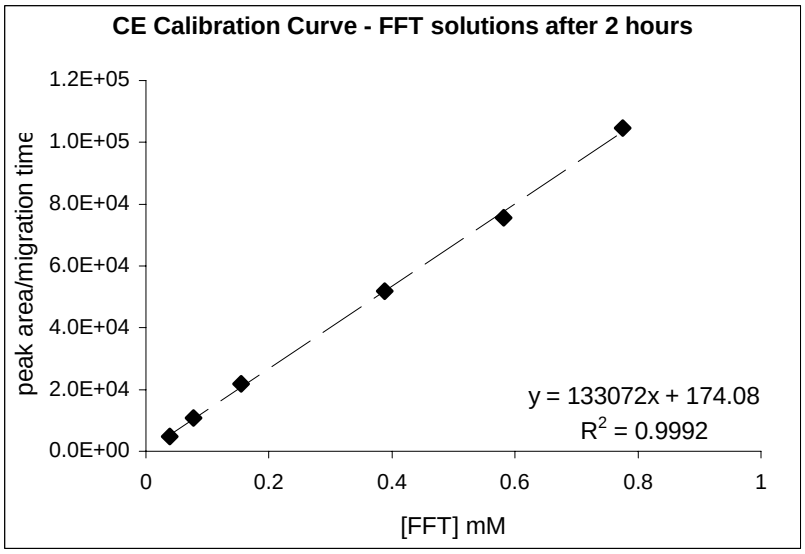

Table 4.2. Comparitive quantification of FFT in solid complexes by CE and ICP-MS. Statistical analysis (paired t-test) indicated no difference in value (P=0.11).

	Sample (Portion #)					
Method	1(1)	1(2)	1(3)	2(1)	2(2)	2(3)
CE	55.9	57.8	59.6	57.9	58.7	60.3
ICP	55.8	50.7	60.2	50.0	59.7	59.7

4.3.2 Comparison of the Initial FFT Loading Values

Loading values for this work are defined as the FFT content for each solid prepared immediately after the last step in the preparation protocol. The quantified FFT loading values and their respective standard deviations are displayed in Figures 4.2 and 4.3; these values represent the grand average and standard deviation of a sample population consisting of the singular loading values quantified in each of the triplicate portions subjected to CE quantification, for each solid complex prepared of a given M/T combination of Table 4.1 (e.g. **Medium II/No Fatty Acid Treatment** = 3 portions quantified by CE per each complex * 2 complexes prepared = sample population of 6). It should be noted that this work made no attempt to maximize FFT loading with β-CD in each of the M/T combinations. The general preparation protocol was used as described earlier, and the FFT loading comparison offers some insight into how the different Medium/Treatment combinations affect the FFT loading under identical temperature and time conditions. Data trends are discussed first, followed by interpretation of the results.

4.3.2.1 Effects of Different Fatty Acid Treatment in the Same Medium (Figure 4.2)

In **Medium I.**, a significant negative relationship exists between FFT loading and saturated fatty acid presence. This is not as apparent for the unsaturated fatty acids, with C_6=$C_2O_2^-H^+$ and C_7=$C_2O_2^-H^+$ resulting in an equivalent FFT load, but both are greater than

$C{=}C_9O_2^-H^+$. However, all three unsaturated FAs inhibit FFT complexation with β-CD more so than any of the saturated auxiliary agents. This finding could be produced from either of the

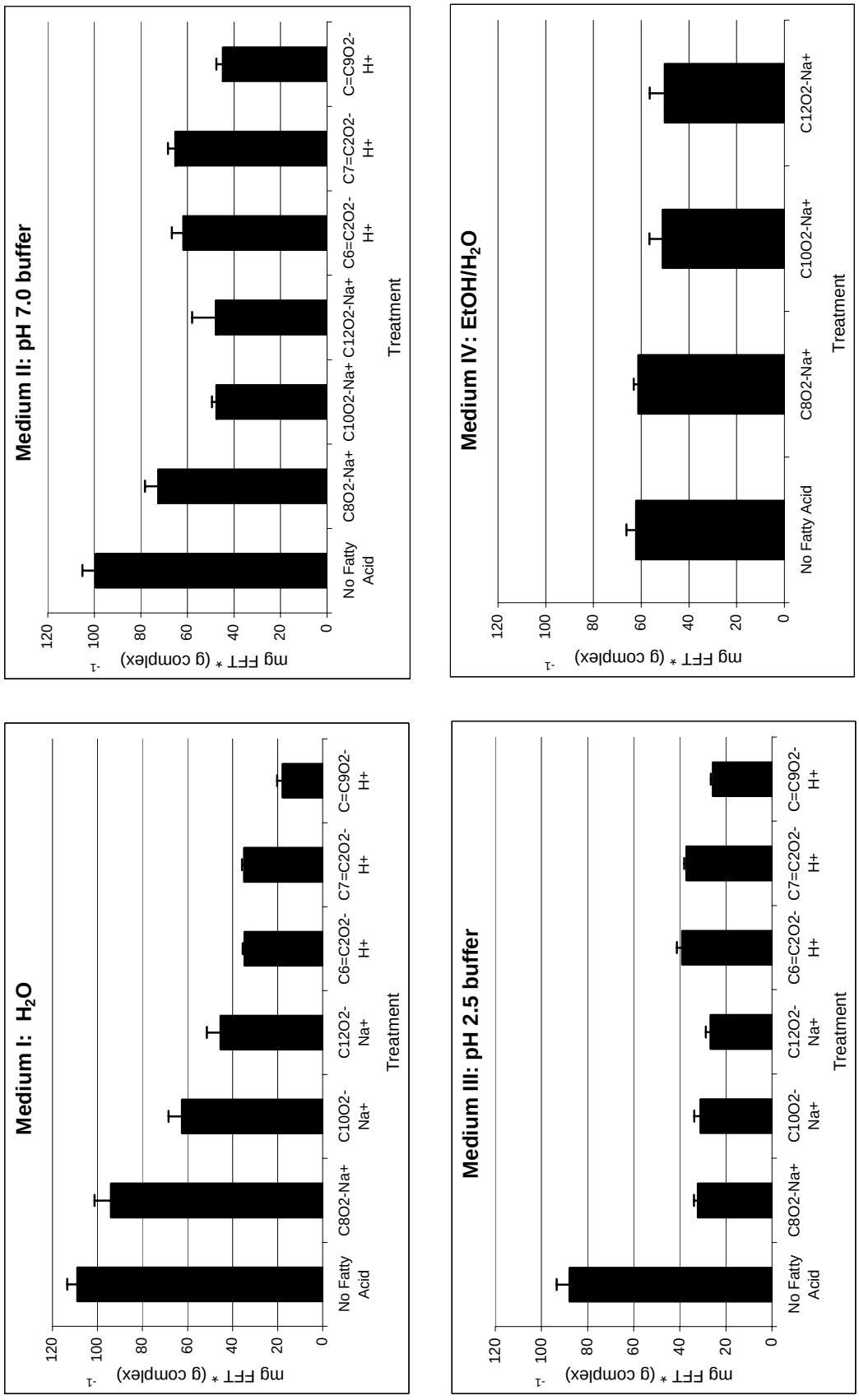

Figure 4.2. FFT loading in the different media as a function of fatty acid treatment.

following differences between saturated and unsaturated FAs: 1) the presence of an alkyl chain double bond, or 2) different FA ionization states for the saturated versus unsaturated FAs when added to the preparation solution. The latter difference arises from the use of an unbuffered aqueous medium, where at the FA concentrations used in this work (~ 75 mM) the saturated salts and unsaturated acids should result in pH values of ~9 and 3, respectively[†]. This difference in ionization states could contribute to the inhibited FFT loading seen for the unsaturated compared to saturated FAs observed in **Medium I**.

To investigate the role of fatty acid ionization state, the complexation procedure was performed in phosphate buffers at pH 7 and pH 2.5 (**Media II** and **III**, respectively). It can be seen in Figure 4.2 that charge state does play a role for decreased loading in the presence of unsaturated acids as observed in **Medium I**, and it is not simply a result of unsaturation in the alkyl chain. Evidence for this lies in the observation that in either buffer, fatty acid alkyl chain unsaturation is not a critical factor (as in **Medium I**) in determining the quantity of FFT loading in the isolated solid. The presence of a FA, either its anionic or neutral ionization states, decreases FFT loading, compared to the "no fatty acid" treatment.

However, visual inspection of Figure 4.2 reveals that FA *identity* appears more important when present in the anionic ionization state. There is a rough trend correlating FA/β-CD binding strength (as detailed in Chapter 3) to FFT loading in **Medium II**, but this becomes more vague as FA chain length is increased to C_{10} (saturated and unsaturated) and beyond. This is not present in **Medium III**, where all FAs affect FFT loading to relatively the same extent. It therefore could be argued that FFT loading in the solid is more sensitive to FA identity in the anionic versus neutral ionization state. This can be observed as the range of FFT loadings between the

[†] Actual pH_{sat}=7-8.5; pH_{unsat}=3-3.5

FA giving the highest and lowest loadings in each medium; for **Medium II** (pH 7) this range is 27.8 (mg FFT/g complex) compared to only 13.3 (mg FFT/g complex) in **Medium III** (pH 2.5). This seems to suggest that a feature of the FFT/β-CD complexation process dependent upon FA *identity* is amplified when the FA is ionized, whereas neutralization of the acid moiety diminishes these effects and renders all FAs investigated more or less similar to each other in their effect on the FFT/CD interaction.

In the ethanol/H_2O mixed solution (**Medium IV**), the effect of fatty acid presence is much less pronounced. In fact, the presence of $C_8O_2^-Na^+$ results in equivalent FFT loading to just using β-CD alone, within statistical limits. Furthermore, the two longer chain FAs used in this medium give equivalent FFT loadings with respect to each other, within statistical limits. The relative independence of FA identity on FFT loading is observed by the difference between the $C_8O_2^-Na^+$ and $C_{10}O_2^-Na^+$/$C_{12}O_2^-Na^+$ treatments from highest to lowest loadings being approximately 11 (mg FFT/g complex) in this medium, as compared to approximately 49 (mg FFT/g complex) in **Medium I**. It is therefore important to note that the presence of EtOH for FFT/β-CD complexation nearly negates any significant effect FA *presence* and *identity* has on FFT loading in other media; in **Medium IV**, the FAs appear to play no significant role in defining the loaded quantity of FFT.

4.3.2.2 Effects of Different Media for the Same Fatty Acid Treatment (Figure 4.3)

The data presented in Figure 4.2 is recast in Figure 4.3 to highlight the comparison of using the same fatty acid treatment in different solution media, and the resulting effect on FFT

loading. In all FA treatments, higher FFT loading was obtained in **Medium II** than **Medium III**, indicating that the presence of a neutral FA impedes FFT loading greater than its anionic form.

The addition of EtOH, compared to **Medium I**, decreases the quantity of FFT loaded in the solid complex for the "no fatty acid" treatment, as well as for two of the three FAs used in this medium. However, FFT loading in the presence of EtOH is less affected as the hydrophobic nature of the FA is increased. Indeed, the $C_{12}O_2^-Na^+$ treatment results in equivalent loading in **Medium I** and **Medium IV**.

Figure 4.3. FFT loading for the fatty acids treatments as a function of different media.

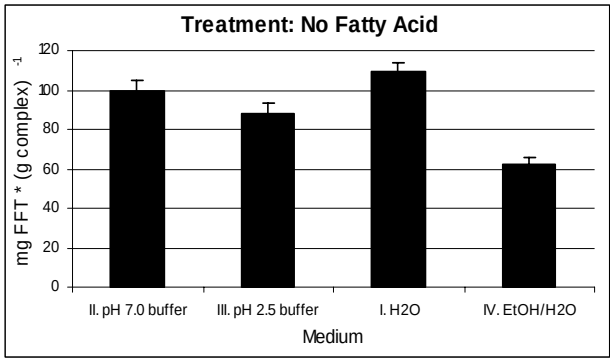

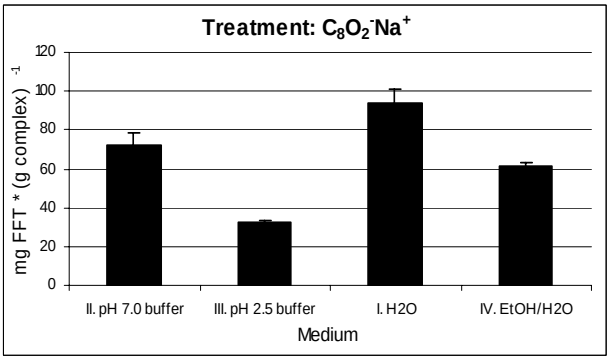

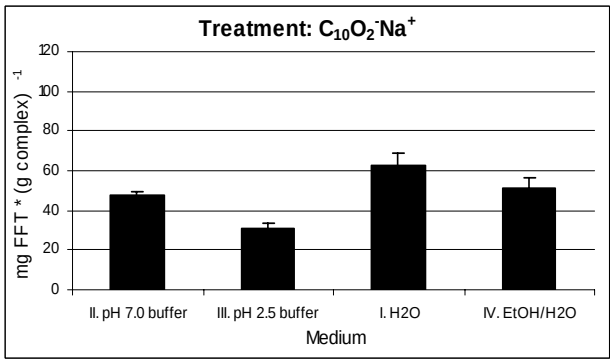

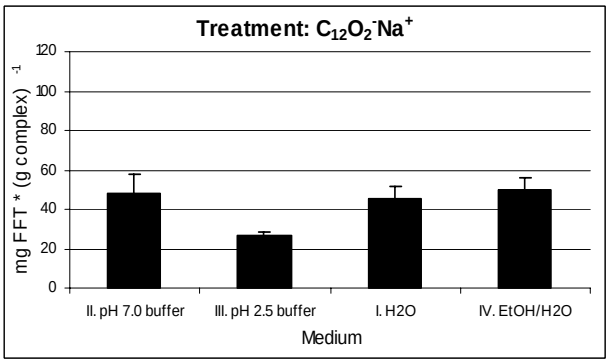

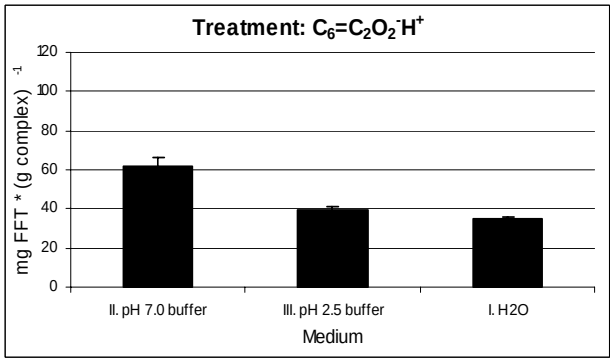

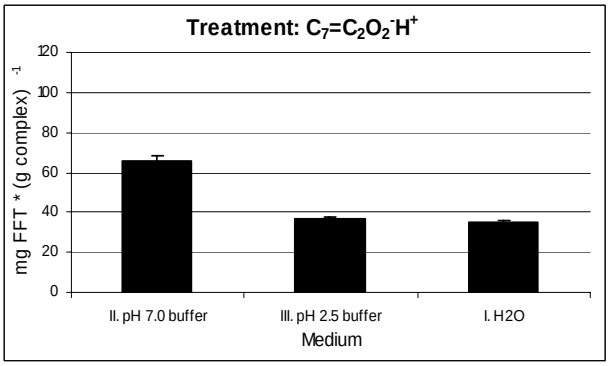

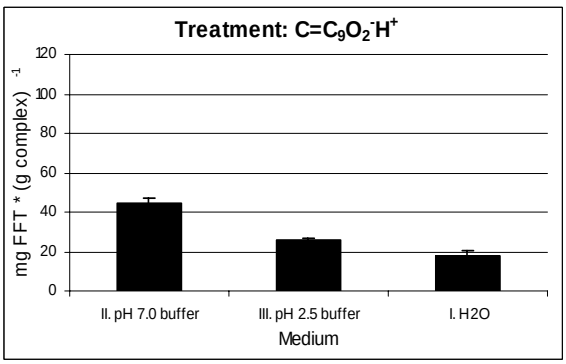

4.3.2.3 Interpretation of the Loading Results

It is evident that in media not containing EtOH, the presence of the FAs inhibits the quantity of FFT that is recovered in the solid product. Fatty acid inhibition of FFT loading could be reasoned by one the following, but is likely a combination dependent upon the medium discussed: 1) competitive binding of FA for the CD cavity, effectively blocking FFT inclusion, or; 2) micellar sequestration of FFT by FAs above their critical micelle concentration (cmc). The assumption of competitive binding is the easiest to infer, where occupation of the CD cavity by the FA should follow a trend based upon FA/β-CD binding strength (Chapter 3); such a trend is seen for the saturated acids in **Medium I.** This is also observed in **Medium II**, where all FAs are present in their anionic state at pH 7.0, and the unsaturated acids are included in the trend.

Micellar sequestration and subsequent inhibition of CD inclusion complexation has been reported in the presence of surfactants in the solution media [19,20]. In these previous studies guest displacement from the CD cavity occurred as the surfactant concentration exceeded the cmc, and ternary CD complex formation was replaced by incorporation of the guest into the hydrophobic micellar core. In the present work, all FAs were added at ~75 mM, and literature estimates [21,22,23] are approximated as 400 mM, 50-100 mM, and 30 mM for $C_8O_2^-Na^+$, $C_{10}O_2^-Na^+$ and $C_{12}O_2^-Na^+$, respectively. Using these values, this equates to $C_8O_2^-Na^+$ as fully present in its free, non-micelle form, and $C_{10}O_2^-Na^+$ and $C_{12}O_2^-Na^+$ capable of forming micelles. This difference could be reason (along with the competitive binding theory) for greater inhibition of FFT loading in **Media I** and **II** as FA alkyl chain length is increased (Figure 4.2).

Furthermore, both the competitive inclusion and micelle sequestration theory can possibly be used to explain the differences in FFT loadings for a given FA between **Media II**

and **III**. The anionic acid possesses a lower affinity for the CD cavity than its neutral form [24,25]; this should equate to greater FFT/CD loading when the FA is anionic, if the competitive inclusion theory is to be assumed as an explanation for medium effect. The micelle sequestration theory applies in this comparison because micelle formation is more readily achieved in the neutral state; for example, the cmc value for $C_{10}O_2^-H^+$ decreases to below 2.5 mM, much lower than for its anionic ionization state [26]. It is not unreasonable to assume a similar reduced cmc for the other FAs used in this study in their neutral states. With micelles being more readily formed at pH 2.5, this could account for decreased FFT/CD loading for each FA treatment when employing **Medium III** instead of **Medium II**.

Additionally, the micelle sequestration hypothesis could also explain why as anions, FA *identity* does possess some importance in FFT/CD loading, and while as neutral acids, this importance is lost (Figure 4.2). This is based on the previously discussed assumptions that all FAs are capable of forming micelles, with subsequent FFT entrapment in their hydrophobic cores, in **Medium III** (pH 2.5), and not all FAs form micelles in **Medium II** (pH 7). It is noted that as a consequence of using the micelle sequestration hypothesis to explain observed differences when comparing these media in this way, it inherently suggests that micelle formation leaves all FAs nearly equal in inhibiting FFT interaction with β-CD.

In **Medium IV**, the presence of EtOH once again renders all FAs nearly identical in their affect on FFT loading. Under the assumption of FA competitive binding, the role of EtOH could lessen the intrinsic attraction of the FA for the CD cavity. By exerting such a solution polarity effect [27], FA occupation of the cavity would be lessened and access is no longer denied for FFT inclusion. The effective diminishing of loading in a solution containing only FFT and β-CD (no FA) is another indicator that a solution polarity effect is indeed introduced by the presence of

EtOH; the more hydrophobic solvent system presumably lessens the "driving force" for complexation, thereby leading to decreased FFT content in the solid product. Occupation of the cavity by EtOH in a competitive fashion offers another possibility for this observation [5].

In another, seemingly contrasting role, EtOH could also be acting as a modifier of the cavity microenvironment. Alcohols acting in this role have been reported previously [28], in which their presence induces a more hydrophobic CD cavity environment compared to using H_2O solvent alone. This effect would intrinsically enhance FFT's attraction for the CD cavity. This effect might also result in FFT having a greater attraction to the cavity than the FAs, and as such presents another possibility for the apparent lacking dependence of FFT loading on FA presence and identity in **Medium IV**.

4.3.3 Evaluating Solid Complex Performance During Storage

The amount of FFT in the solid materials was quantified on a weekly basis to assess the performance of the prepared solids in preventing FFT loss during room temperature storage in the ambient atmosphere. This was done for every complex of a given M/T combination, and FFT content appeared to stabilize after 4 weeks. FFT retention results during this 4-week storage period are displayed in Figures 4.4 and 4.5, and the values are presented as %FFT retained relative to initial FFT loading quantified immediately after preparation. Evaluating the FFT content in each of the solids this way serves as a better indicator of the solid complexes' performance, and further clarifies the role of different media and treatments on the actual FFT/β-CD complex performance.

4.3.3.1 Effects of Different Fatty Acid Treatment in the Same Medium (Figure 4.4)

For complexes prepared in the unbuffered, purely aqueous **Medium I**, $C_{12}O_2^-Na^+$ is the only saturated fatty acid whose presence showed more than marginal deviation in FFT retention from those complexes prepared without FA. Furthermore, the complexes made with unsaturated acids in the preparation solution were significantly worse than any of the saturated acids in retaining FFT over the course of the 4-week period. This finding may be once again an artifact of the unsaturated acids being added to solution in their neutral states that should result in a rather acidic (pH ~3) solution, while the saturated acids were added as their sodium salts. Without pH control of this medium, this difference may again be responsible for the observed differences in FFT retention between the saturated and unsaturated groups. This finding does, however, indicate that FA ionization state plays a role in defining the ability of the complex to retain FFT. By using buffered media to prepare the complexes in the presence of the 6 fatty acids chosen for this work, the effect of fatty acid ionization in the preparation solution on complex performance is elucidated.

Figure 4.4. FFT retention after 28 days room temperature storage in the different media as a function of fatty acid treatment.

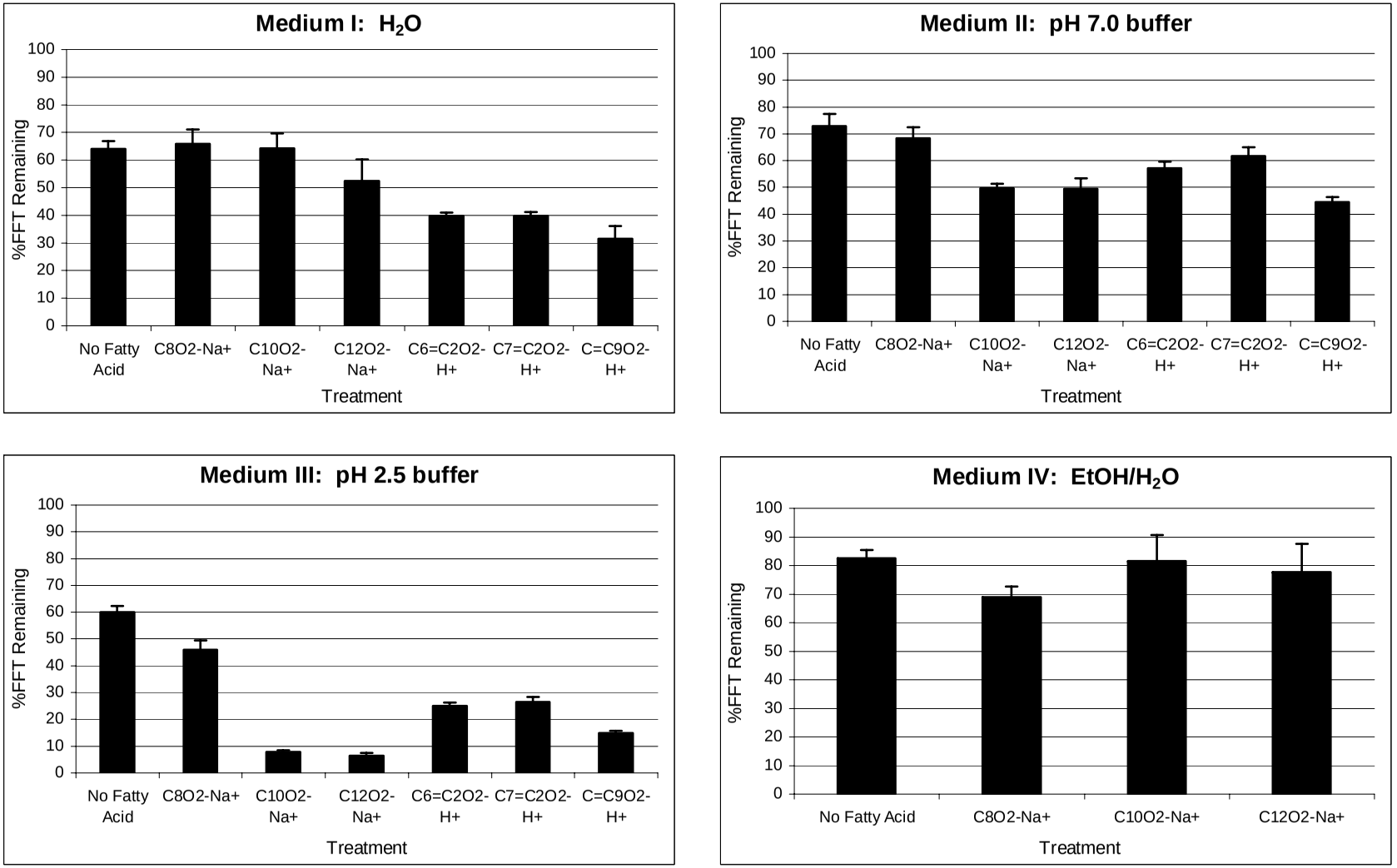

The presence of fatty acids in the preparation medium at pH 7.0 and pH 2.5 results in complexes that are decreasingly capable of preventing FFT loss, when compared to complexes prepared in their absence. This trend roughly correlates to FA size for both the saturated and unsaturated acids. The effect is much more pronounced for complexes prepared at pH 2.5 than pH 7.0, suggesting that the neutral acids severely affect the FFT retention properties of the solid material. While the effect of FAs cannot be defined by these datasets, their presence in these preparation media (**II** and **III**) cannot be ignored as a component in altering the mode of FFT/β-CD interaction.

The addition of ethanol to the encapsulation medium results in less obvious differences in FFT retention between complexes prepared with and without FAs. This limited dataset seems to suggest that the role of FAs on FFT retention properties of complexes prepared in other media, previously discussed, disappears in the mixed solvent system. Furthermore, this observation fits well to the discussion on FFT loading in the presence of FAs in the EtOH/H_2O medium in Section 4.3.2.1; in loading and in FFT retention, EtOH deems all FAs nearly identical in their role seemingly by negating their involvement in the FFT/CD complexation process.

4.3.3.2 Effects of Different Media for the Same Fatty Acid Treatment (Figure 4.5)

The comparison of medium composition for FFT complexes prepared in the presence of the same FA revolves around two major trends. The first reiterates the discussion that FA charge plays a key role in defining the capability of the solid complex to maintain FFT content. Again,

in the neutral state, all FAs lead to complexes that perform poorer than their anionic medium counterparts.

For every treatment prepared, regardless of FA presence and identity, the addition of EtOH led to complexes that retained FFT content better than every other medium investigated; this is the second major observation of these comparisons. Because this trend is apparent for all CD and CD/FA combinations, and because retention is relatively FA identity independent (Figure 4.4), the role of EtOH must be more decisive in defining the FFT retention capability than FA presence and identity. It must also play a role in complex formation that is absent in the purely aqueous **Medium I**.

Figure 4.5. FFT retention after 28 days room temperature storage for the fatty acid treatments as a function of different media.

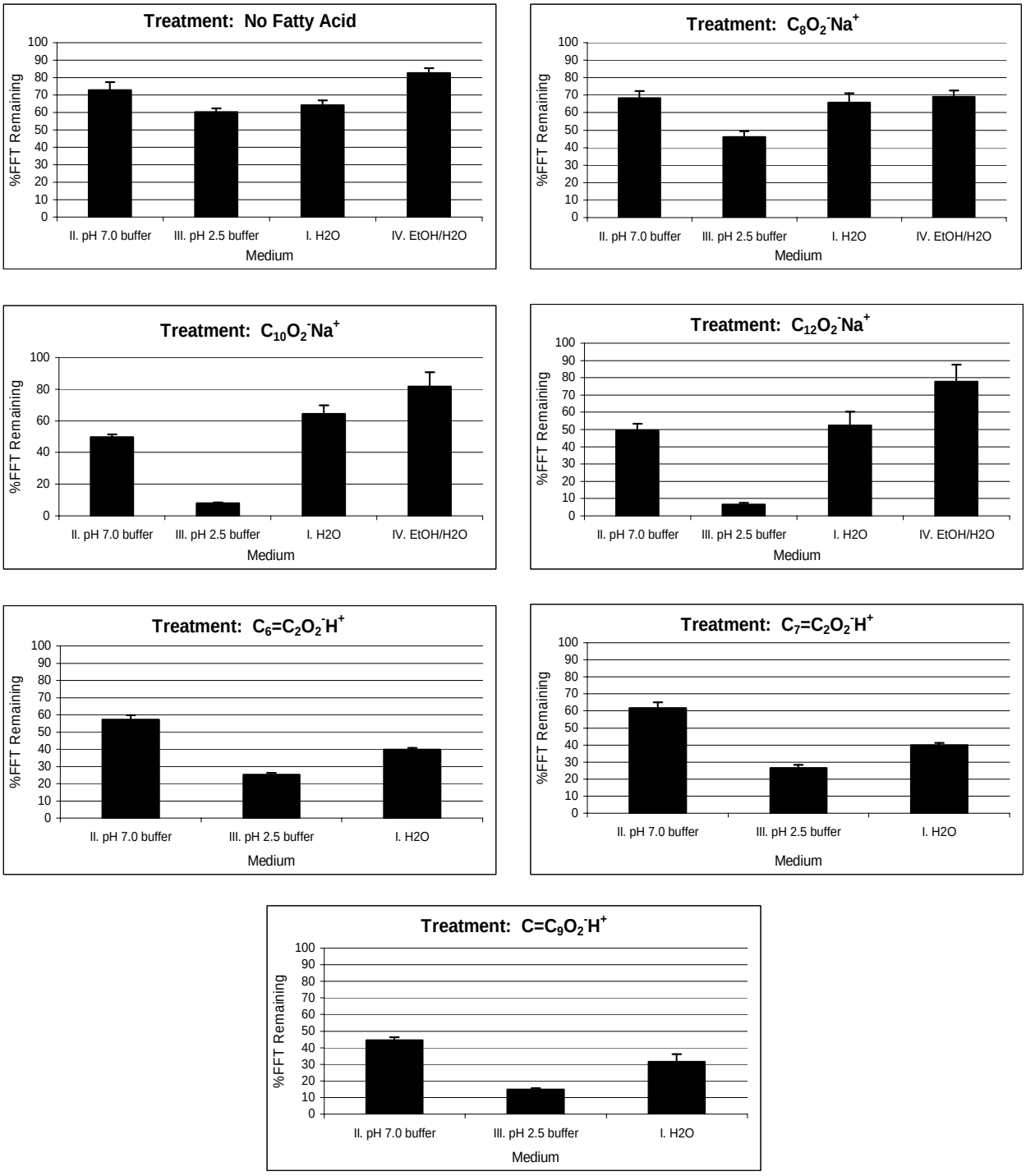

4.3.3.3 Interpretation of the FFT Retention Results

Assuming that FA presence only affected the *quantity* of FFT loaded during the preparation procedure and not the *mode* of FFT/CD interaction, then all solids should perform more or less equally during the time storage study regardless of FA treatment or medium. This was observed, without much deviation, for the saturated FAs in **Medium I** and **IV**. Therefore it is suggested that the use of FAs in these media does not have a significant effect on the retention properties of the formed solids, and seems to indicate the FFT/β-CD mode of interaction is not affected. However, the FA treatments in buffered **Media II** and **III** do affect the FFT retention properties of the prepared solids, suggesting some change in FFT/β-CD interaction when using the FAs in these media. Further studies are required in order to determine the effect on the FFT/β-CD interaction with these M/T combinations.

Interestingly, as noted previously, the use of EtOH in the preparation medium (**IV**) resulted in complexes that performed the best with regards to FFT retention properties, suggested again that the FFT/β-CD interaction *mode* is altered. Because EtOH presence appears to be more decisive in determining FFT loading and retention than any fatty acid treatment, discussion of its effect is offered in the following section.

4.3.4 Preliminary Investigation into the Role of Ethanol on Complex Formation and Performance

Short-chain linear and branched alcohols have been evidenced to be involved in the inclusion complexation of various guests with CDs. This role has been defined as one or a

combination of the following: 1) altering bulk solution polarity [27]; 2) co-competing for the CD cavity [5]; 3) modifying the cavity microenvironment [28]; and 4) filling void space in the cavity after guest/host association [29,30]. The suggestion that EtOH, performing one or both of the first two roles in this work, could seemingly be responsible for decreased FFT *loading* in the presence of EtOH compared to loading in its absence. This has already been discussed in Section 4.3.2.3.

The modification of the cavity microenvironment, and filling cavity void space, by small alcohols can enhance complex formation and help realize guest compound *retention*. By interacting with the CD host, alcohols can alter the surrounding cavity environment making the CD molecule more favorable for guest compound inclusion [28]. By acting as a space regulator, alcohols can fill the void space resulting from imperfect geometry matching between the guest and host cavity, thereby leading to the formation of a 'tighter' ternary complex [29,30]. In this way, the guest molecule is more effectively trapped in the CD cavity, helping to realize the potential benefits of CD inclusion complexation. In relation to this work, because EtOH was found to enhance the FFT retention properties of the CD complexes, it was hypothesized that EtOH's presence could be defined as one of these roles.

NMR spectroscopy was used for preliminary screening of these complexes. Analysis of each complex prepared in the presence of EtOH, with and without FA, revealed an NMR signal at ~1.00 ppm, characteristic of the H_3C moiety of EtOH (Figure 4.6). This resonance is easily distinguishable from other signals in the spectrum, whereas the methylene and hydroxyl protons are severely interfered with by signals of other constituents of the complex. Integration of the anomeric (H1) proton of β-CD and the H_3C signal of EtOH returned a molar ratio of ~5:1 (CD:EtOH). Analysis of a portion of each complex, during the same time-course investigated

for FFT quantification by CE, revealed this molar ratio as steadily increasing, relaying that EtOH was being continually lost from the solid complex. If the ternary FFT/EtOH/CD complex is indeed formed, its performance must be comprimised over time as evidenced by the simultaneous reduction of FFT and EtOH content in the solid material. If EtOH is simply associated with the solid in a different manner, then its role in enhancing the FFT retention properties of the solid could be that of influencing the mode of FFT/β-CD complexation without co-inclusion, such as altering depth or orientation of penetration of FFT into the cavity. From this preliminary investigation, however, it cannot be concluded either way that a weak ternary FFT/EtOH/β-CD complex is formed, or that EtOH plays a different role that positively affects the relative FFT content remaining in the solid complex after 4 weeks of room temperature storage.

Figure 4.6. ^{1}H NMR spectrum acquired immediately after preparation of a FFT/β-CD complex prepared in **Medium IV**. No fatty acid was in the preparation medium.

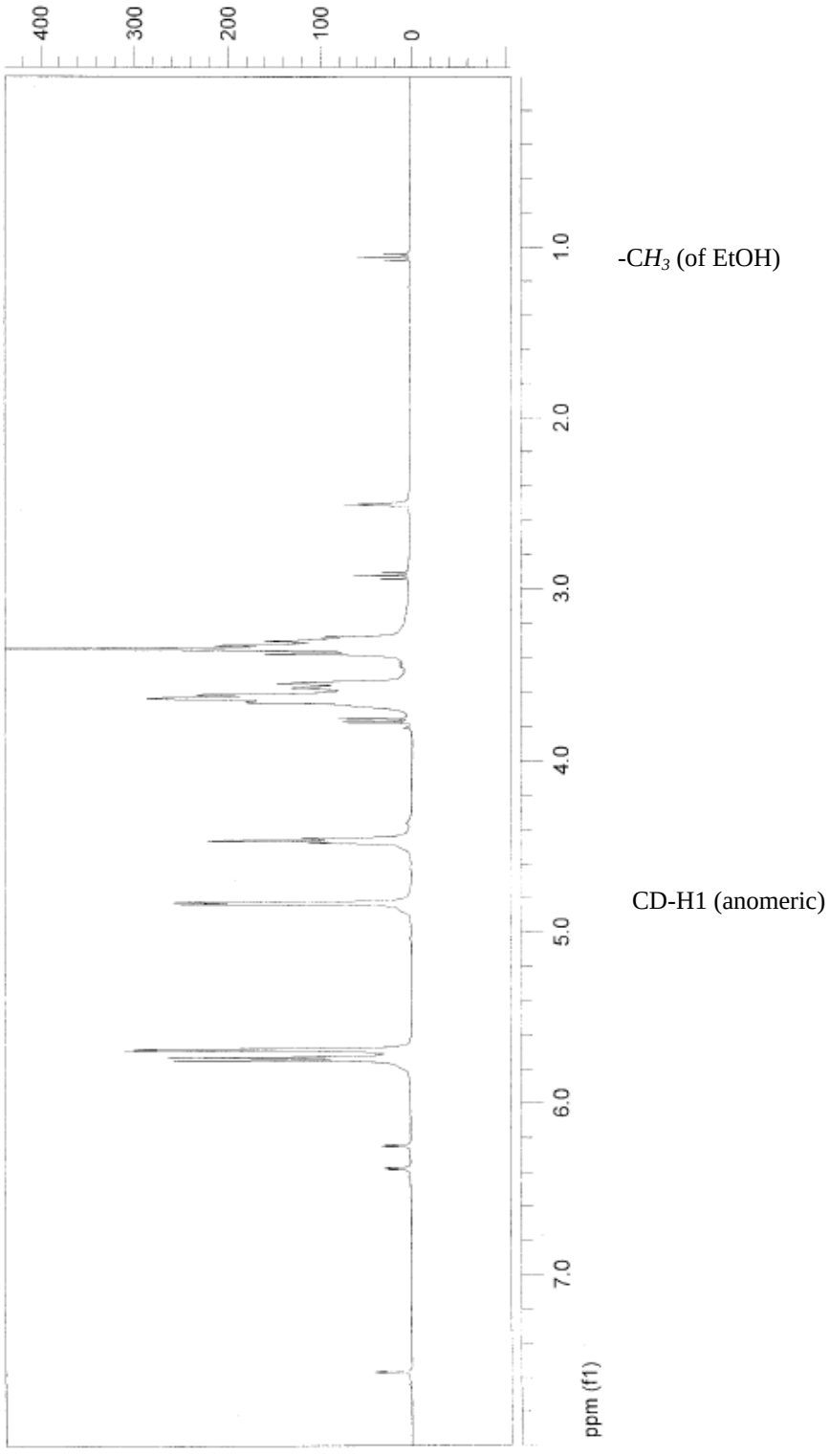

4.3.5 Long Term Storage Results

All complexes, regardless of the media they were prepared in, appeared to reach an FFT retention plateau after 4 weeks of storage at room temperature. The FFT content of some complexes was again quantified after an additional 5 weeks under the same storage condition (9-weeks total) to further assess their utility. All complexes displayed further FFT content loss, apparently suggesting that additional processes, such as FFT oxidation, cumulatively affect the FFT retention properties of the solid complexes longer than what appeared in the preliminary time course studied of this work.

4.4 Summary

The presence of ethanol in the complex medium generally led to decreased FFT loading in the solid products. However, this addition produced solid complexes with the greatest ability to retain FFT content throughout a 4-week storage period. Analysis of the complexes by NMR revealed the presence of EtOH in the final solid products, but is presence is not maintained over the course of storage. Both effects were independent of saturated fatty acid content under the experimental guidelines, suggesting non-participation of the FAs in complex formation in this medium.

In media not containing ethanol, the effect of fatty acid presence in the FFT/β-CD complex preparation medium under the same preparation conditions led to decreased FFT loading in the solid product. This observation is more prevalent when the fatty acids are used in their neutral state, presumably because of reduced FFT/CD interaction resulting from a

combination of greater intrinsic attraction for the CD cavity by protonated FAs or because of a micellization phenomenon. Furthermore, evaluation of the ability of the solid products to retain FFT content over time revealed that complexes prepared with FAs in the media generally performed worse than complexes prepared in their absence. These results indicate that FA/β-CD or FFT/β-CD are indeed present in product formation, and use of FA negatively alters the FFT retention characteristics of the CD complexation by altering the mode of FFT/CD interaction.

In comparison to earlier work on the β-CD encapsulation of FFT [1,2], the results of this study seem to offer support to both claims. When prepared in a purely aqueous encapsulation medium, FFT content is initially high but is lost over the course of a just a few weeks; this seems to support the finding of Rennicius, et al [2]. Following the work by Szente et al [1], the addition of EtOH produced complexes displaying enhanced encapsulation properties, and the FFT loading values are comparable (6.2% w/w this work, 6.8% w/w Szente et al). However, the results presented in this Chapter do not support their claims that the β-CD complex can retain 100% of initially loaded FFT content.

4.5 References

[1] L. Szente, J. Szejtli, J. Food Sci. 51 (1986) 1024.

[2] T.A. Reineccius, G.A. Reineccius, T.L. Peppard, J. Food Sci. 67 (2002) 3271.

[3] L. Szente, J. Szejtli, Trends Food Sci. Technol. 15 (2004) 137.

[4] J. Szejtli, L. Szente, E. Banky-Elod, Acta Chim. Hung. 101 (1979) 27.

[5] L. Szente, in J. Szejtli, T. Osa (Editors), Comprehensive Supramolecular Chemistry, Vol 3, Cyclodextrins. Permagon, Oxford, 1996, p. 243.

[6] Z. Qi and A. Hedges, in C. Ho, C. Tan, C Tong (Editors). Flavor Technology: Physical Chemistry, Modification, and Process. American Chemical Society, Washington D.C. 1995, p. 231.

[7] J. Szejtli, Cyclodextrin Technology. Kluwer Academic Publishers, Norwell, MA, 1988, p.91

[8] F. Giordano, C. Novak, J.R. Moyana, Thermochim. Acta 380 (2001) 123.

[9] V.T. Karathanos, I. Mourtzinos, K. Yannakopoulou, N.K. Andrikopoulos, Food Chem. 101 (2007) 652.

[10] M.E. Cortes, R.D. Sinisterra, M.J. Avila-Campos, N. Tortamano, R. G. Rocha, J. Inclusion Phenom. Macrocyclic Chem. 40 (2001) 297.

[11] B.R. Bhandari, B.R.D'Arcy, I. Padukka, J. Agric. Food Chem. 47 (1999) 5194.

[12] H. Shiga, H. Nishimura, H. Yoshii, T. Furuta, P. Linko, J. Chem. Eng. Jpn. 35 (2002) 468.

[13] T.A. Reineccius, G.A. Reineccius, T.L. Peppard, J. Agric. Food Chem. 53 (2005) 388.

[14] M. Schultz, P. Hebeisen, β-Cyclodextrin-Furfuryl Mercaptan Complexes. Test Report. (2001)

[15] I. Blank, E. Pascual, S. Devaud, L.B. Fay, R.H. Stadler, C. Yeretzian, B.A. Goodman, J. Agric. Food Chem. 50 (2002) 2356.

[16] T. Hofmann, P. Schieberle, W. Grosch, J. Agric. Food Chem. 44 (1996) 251.

[17] D. Rowe, K. Auty, S. Jameson, P. Setchell, G. Carter-Jones, Perfumer & Flavorist 29 (2004) 2.

[18] J.H. Zar, Biostatistical Analysis, Fourth Edition. Prentice-Hall, Upper Saddle River, NJ, 1999, p. 360.

[19] H.E. Edwards, J.K. Thomas, Carbohydr. Res. 65 (1978) 173.

[20] E.A. Cummings, T.T. Ndou, V.K. Smith, I.M. Warner, Appl. Spectrosc. 47 (1993) 2129.

[21] K. Shinoda, J. Phys. Chem. 58 (1954) 1136.

[22] A. Gonzalez-Perez, G. Prieto, J.M. Ruso, F. Sarmiento, Mol. Phys. 10 (2003) 3185.

[23] T. Namani, P. Walde, Langmuir 21 (2005) 6210.

[24] K.A. Connors, *Supplemental Material* to J. Pharm. Sci. 84 (1995) 843.

[25] E. Schneiderman, A.M. Stalcup, J. Chromatogr. B 745 (2000) 83.

[26] S. Lima, B.J. Goodfellow, J.J.C. Teixeira-Dias, J. Phys. Chem. B 107 (2003) 14590.

[27] E. Junquera, E. Aicart, J. Phys. Chem. B 101 (1997) 7163.

[28] G. Patonay, K. Fowler, A. Shapira, G. Nelson, I.M. Warner, J. Inclusion Phenom. 5 (1987) 717.

[29] A. Nakajima, Bull. Chem. Soc. Jpn. 57 (1984) 1143.

[30] A. Munoz de la Pena, T.T. Ndou, I.M. Warner, J. Phys. Chem 94 (1991) 6701.

Chapter 5

Conclusions and Future Directions

5.1 Conclusions

The work presented in Chapter 2 provides evidence for cavity inclusion of 2-furfurylthiol (FFT) with β-cyclodextrin (β-CD), thus validating earlier work assuming that inclusion complexation was possible for this guest/host system. Furthermore, an inclusion complex structure was proposed based upon induced chemical shifts of FFT and β-CD during NMR titration experiments. Preliminary 2-D NMR experiments for validating the proposed structure is hypothesized to have failed assuming weak guest/host interactions, defined as a poor geometric match between the aromatic moiety of FFT and the β-CD cavity; past studies of CD complexation have proven this factor to be critical in forming stable complexes. Estimation of a binding constant for FFT/β-CD inclusion provided further evidence for weak interaction between these two compounds.

Chapter 3 detailed the first use of CE and ITC to study the interaction between the proposed fatty acids (for ternary complex formation) and β-CD. This work adds further information on the affect of FA structural characteristics on binding constants and thermodynamic parameters of binding to the often-studied FA/β-CD system. Additionally, our results support 1:1 binding adding more experimental results to the debate on the preferred stoichiometry of interaction between these FAs and β-CD in solution. At the same time, the discussion on factors affecting the accuracy of the ACE measurement of binding constants

displays the necessity of evaluating the experimental setup, and can serve as a guide to future investigations of host/guest chemistry using this technique in the Stalcup group.

The final chapter detailing experimental work, Chapter 4, carried the focus of this dissertation into the solid state, a move that was necessary for evaluation of the proposed ternary system for potential use in industrial applications. Fatty acid presence and complexation medium effects were observed, indicating that FA presence and ionization state was a key factor in determining FFT/β-CD loading values and retention properties. The use of a competitive binding and micelle sequestration theories might explain observed trends in FFT loading. The fact that FA presence in the preparation medium (without ethanol) affected FFT retention properties of the isolated solids suggests alteration of the mode of FFT/CD complexation. The best FFT retention was obtained for complexes with ethanol present in the complexation medium, suggesting an active role of this additive on the mode of FFT/β-CD complexation. At this point it is not known if the formation of a ternary FFT/EtOH/β-CD complex is formed, or EtOH affects binding in solution by altering the cavity microenvironment. This solid-state FFT/β-CD inclusion study could not reproduce earlier reports suggesting nearly 100% FFT retention and anti-oxidant properties of the β-CD encapsulation technique.

5.2 Suggestions for Future Work

5.2.1 Additional NMR Studies to Investigate FFT/β-CD Interaction

As suggested during conversations with Dr. Pearl Tsang at the University of Cincinnati, modifications of experimental design could be investigated to potentially gather 2-D NMR data

representative of the FFT/β-CD inclusion complex. Lowering experimental temperature may prove to be beneficial by slowing the kinetics of interaction, and hopefully enabling detection of NOE (or ROE) signals. Additional experiments could at least investigate using a large excess of one binding partner over the other to increase the probability of complex formation for one of the components; this strategy has been used in past literature reports for systems expected to give weak correlation signals because of a low complex population in a simple 1:1 molar solution [1]. And as noted in Chapter 2, more complicated 2-D NMR pulse sequences could also be attempted.

Although not noted in Chapter 2, 1-D NOE experiments could also be conducted to elucidate the FFT/β-CD complex structure. Advantageously, 1-D NOE offers a more rapid analysis compared to 2-D NOESY experiments, and perhaps should be considered instead of continued 2-D work. Enhancement of the FFT aromatic proton signals resulting from selective irradiation of the CD cavity protons would provide information into the spatial relationship of guest/host protons in the formed complex. Reversal of the approach and selective irradiation of the guest FFT protons could offer further confirmation of proposed inclusion structures.

Titration experiments in the presence of deuterated EtOH might provide information highlighting the effect EtOH has in solid complex formation. It is advised that non-deuterated EtOH not be used; preliminary experiments not discussed in this dissertation were unsuccessful as EtOH dwarfed the analyte peaks of interest.

5.2.2 Further Ternary Complex Investigations

It would be extremely beneficial to the investigation of ternary complex formation as a possible strategy to encapsulate FFT if screening experiments could be performed in solution to assess the utility of different proposed auxiliary binding agents Possibilities include NMR, CE (dependent upon the nature of the auxiliary compound), and computational studies to fulfill this need. An obvious advantage of developing screening methods would be identification of feasible auxiliary binding agents to enhance FFT/β-CD binding, before solid complexes are prepared and tested.

The literature support garnered for the inclusion of small linear and branched alcohols in ternary CD complexes offers another interesting avenue of research to investigate for FFT encapsulation by β-CD. Although use of these types of auxiliary binding agents is potentially limited because of GRAS (Generally Regarded As Safe) regulations in place by the FDA, information gleaned from such a study investigating size/structure relationship on the formation of FFT/alcohol/β-CD ternary complexes could possibly be expanded to auxiliary binding agents that do meet FDA approval for use in foods.

5.2.3 Miscellaneous

It would be interesting to further examine the possibility of micelle sequestration of FFT by FAs. This could potentially add validity to the arguments offered in Chapter 4, specifically that FFT/β-CD binding is decreased because of entrapment of FFT by FA micelles in solution. Initial work should focus on determination of the critical micelle concentrations (cmc) for all of

the fatty acids investigated in this work, to further validate the estimates offered by limited literature information for these compounds. Current monitoring techniques using available capillary electrophoresis instrumentation [2,3] are discussed in the literature and can be adapted to studying the fatty acids of our work. It should be noted that, while current monitoring techniques are rather straightforward for charged FAs, cmc determination for the neutral FAs would present more challenges, but measurements of solution surface tension and light scattering could be considered [4,5,6,7].

A study on the interaction between FFT and FA micelles could be performed quite easily in our lab using capillary electrophoresis. Assuming inclusion of FFT into the hydrophobic micellar core, this would theoretically induce an electrophoretic mobility for (neutral) FFT resulting from interaction with negatively charged FA micelles in the electrophoresis background electrolyte [3]. Again, this approach would be rather straightforward for FAs in their anionic form, but studying the FFT/micelle interaction for neutral FAs would present more challenges.

In addition, if micelle sequestration is indeed responsible for some of the observations of work presented in Chapter 4, it would emphasize the necessity of investigating other solid complex preparation techniques that could be done in solution to potentially form FFT/FA/β-CD ternary complexes without introducing micelle formation. Furthermore, it could open the door to studies on the use of FAs or other surfactants or surfactant-like compounds for extraction of guest species included in the CD cavity in other applications where removal may be advantageous.

5.3 References

[1] T. Carofiglio, R. Fornasier, L. Jicsinszkyu, G. Saielli, U. Tonellato, R. Vetta, Eur. J. Org. Chem, (2002) 1191.

[2] A. Cifuentes, J.L. Bernal, J.C. Deiz-Masa, Anal. Chem. 69 (1997) 4271.

[3] C.E. Lin, J. Chromatogr. A. 1037 (2004) 467.

[4] M.J. Lawrence, S.M> Lawrence, D.J. Barlow, J. Pharm. Pharmacol. 49 (1997) 594.

[5] I. Pepic, J. Filipovic-Grcic, I. Jalsenjak, Colloids Surf.,A 327 (2008) 95.

[6] M. Jamroz-Piegza, W. Walach, A. Dworak, B. Trzebicka, J. Colloid Interface Sci. 325 (2008) 141.

[7] P.K. Sharma, M.J. Reilly, D.N. Jones, P.M. Robinson, S.R. Bhatia, Colloids Surf., B 61 (2008) 53.